THE USE OF LATE TIME RESPONSE FOR STAND OFF ONBODY CONCEALED WEAPON DETECTION

ALI SAIED MILAD ATIAH

A thesis submitted in partial fulfilment of the requirements of the
Manchester Metropolitan University for the degree of
Doctor of Philosophy

Department of Electrical Engineering
The Manchester Metropolitan University
2012

Abstract

A new system for remote detection of onbody concealed weapons such as knives and handheld guns at standoff distances presented in this thesis. The system was designed, simulated, constructed and tested in the laboratory. The detection system uses an Ultra-wide Band (UWB) antenna to bombard the target with a UWB electromagnetic pulse. This incident pulse induces electrical currents in the surface of an object such as a knife, which given appropriate conditions these currents generate an electromagnetic backscatter radiation. The radiated waves are detected using another UWB antenna to obtain the Late Time Response (LTR) signature of the detected object. The LTR signature was analysed using the Continuous Wavelet Transform (CWT) in order to assess the nature and the geometry of the object.

The thesis presents the work which divided into two related areas. The first involved the design, simulation, fabrication, and testing of an Ultra-wide Band (UWB) antenna with operating bandwidth of $0.25 - 3.0$ GHz and specific characteristics. Simulated and measured results show that the designed antenna achieves the design objectives which are, flat gain, a VSWR of around unity and distortion less transmitted narrow pulse. The operating bandwidth was chosen to cover the fundamental Complex Natural Resonance (CNR) modes of most firearms and to give a fine enough time resolution. The second area covered by this thesis presents a new approach for extract target signature based on the Continuous Wavelet Transform (CWT) applied to the scattering response of onbody concealed weapons. A series of experiments were conducted to test the operation of the detection system which involved onbody and offbody objects such as, knives, handheld guns, and a number of metallic wires of various dimensions. Practical and simulation results were in good agreement demonstrating the success of the approach of using the CWT in analyzing the LTR signature which is used for the first time in this work. Spectral response for every target could be seen as a distribution in which the energy level and life-time depended on the target material and geometry. The spectral density provides very powerful information concerning target unique signature.

List of Publications

A. Atiah, N. Bowring, (2011), “Design of Flat Gain UWB Tapered Slot Antenna for onbody Concealed Weapons Detections,” *PIERS*, vol. 1. Marrakesh, Morocco, PIERS proceedings, pp. 581-585.

A. Atiah, N. Bowring, (2010), “Detection and Identification of Buried Objects Based Late Time response”, The Libyan Arab International Conference on Electrical and Electronic Engineering LAICEEE, Tripoli, Libya, vol 2, pp. 232-237

D. A. Andrews, N. Bowring, N. D. Rezgui, M. Southgate, E. Guest, S. Harmer, and A. Atiah, (2008), "A multifaceted active swept millimeter-wave approach to the detection of concealed weapons,", proc. SPIE, 7117, UK, Cardiff , pp 707-711.

Acknowledgements

I would like to thank God for giving me wisdom, patience, guidance and capabilities that has allowed me to complete this PhD. This research would not have been completed without the support and assistance from a large number of people. First, I would like to express my deepest appreciation and sincere gratitude to my director of study Professor Nicholas Bowring and Dr Alhussain Albarbar for their guidance and support without which this work could never have been completed. They have given me many degrees of freedom to explore different possibilities in this research and have always been supportive of my ideas. I admire them for his knowledge and strong determination.

Many thanks are due to my colleagues in the Concealed Weapon Detection Group, Dr. N. Rezgui, Dr. S. Harmer, Dr. D. Andrews, Mr. M. Southgate, Miss S. Smith and Mr. S. Colleen for their fruitful discussions and suggestions and for their friendship for the past few years which has made this PhD journey more enjoyable.

Last but not least, I would like to thank my parents, my wife and my children for their endless understanding, patience and support.

Statement of Originality

I hereby certify that all of the work described within this thesis is the original work of the author. Any published (or unpublished) ideas and/or techniques from the work of others are fully acknowledged in accordance with the standard referencing practices.

(Ali Atiah)

(May 2012)

Table of Contents

List of Figures

List of Tables

List of Abbreviations

ATR	Automatic Target Recognition
CNR	Complex Natural Resonance
CWT	Continuous Wavelet Transform
DR	Discrimination Ratio
ED	Exponential Distribution
EDN	E-Pulse Discrimination Number
ETR	Early Time Response
EMD	Empirical Mode Decomposition
FDTD	Finite-Difference Time Domain
FFT	Fast Fourier Transform
GLRT	Generalized Likelihood Ratio Test
GPOF	Generalized Pencil-of-Function
GTD	Geometrical Theory of Diffraction
HWSEM	Hybrid Wave front Singularity Expansion Method
IFFT	Inverse Fast Fourier Transform
LP	Linear Prediction
LTR	Late Time Response
MPM	Matrix Pencil Method
MUSIC	MUltiple SIgnal Classification
PEC	Perfect Electric Conductor
PML	Perfectly Matched Layer
LTI	Linear Time Invariant
MoM	Method of Moments
MIMO	Multi Input Multi Output
PCA	Principal Component Analysis
PWVD	Pseudo Wigner-Ville Distribution

RCS	Radar Cross Section
RSP	Reassigned Spectrogram
RSPWVD	Reassigned Smooth Pseudo Wigner-Ville Distribution
SEM	Singularity Expansion Method
SNR	Signal-to-Noise Ratio
SP	Spectrogram
SPWVD	Smooth Pseudo Wigner-Ville Distribution
STFT	Short-Time Fourier Transform
SVD	Singular Value Decomposition
TF	Time-Frequency
TFD	Time-Frequency Distribution
TSA	Tapered Slot Antenna
VSWR	Voltage Standing Wave Ratio
UWB	Ultra Wideband or Ultra wide Band
WVD	Wigner-Ville Distribution

Chapter 1

Aims and objectives

1.1 Introduction

During the last few years the demand to remotely and automatically detect concealed weapons at the entrance of public places such as airport and government buildings has been a major security challenge. This approach is not currently available by the application of access control technologies or imaging systems which are time consuming and do not preserves the privacy of people. In order to detect and classify an unknown concealed object by remote sensing, certain electrical properties of the object to be detected are required. To identify the unknown object accurately at a standoff distance, one approach is to illuminate the object by an ultra-wideband electromagnetic pulse. The transmitted pulse induces electrical currents on the target. This current flows on the target surface and radiates electromagnetic waves. Strong resonances will occur when the frequency of the incident wave coincides with the period of the oscillation of an induced current. This occurred resonance called the complex natural resonance frequency CNR of the conducting body related to the object's geometry. Each object has a unique signature involving dependent and independent aspects. The effects of these frequencies in the scattered response of a target mostly exist in the late time period LTR of the scattered response of a target which is mainly related to the construction features of the target such as overall shape and size. An initial forced response happens with direct reflection from the illuminated target and is generally called an early time response (ETR), in which

forced and natural responses exist together. A feature extraction techniques that relies on nature resonances should avoid using the ETRs of the scattered field since this addresses the object localization only and does not carry any aspects of target characteristics and features, Harmer et al. (2009).

The complex natural resonance behaviour in linear time invariant systems was formulized as the singularity expansion method (SEM) by Baum in 1976 in which the first mathematical model to represent the LTR using the independent resonance frequencies of the target was proposed. Since CNR frequencies are independent of incident angles it should be possible to extract the same complex resonance frequencies for any incident angle from its corresponding impulse response.

The problem of detecting a concealed object and classifying it from the scattered electromagnetic field is very difficult to solve for the following reasons: The scattering mechanism is very complicated even for simple geometry objects, and also these scattered signals are strongly dependent on the signal polarization and aspect angle of incident and reflection. In fact, the aspect dependency of the scattered fields makes the problem more complicated since it may cause two types of error in classification problems. The first one is that the scattered response at two different aspects of the same object could incorrectly be identified as two different concealed objects, while the second one is that the scattered response of two different concealed objects could be classified as one concealed object, (Agurto et al., 2007). An extraction feature which is insensitive to aspect variations is needed to accurately detect and characterize the concealed objects.

For discrimination of the concealed objects based on the late time target response, accurate extraction of these frequencies from a measured transient response is very important. Necessary requirements are automatic operation (no initial guesses required), insensitivity to noise and to estimation of the model order (number of frequency modes). It is not necessary that the concealed weapons detection system uses the whole electromagnetic band, however it is necessary that a large band of frequencies have to be used for the following reasons: firstly, to ensure that the resonances from all kinds of weapons are detected. Secondly, to identify the weapon by its profile as a function of frequency, (Harmer et al., 2009).

Key for the successful detection of onbody concealed objects, such as guns and knives, is an effective detection system with high resolution and dynamic range, the transmitting/receiving UWB antenna should be flat gain (non-zeros resonant) as much as possible, have distortionless pulse transmission, reception and be directive with high-radiation efficiency. Of particular interest are the aspect independent resonances and their associated damping which can be measured by a receiving UWB antenna, the amplitude and phase of such backscatter is aspect dependent relative to the linear polarization. For an effective detection system with high resolution and dynamic range, the transmitting/receiving UWB antenna should be flat gain (non-zeros resonant) as much as possible, have distortionless pulse transmission, reception and be directive with high-radiation efficiency. For radar systems used for the detection of weapons concealed under clothing, onbody or within carried bags at standoff distance, a flat gain directional

antenna and VSWR around unity is advantageous. This criterion is required to enable effective de-convolution of the antenna response from the received scattered signal, which is essential to enable successful extraction of CNR modes. Nevertheless, having a less than desirable antenna response, may lead to a detection system having unauthentic resonances as any antenna resonance could mask concealed onbody objects. The bandwidth of the antenna must be sufficiently wide to cover all of the basic frequencies of the most common firearms. In this thesis, a compact UWB antenna with exponentially tapered slot with a bandwidth of operating frequencies 0.25 to 3 GHz will be developed. This operating bandwidth was chosen to cover the fundamental CNR modes of most firearms and to give a fine enough time resolution to resolve these CNR, and to minimize clutter from the human subjects and other objects in the surveillance area.

An analysis of the LTR of a range of complex objects such as knives, mobiles phones and handguns over a range of aspects was carried in this research to form a theoretical and simulation knowledge of the LTR with a co-polarized and a cross polarized detector, to find out which of the aspect independent components could be applied to allow the target to be identified in an effective manner. A range of objects was modelled using a finite element program CST microwave studio transient solver at the range of frequencies proposed here. The signal processing algorithms and software necessary to pick out these signals were developed in order to detect the signature of the concealed threat objects at standoff distance, initially using the approach taken by Novak et al. (2006) and Ibrahim et al. (2007).

1.2 Aims

The aim of this research is to develop a new method to detect threat items such as handguns and knives at standoff distance by:

- Designing and fabricating a high gain wideband free wave antenna working within the frequency band 0.25 - 3GHz. The proposed antenna should be capable of offering both flat gain and a wide operational frequency range to identify the object by using the natural resonant frequency produced by concealed weapons which are dependent only on the size and shape of the target and independent on the way the target is excited.
- Develop signal processing algorithms to extract the unique target signature from the LTR signals.

1.3 Objectives

The block diagram of figure 1-1 presents the objectives of this thesis, also summarized by the following points.

- To study, investigate and design relatively flat gain ultra-wideband antenna in the frequency range of 0.25-3 GHz.
- To capture the LTR scattered from the onbody concealed objects and off body objects using the designed and purpose built antenna.
- To study and analyse the LTR of complex objects such as knives, and handguns for a range of aspects to provide theoretical, simulation and experimental knowledge of the LTR of onbody and off body, with normal and cross

polarization sensors, in order to find out which of the aspects independent components data can be used for target identification.

- To develop novel signal processing algorithms that will extract the LTR of onbody concealed target signature from the backscattered electromagnetic signals.
- To compare the new developed signal processing algorithms with one of the exist methods such as Generalized Pencil off Function GPOF.

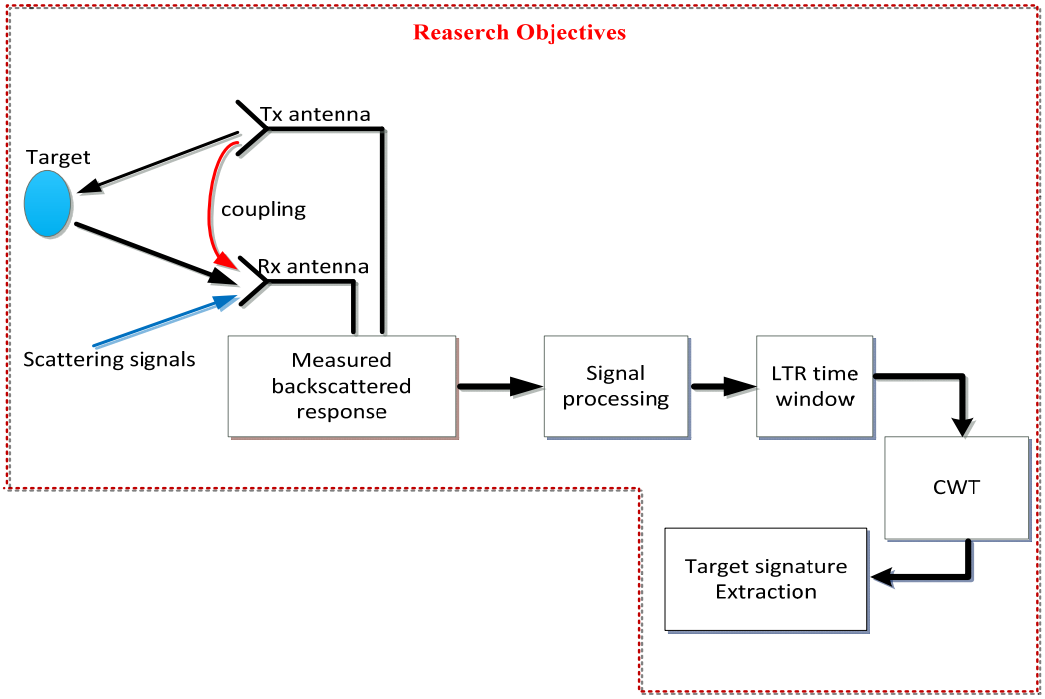

Figure 1-1 Research objectives block diagram

1.4 Methodology

This research aims to develop methods for remote detection of concealed weapons at a given distance and specify the required sensors. To obtain a practical system the following areas will be investigated.

- ✓ Running and analysing a series of computer object modelling simulations by using CST microwave studio transient solver method and MATLAB software.
- ✓ Modelling the response of complex objects such as knives, and handguns at the range of aspects to gain theoretical and simulation knowledge of their LTR and direct response with normal and cross polarization detectors.
- ✓ Modelling of proposed antenna by using CST microwave studio.
- ✓ Develop and build high gain wide-band antenna to permit the standoff detection of these responses.
- ✓ Design signal processing algorithms to extract the LTR. A series of laboratory experiments will be carried out to validate the results.

1.5 Scope of thesis

The thesis contains two parts. The first focuses on antenna requirements for successful detection of concealed weapons based on the backscattered response of the target being detected. The second part focuses on the novel application of the Continuous Wavelet Transform (CWT) to concealed weapon detection. The thesis contains six chapters; an outline of each chapter is given as follows.

Chapter two discusses the current state of the art of concealed weapons detection technology. It describes the behaviour of antennas in the UWB range. It also presents LTR extraction methods available at present and points out some major drawbacks related to these systems for this application.

Most detection systems need antenna to transmit the radar pulse and receive the backscatters from concealed objects. Chapter three focuses exclusively on UWB a Tapered Slot Antenna TSA, its principle of operation, design methodology and characteristics are illustrated and discussed. Some simulated and measured results of the developed antenna performance and far field radiation results are also presented here.

Chapter four addresses the experimental setup to validate the performance of the designed and fabricated antenna in capturing LTR from various simple and complex objects such as wires, knife and handgun.

The captured late time response of the target being detected is subject to new signal algorithms based on the CWT to extract unique signature of the target. This approach is presented in chapter five. Extensive experimental measurements are reported in this chapter, in which response of wires of different dimensions and complex objects such as a knife and a handgun, are analysed using CWT. contribution to knowledge and suggestions for future work are presented in chapter seven.

Chapter 2
Literature Review

2.1 Introduction

There is little doubt that security detection provides a significant deterrent to criminals and terrorists in the fight against crime and recent tragedies have provided new impetus for more intensive research in the use of electromagnetic wave technology for advanced security detection systems, (Agurto et al., 2007). Most current screening of concealed weapons such as knives and handguns take place in access areas to controlled buildings such as the entrances to the shopping centres, government buildings and airports. However the methods currently applied are not always effective in preventing weapons from getting through. (J.Young, 1976; Gordon et al., 2001; Appleby, 2004; Appleby and Anderton, 2007).

Just as the vibration frequency of a tuning fork is controlled by its physical shape, size and material, the same thing applies to complex natural resonances (CNR). With electromagnetic scattering when a hidden object is excited by an incident UWB short pulse, a current on its surface will be induced which will radiate electromagnetic waves. Resonances occur when the frequency of the incident wave coincides with the period of the oscillation of one or more of the CNRs of the induced current.

The induced CNR of a target consists of two parts which are sequential. The first part is the forced response due to the incident electromagnetic wave. This is called Early Time Response (ETR) and this normally addresses the location of the target. The latter part

occurs after the initial electromagnetic pulse and represents the decay of the response. This is called the Late Time Response (LTR) and is related to the target's unique signature. The LTR is aspect independent of the target position and orientation Baum, (1991).

This review of current and previous research into detection of concealed weapons is based on the phenomenon of back scattering. The review begins with a discussion of technology in current use; next the use of CNRs is presented after which there is a short review of the state of the art of antennas, and finally, some of the methods used to extract LTR signature of concealed targets are discussed.

A literature search shows that Heyman and Felsen (1983) were the first to attempt to produce a comprehensive hybrid model including both ETR and LTR. This hybrid model is based on a wave front interpretation using the singularity expansion method (SEM) Leopold B. and Felsen (1984), although it has not yet been applied to target recognition, it has provided useful insight into scattering phenomena which has proved useful for a better understanding such as time-frequency (TF) plots of target response, see Chapter five. Because ETR and LTR are different in nature, it is usual to consider scattering as two distinct procedures: With wave front analysis used for the ETR and SEM for the LTR. Heyman and Felsen (1985) were also the first to study scattering by a convex perfect electric conductor (PEC) target and used a mathematical treatment which included a combination of the Green's function with a hybrid formulation of the time domain transient response named the "Hybrid Wave front Singularity Expansion

Method" (HWSEM) to relate the wave front and the SEM. Because of the lack of clarity and over-complexity of this model, Heyman and Felsen (1983), progressed to a model of the entire scattering phenomena based on consideration of the wave front and flow graph representation. They found it possible for high-Q targets with selected scattering centres to synthesize multiple interactions between the centres which corresponded to partial resonances which could approximately identify subgroup of global resonances under the SEM. These findings help define the origins of resonances in targets, and the flow graph helps to provide physical insights into the resonances in composite environments.

The example of the flat strip has been extensively studied by, amongst others, H. Sharai and Felsen (1986 and Shirai et al (1986). The resonances of the flat strip were obtained using a modified Geometrical Theory of Diffraction (GTD) model and matched with numerical results from the method of moments (MoM). It was found that including low frequency correction terms provided improved accuracy and a better wave front model (Shirai and Felsen, 1986). The results presented in Shirai and Felsen (1986) were not confirmed because at that time there was no rigorous method of synthesizing the multiple diffracted fields over the frequency range of interest. However, when low frequency components dominate the diffracted and scattered fields, the model does provide accurate results for targets. This was studied using a flat strip wave front model proposed by Shirai and Felsen (1986), but using a cosine pulse window so that the frequency response modelled an excitation signal with low frequency cut-off. The results were verified using an exact solution generated by an Eigen function expansion.

A significant part of the work presented in this thesis relates to the study of the target response in the time frequency domain (TFD) based on continuous wavelet transform (CWT). In the TFD, the temporal occurrence of the scattering phenomena can be clearly observed. The HWSEM model provides insight into the physics of scattering phenomena and helps interpretation of the target response in the TFD.

2.2 Complex natural resonant extraction

In the early 2000's Van Blaricum and Mittra (1988) proposed Prony's Method to extract the CNRs and residues from the LTR. This has attracted much attention in the literature because it can be applied to measured target signatures and the resonances can be extracted directly from the target's LTR. Theoretically, all the natural resonances of the target embedded in the LTR can be extracted directly. Unfortunately, Prony's Method is highly sensitive to noise, so improving Prony's method noise immunity became a major objective for SEM research in the last years (VanBlaricum and Mittra, 1978).

Numerous techniques have been used to provide greater accuracy of measured CNRs when the target response is corrupted by noise. Some of these are: Genetic Algorithms (Ilavarasan et al., 1995), Variation Method, (Mittra and Pearson, 1978), Continuation Method (Drachman and Rothwell, 1988), Least Square and Modified Least Square Prony's Method (Marple S. L. 1987), Evolutionary Programming based CLEAN technique (Choi et al., 2003). In addition, target recognition schemes have been developed: K-Pulse technique with genetic algorithm (Turhan-Sayan and Kuzuoglu, 2001) and the E-Pulse technique (Rothwell et al., 1987; Lui et al., 2005).

Another problem with Prony's method is the modal order of the system (number of CNRs modes), Van Blaricum and Mittra (1978). The number of modes seriously affects the algorithm's accuracy. If the number of modes is greater than the number of poles contained in the data, Prony's method will generate extraneous or spurious poles over and above the true poles which results in inaccuracies in the true poles. If the number of modes is less than the number of poles, then poles may be missed and those found may deviate substantially from the true poles. VanBlaricum and Mittra (1978), present proposed solutions to the spurious poles problem which include use of Eigen value and Householder Orthogonalization method. Other researchers have suggested alternative methods of modal order estimation, for example, the Generalized Pencil-of-Function method (GPOF) (Lee and Kim, 2008) and E-Pulse techniques (Gallego et al., 1991). Today, modal order prediction is usually achieved by Singular Value Decomposition (SVD) which predicts the desired number of poles, *M*, and reduces noise in the sample data, Sarkar, T. K. and Perira, O. (1995).

Improving the algorithm is one approach to better accuracy of extracted poles (and residues) however, resonance extraction can also be enhanced by the alternative techniques of using much larger and multiple data sets of responses from the same target (Ksienski, 1985; Li et al. 1998; Shuley and Longstaff, 2004). CNR extraction has been achieved with multiple aspect incidence data obtained by applying the same resonance extraction procedure to a number of responses from one target. These results in multiple sets of poles (and residues) either measured or computed for the various incident aspects

but the literature reports no formal discussion on how to rationalize these multiple sets to produce a unique set of features for a given target that can be used for identification applications. Ilavarasan et al (1995) obtained a single set of resonant frequencies that could be used for target recognition by applying a genetic algorithm to multiple data sets. Sarkar and Pereira (2000) produced a new version of the Matrix-Pencil-Method (MPM) which considers multiple target responses for various aspects and combines these to produce a single set of poles with multiple residues. This method has two important advantages: (i) compared to other methods such as Ksienski (1985), Li et al (1998), Shuley and Longstaff (2004), it is not necessary to choose a set of CNRs from the multiple sets of poles to characterize the radar target, and (ii) when the data is corrupted by noise, a number of spurious poles will also be extracted and when selecting poles from multiple sets, it is very possible that some true poles will be omitted or spurious poles included. There is thus a significant possibility that false information will downgrade the recognition performance. To avoid this problem the true CNRs or at least the resonant frequencies are found beforehand using alternative methods, such as TF or Fourier analysis of target signatures. Sarkar and Pereira (1995) pointed out that in the actual resonance extraction procedure multiple data sets are used for resonance prediction, and thus the accuracy of the CNRs should be better than for a single extraction from one signal.

2.2.1 Matrix Pencil Method (MPM)

Researchers are investigating alternative methods with better resonance extraction performance than Prony's method. One such method is the MPM also known as Generalized Pencil-of-Function method (GPOF) (Hua and Sarkar, 1989). The MPM originated from the Pencil-of-Function method (POF) developed by Jain (1974), Sarkar et al. (1980), Mackay and McCowen (1987), Ross et al. (1988), Jain et al. (1974). The POF was first applied to filter analysis problems in the mid-70s by Jain (1974). Sarkar and Jain then separately applied the POF to system identification and then to applications requiring a damped exponential model. Next Mackay and McCowen developed an improved POF method based on Jain's work, and later Sarkar et al. (1980) introduced the GPOF. The major difference between the MPM and POF is that the MPM is computationally more efficient. The POF has the same bottlenecks found with Prony's method because it also requires finding the roots of a polynomial which needs two distinct steps.

A number of researchers including Hua and Sarkar (1989),Lee and Kim (2008), Gashinova et al. (2008), Harmer et al (2010) and Ye and Jin (2010) extensively studied the GPOF, or the MPM. The performance of the algorithm under noisy conditions has been addressed by Hua and Sarkar (1990). The performance of the GPOF algorithm with different pencil parameters have been studied using perturbation analysis and it was found that the GPOF method approximately reached the Cramer-Rao bound which specifies the "absolute" best result that any technique can achieve in the present "noisy"

environment (Hua and Sarkar, 1990); Baum et al., 1991); Sarkar and Pereira, 1995). Chen and Shuley (2010) have compared the performance of the MPM with the polynomial method of Kumaresan and Tufts (2003) and Tufts and Kumaresan (2005). The results show the MPM is less sensitive to noise and more computationally efficient. Sarkar and Pereira (1995) have compared MPM to Prony's method and found it to be more computationally efficient and to possess better statistical properties for estimation of the CNRs. Different versions of POF can be found in the literature, Hua and Sarkar (1989) and Harmer et al., (2010).

2.3 Review of time-frequency domain analysis

In standard Fourier analysis a stationary time domain signal of infinite extent is decomposed into its individual frequency domain signals but it does not provide information about frequency components that occur simultaneously or change with time. One way to study the behaviour of time-varying frequency content of the signals is with TF signal analysis (Cohen, 1989; Abbas-Azimi et al., 2007; Ceravolo, 2008).

Here either the time domain or the frequency domain signals are converted to the Joint TF domain, and represented into the 2-D time-frequency space. Now the changes in frequency content can be observed visually. Using TF analysis to a moving window is applied to the signal in the time domain with its Fourier transformed results converted to the frequency domain. The resultant distribution is known as the Short-Time Fourier Transform (STFT). Its magnitude is identified as the Spectrogram (SP) which in the 1940s was applied to analysing audio signals. The limitation of the STFT is that due to

the constraint of the uncertainty principle, it is not possible to get accurate time and frequency resolution together i.e. to get the fine resolution in the frequency domain, the resolution in the time domain should be in that order degraded and vice versa. The Wigner-Ville Distribution (WVD) is use to resolve this resolution issue. It is able to provide good TF resolution when compared to other Time-Frequency Distributions (TFDs), although, the price paid is labelled as cross term interference. Cross terms do not offer any physical analysis of the signal and to suppress these cross terms a great amount of work has been carried, (L. Cohen, 1989 and1995; B. Boashash,1992 and 2003).

For example, one technique is to smooth the WVD using specific time and frequency spaces thus ensuing in the Smooth Pseudo Wigner-Ville Distribution (SPWVD or Pseudo Wigner-Ville Distribution (PWVD). The alternatives of the WVD reduce the cross terms using special kernels, (P. Flandrin, 1984). The capability of suppressing the cross term interference is also demonstrated by extending the notion of time-scale from the wavelet transform to TFD's also called affine TFDs. The Time Frequency Distribution Series is a result of a series of functional decompositions of the WVD (Qian and Chen, 1999). The dominant components of the cross term interference are the main self-term of the WVD's. As the signal is smooth in the TF domain, the SPWVD localization will be degraded. Likewise when the cross-term and self-terms do not overlapped the Time Frequency Distribution series is valuable. By using relocation on the TFDs the cross-term destruction can be overcome, (Auger and Flandrin, 2002). The expansion of the frequency components can be easily seen using 2-D frequency space. The TF is obtained

by applied a moving window to the signal in the time domain and then Fourier Transform results to the frequency domain. This transformation is the Short-Time Fourier Transform (STFT) and it produces the spectrum of the time domain signal contained within the window.

Fourier analysis transforms a time domain signal into its individual frequency components but is only suitable for use with stationary signals because of the time resolutions. For the frequency content of time-varying signal more sophisticated methods are necessary such as TF signal analysis,(1999, Boashash, 2003). In TF analysis, the original signal (whether time or frequency domain) is transformed to the TFD, and represented in a two-dimensional time-frequency space where the frequency components are especially easy to observe visually. An early application of TF analysis used a moving window on the signal in the time domain, and used a Fourier transform on the resulting signal to obtain the frequency domain. This is known as the Short-Time Fourier Transform (STFT) and was first applied in the 1940s, (Cohen L, 1989).

However a serious limitation of the STFT is that it cannot provide fine time and frequency resolution simultaneously - due to the constraint imposed by the uncertainty principle (Cohen L, 1989 and Cohen, 1995). That is, fine resolution in the time domain can only be achieved at the expense of poor resolution in the frequency domain. One solution to this matter is to utilize the Wigner-Ville Distribution (WVD) which produces the best resolution of all the TF distributions (TFDs) (Chen, 2002; Cohen, 1995; Boashash, 2003). However, the WVD suffers from "cross-term interference", spurious

features which usually do not provide any physical interpretation of the signal. Extensive and wide work done to suppress the WVD cross terms, for example the Smooth Pseudo Wigner-Ville Distribution (SPWVD) that smooth the WVD using time and frequency windows (Flandrin, 1984). However, with the SPWVD the localization of signals will generally be degraded with smoothing of the signal in the TFD.

Other variants of the WVD use computational techniques to reduce the cross-terms, which have been extended to the so-called affine TFDs which demonstrate the capability of suppressing cross-term interference (Sejdic et al., 2009; Choi and Williams, 1989; Zhao et al., 1990, Oh and Marks,1992). The TFD series is only useful if the cross-terms and self-terms of the WVD do not overlap.

The WVD can be decomposed into a Time Frequency Distribution Series which allows the cross-term interference to be suppressed by considering the dominant components in the series which contain mainly the self-terms of the WVDs (Qian and Chen, 1999; Narasimhan et al., 2008).

Studies have shown that to overcome the shortcomings of the above methods and further improve the performance of TF Distributions, cross term suppression can also be done by reassigning the TF Distributions in two dimensional time-frequency space and using such techniques as Time-scaled Distributions (Auger and Flandrin, 1995; Sejdic et al. , 2009).

Much work on TFDs has been undertaken to determine whether they preserve desirable properties such as: real valued, preserved time and frequency shift, time and frequency margins, instantaneous frequency, group delay, non-negativity, etc. (Cohen, 1995;

Cohen, 2000; Jeong and Williams, 1989; Hlawatsch and Boudreaux-Bartels, 1992; Ceravolo, 2008; Bastiaans, 2009).

This thesis focuses on the application of TFDs to the study of the frequency of the scattering off radar targets and temporal occurrences. The remainder of this section provides a review of various TFDs that could be suitable: in particular, reducing interference using particular kernels and the reassignment method.

TF techniques have been applied in biomedicine, engineering, speech processing, wireless communication, and sonar and radar applications. In the latter, with stationary targets, most work has been carried at frequencies below 2 GHz (Gaunaurd and Strifors, 1996). With UWB radar there has been extensive work on feature extraction, range profiles for stationary targets and TF analysis of backscattered signals (Ling and Kim, 1992; Turhan-Sayan, 2003; Turhan-Sayan, 2005; Ersoy and Turhan-Sayan, 2005; Kim and Ling, 2008). For these applications the frequency of operation lies beyond the fundamental resonant modes in the quasi-optical range, and interest is focused on high frequency scattering phenomena such as what happens at corners and edges. Such phenomena can be described by the geometrical theory of diffraction (GTD) in the electromagnetic context, (Balanis, 1989).

The Wavelet transform is introduced as alterative approach to overcome the STFT resolution limitation, a detailed explanation of the wavelet theory could be found in Moghaddar and Walton (1991), Hwil and Walnut (1989). Particularly, the wavelet transform utilizes the wavelet as a ‘window’ and also as a fundamental for the analysis of

multi resolution, (Kaiser, 1994). To provide good time resolution (small scales) at high frequencies the 'mother' wavelet is compressed so that the wavelet of the time response provide effective resolution in detecting the presence of high frequencies. To have a good frequency resolution at low frequencies the mother wavelet is expanded (large scales), by which the wavelet transform has effective resolution in frequency domain in detecting the appearance of the low frequencies. In fact, in this research the CWT approach is proposed to extract the target signature and represent the LTR in time frequency domain. A Morlet wavelet is used as the mother wavelet within the CWT algorithm because it is simple and well suited for time frequency localization and resolution for concealed weapon application. The CWT provides coefficients in which the degree of correlation is proportional to the peaks or amplitude. Another perspective is that the analysed signal decomposes into a superposition of scaled mother wavelets by the wavelet transform.

The scattered response of the concealed weapons involves a forced (direct) return response from an early time event which aspect target dependent and resonance at the late time event which is aspect independent to the target. In order to extract the target signature that appears in the late time response it is desirable to use good time resolution in the ETR and good frequency resolution in the LTR, a CWT with a 'Morlet' wavelet mother is used for this purposes.

The multi-resolution features of the CWT provide an alternative to TF analysis. Ling amongst others has carried out TF analysis for electromagnetic scattering using the

spectrogram (SP) and CWT (Moore and Ling, 1993; Chen and Ling, 2002; Ozdemir and Ling, 2002; Ling and Kim, 1993; Chen, 2008; Kim and Ling, 2008; Lazaro et al., 2009; Thayaparan et al., 2010; Liu et al., 2010). However, Ling and his co-workers have defined the CWT somewhat differently from that found more generally in the literature and as presented here.

2.4 Overview of standoff concealed weapon detection

There is currently an urgent demand for a system that has the ability to remotely detect firearms concealed on the body in real time. However, such technology is not available yet. Most current technologies are access control (imaging systems) and time consuming (Costianes, 2006; Agurto et al., 2007). Hunt et al., (2001) have suggested using UWB LTR to detect concealed weapons. However, the need for clear explanation of LTR object signatures for object detection and a reliable system approach (include complete model) has not yet been met.

Standoff detection of concealed handguns using the SEM is presented in Rezgui et al. (2008), prior to that it is utilized to identify complex objects such as aircraft by extracting aspect independent information from the LTR. Smaller targets have less conducting area than large targets, so their response will be smaller with less transmitted power. The aspect independent response is utilized to classify the object. Dimensional information about an object can be found from the Fourier transform using a wide frequency sweep which is equivalent to using fast-pulsed signals.

It has been shown that targets can be identified using complex resonances (Novak et al., 2006). The unique fingerprint of the target being detected was identified using a matching filter. This method depends on the response and characteristics of the filter being used and is very sensitive to interference.

The MUSIC algorithm which splits the data into the signal subspace and the noise subspace and incorporates an averaging algorithm called the forward-backward averaging method to extract the signature of an object has been used by Ibrahim et al. (2007). Here a database of signatures of a number of threat objects in the frequency band (26-40 GHz) is used.

It has been shown that a gun can be detected from its radar signature using polarized waves, a technique which the authors claim provides additional information for decision making, (Hausner and West, 2008). Xia et al. (2008) considered the position problem of multiple targets for a MIMO radar system, the non-singular conditions is almost the reason of covariance as it is illustrated. More effective estimation of the object could be obtained with multiple transmitted antennas.

Another way to identify the radar target by using both ETR and LTR was based on TF analysis, the principle component analysis was used to stop redundancy in the feature vector. However, the effect of background and radar antenna response was ignored (Kim et al., 2002). As the antenna response and the background effect are ignored, the proposed method of using the Principle Component Analysis (PCA) does not give an exact target signature for real data as this most affected by these factors.

Chauveau et al. (2007) used the Singularity Expansion Method SEM with narrow frequency bands instead of UWB to collect the target poles using step by step tuning with a minimized frequency band. However, it is possible by using this technique that important information related to the target signature will be lost.

Gashinova et al. (2007) and Harmer et al. (2010) have presented a method to detect onbody concealed weapons using GPOF. The object is illuminated by an UWB short pulse and the LTR of the object collected. It was reported that the basic frequency (dominant frequency) rather than the whole band of backscattered frequencies could be used for the pole extraction algorithms.

A late time evolution programming algorithm has been proposed by Choi et al. (2004) and Choi and Kim (2008). This algorithm is applied to extract the LTR from the backscattered natural frequency of a radar target, in which the phase and amplitude is estimated by evolutionary programing. This method is not sensitive to random noise; however it has not been validated by real data by the authors.

Kim at al. (2002) developed one-dimensional range profiles to classify the type of target using multiple signal classification algorithms. The MUSIC algorithm and central moment features with appropriate pre-processing were used for the target identification. However, accuracy of target identification obtained in this way is very sensitive to the data range resolution.

Jang et al. (2004) have used ETR and LTR to develop an approach that estimates the damped sinusoid parameters and impulse. Fractional Fourier transform (FRFT) with

optimization of parameters was used to extract the pulse-like components from the damped exponentials. MPM was used to estimate the starting point.

Many researchers investigated extraction of LTR in different frequency bands, but with limited success. Cheville et al. (2002) describe a Terahertz impulse ranging system used to extract the LTR of dielectric objects. They used the inverse Fourier transform to determine frequency domain scattering, however many important parameters are not mentioned including the influence of the antenna.

Radar target identification via combined E-pulse and Prony methods have been demonstrated by Younan (2002). First the Singular Value Decomposition (SVD) and Prony method was used with a data processing algorithm to calculate precisely the CNRs of a target. Identification of the target was obtained by convolving that response with the corresponding LTR using the E-pulse.

Choi and Kim (2007) demonstrated how to apply the evolutionary adaptive wavelet transform to feature extraction of a radar target. Evolutionary programming was used instead of the Fast Fourier transform (FFT) to extract the backscattered target signature.

The Wavelet transform as proposed by Arivazhagan and Ganesan (2004) and Mohamed et al. (2009) claims to recognize the radar target automatically. The algorithm presented gave satisfactory results for a number of different radar targets, which make it useful for finding the flaws in any target by its visual characteristics. Time-frequency analysis of the target scattered response using a wavelet transform was presented by Kim and Ling (2008) and Ikuno and Nishimoto (1999). The resonant frequency is accurately extracted

and the simulated results show that wavelet analysis is very effective in electromagnetic target response detection. One method of how to apply the wavelet transform in feature vector representation is given by Le-Tien et al. (1997) and Wei et al. (2010). Here the range profile in absolute value form is transformed to build a data base in which only the extreme points that exceed certain threshold values are stored to form the feature vector. Harmer et al. (2009) have provided onbody and offbody detection of hidden handguns and knives using aspect independent object radiation. The GPOF method was used to obtain target signature poles. Rezgui et al. (2008) have shown that noise clutter in free space and data resolution are severe limitations on this method.

Andrews et al. (2008) used a frequency band (75 - 110 GHz) to detect the presence of explosives concealed onbody. The wavelength here is in order of millimetres and the method is based on measuring backscattering in which the interference between front and back surfaces of the dielectric gives a characteristic frequency variation which can be treated. A super-heterodyne system has been used to detect the range of the object, which enables a signal from a target, such as explosive to be extracted from background clutter. Andrews et al. (2008) have presented a technique of sweeping with millimetre waves to detect concealed objects. Neural networks have been applied to the extracted information, such as optical depth, to detect concealed objects.

Detection of concealed objects using LTR has been described by Vasalos et al. (2010). CNRs are induced in the concealed target by illuminating it with an UWB pulse. The LTR is analysed using a SVD Prony's method and MUSIC algorithm is applied. It was

shown that concealed onbody objects were detected by both methods. However, no details of the illumination pulse were given other than it had a unique frequency response and needed to be deconvoluted out of the returned signal.

2.5 Antenna for concealed weapon detection

Designing a UWB antenna having a non-resonant (flat) gain across all frequencies in the desired band is a key for successfully detecting onbody concealed objects at standoff distance. For an effective detection system with high resolution and dynamic range, the transmitting/receiving UWB antenna should have flat gain, distortionless pulse transmission and reception, and be directive with high-radiation efficiency. A Voltage Standing Wave Ratio (VSWR) around unity is advantageous to enable effective de-convolution of the antenna response from the received scattered signal, which is essential to enable successful extraction of CNR modes to obtain an impulse response from onbody concealed weapon(s), the weapon(s) need to be illuminated in the far field region by a very narrow pulse, equivalent to a UWB frequency sweep.

As the pulse propagates through the concealed objects, omnidirectional reflections and scattering occur at the interfaces, (Harmer et al., 2010). Of most interest are aspect independent resonances and their associated damping which can be measured by a receiving UWB antenna. The amplitude and phase of such backscatter is aspect dependent relative to the linear polarization of the source. The Tapered Slot Antenna (TSA) is a member of the class of aperiodic, continuously scaled, axial mode travelling

wave antenna structures. TSAs, especially the Vivaldi antenna that was first brought out by Gibson in 1979, have been widely used in different radar applications, (Gibson, 2007). The TSA consists of an exponentially tapered flare, and at different frequencies, different parts of the antenna radiate, while the size of the radiating part is constant in wavelength. Theoretically, the TSA has an infinitely wide operating frequency band but in practice this is limited due to certain practical factors such as the feed to slot line transition, finite dimensions of the antenna, etc. (Gazit, 2005). However, the Vivaldi antenna can still provide multi-octave operation and is designated an UWB antenna. These antennas are widely used in microwave imaging, radar systems and wide-band phased array systems, all of which require that the radiation characteristics and phase centre location are known, (Schaubert, 2002).

The main drivers for advances in UWB technology and TSA have been the necessity for increased operating frequency and bandwidth required by military and commercial communication systems, (Mao and Chen, 2006). The very short pulses transmitted by UWB systems ($1x10^{-9}$ second or less) result in effective bandwidths of more than 1 GHz, (Mohammadian et al., 2004). To avoid the fabrication of a large number of metal waveguides which are expensive and heavy, for these applications, there is a growing emphasis on integrated technology, (Yngvesson et al., 1985). The first planar antennas with axial mode radiation were described by Lewis et al. (1974) who presented a strip line fed tapered notch antenna capable of multi-octave bandwidths. Gibson (2007) described an exponential TSA with bandwidth from 8 - 40 GHz. Numerical methods have

been widely used to analyse the performance of these TSAs including radiation characteristics, Janaswamy (2002) and finite difference time domain (FDTD) analysis of the Vivaldi TSA by Thiele and Taflove (2002).

Extensive investigation of TSA have been carried out recently including the development of wideband Vivaldi arrays and interleaving orthogonal single polarized arrays to form dual polarized arrays (Yngvesson et al., 1985; Schaubert and Chio, 2002;). Grazit (2005) introduced the antipodal Vivaldi antenna to overcome the band limiting effect of feed line to slot line transition. Langley et al., (2008) took this idea further to overcome the very high cross-polarization exhibited by the new antenna by developing the balanced antipodal Vivaldi.

Previously, Bowen (1995) showed that for the Vivaldi antenna the H-plane phase centre was situated near the antenna feed and the E-plane phase centre was situated near the wider end of the slot, but as the frequency increased tended to move closer to the feed. Jin et al., (2007) developed an approach to find the 3-D phase centre and Elsherbini et al. (2007) devised a method whereby a dielectric rod could be inserted into a Vivaldi antenna to minimize phase centre variation.

In the past four years many TSAs with improved antenna parameters involving dual exponential TSAs have been developed and optimized for UWB applications and millimetre-wave detection systems: linear TSA, antipodal exponential TSA and dual V-type (Xianming et al., 2008). However, in the frequency range 0.25-3 GHz, none of the improved TSAs has a non-resonant flat gain. Around 10 dB gain is required for

successful standoff detection of concealed weapons based on LTRs, covering all the basic frequencies of objects of common interest.

Abbas-Azimi et al., (2007) have shown that ridged horn antenna shows high antenna gain with UWB, but it does not meet the non-resonant demands needed to cover the fundamental CNR of the target(s) being detected.

TSA arrays (Yang et al., 2008) can usually achieve 10 dB or higher antenna gain covering the frequency range of interest. However, compared with the single TSA element, an antenna array is heavier, larger and more complicated to design and build due to the extra networks required. Most compact UWB antennas presented in the literature exhibit omnidirectional radiation patterns with comparatively low gain and an impulse response with observable distortion (Chen and Chew, 2003). These types of UWB antennas are convenient for short-range indoor and outdoor communication applications.

The bandwidth must be sufficiently wide to cover all of the basic frequencies of the most common firearms and one objective of this thesis is to design and optimize a compact UWB antenna exponentially tapered slot with a bandwidth of the operating frequency 0.25 to 3 GHz. Antenna with these characteristics are not yet available on the commercial market. This operating bandwidth was chosen to cover the fundamental CNR modes of most firearms and to give fine enough time resolution to resolve these modes and to minimize clutter from the human subjects and other objects in the surveillance area. Having a less than desirable antenna response, may lead detection system to have spurious resonances which could mask concealed onbody objects.

2.6 Electromagnetic scattering theory

The CNR radiated from a hidden body subjected to a UWB pulse of radiation, is related to the geometry (overall size and shape) of the object and has a unique signature which found mostly in the LTR. As mentioned earlier, CNR consists of early time response and late time response. However, feature extraction based on the use of natural responses should avoid using the ETR of the scattered field as its represent the target location and does not provide any information for target identification Baum (1991).

CNR frequencies of the target are both waveform and aspect dependent (Equation 2.1) and can be extracted from the target LTR. However to estimate when the LTR commences some target parameters are needed. These might be a dimension of the target, width of the incident pulse and the distance between detector and target, (Balanis, 1989). There are two steps when applying resonance related target detection: the first is to obtain the impulse response from the object being identified and the second is to apply FFT analysis to the time domain of the data sets to obtain the frequency domain impulse response.

The CNR behaviour in linear time invariant system models was formulated as the SEM by Baum (1976) who described the first mathematical model to represent the LTR using the independent resonance frequencies of the target which described as:

$$y(t) = \sum_{t=1}^{M} A_m \cos(\omega_m t + \varphi_m) \exp(-\alpha_m t), \qquad t > T_L \tag{2.1}$$

Where T_L describes the start of the LTR, and M modes are required to describe the time signal. The natural modes consist of amplitude A_m and phase (φ_m), and the CNR ($\omega_m t + \varphi_m$).

The start of the late time period could be estimated using

$$T_L = T_b + 2T_{tr} + T_p \tag{2.2}$$

Where:

T_b, is the travelling time of the incident wave from source to the leading edge of the target.

$2T_{tr}$, is the time trip from the antenna to the target and time travel from the target to the receiver.

T_{tr}, is the one way transient time along the line of sight (antenna to target).

T_p , is the width of the interrogating pulse.

The form of the LTR is dependent upon the time form of the illuminating pulse, since $y(t)$ in equation 2.1 is the impulse response of the target, the LTR can be expected to have the time form.

$$R(t) = X(t) \otimes y(t) \tag{2.3}$$

This represents a convolution process, from which the LTR has the form:

$$R(\omega) = X(\omega)y(\omega) \tag{2.4}$$

Illuminating the target by an UWB short pulse excites a sufficient number of resonances *(M)* of the unlimited set of CNRs with sufficient time resolution in time domain data.

Since LTRs are aspect independent it should be possible to extract the same LTRs of the target from any incident angle related to target corresponding impulse response, (Sarkar et al.,1989; Gashinova et al., 2006)

The problem of detecting and identifying a concealed handgun from its scattered electromagnetic field is very complicated, because the scattered signal is very complex even for objects with simple geometry. Also the scattered signals are strongly dependent on signal polarization and aspect angle of incident and reflection. An extraction feature which is sensitive to aspect variations is needed to accurately detect and characterize the concealed target.

For discrimination of the concealed objects based on the natural resonance frequencies accurate extraction at these frequencies from a measured transient response is very important (Harmer et al., 2010).

2.7 Singularity Expansion Method (SEM)

The linear circuits and system features can be characterized by the impulse response as dictated by the electrical circuit theory and the linear time invariant model. The impulse response of linear circuits in general can be calculated using the singularity values from the re-radiation function in the frequency domain and the relevant values of inductance, resistance and capacitance of the circuit (Oppenheim et al., 1997; Nilsson and Riedel,

2008). Summing up all the harmonics and their product with exponentially damped sinusoids gives the desired impulse response.

The concept of impulse response was further elaborated in 1960s, by Kennaugh and Moffatt (1965) and was used to study the transient re-radiation from radar targets. Using the results, the SEM was described by Baum (1971) who explained the transient electromagnetic scattering theory. SEM is based on the assumption that for a LTR the scattering of electromagnetic waves is linear and time-invariant, meaning it is independent of time. Linear means that the superposition principle holds true in this case. The SEM also assumes that by using the output of a linear, time-invariant system with a sum of damped exponentials, the transient or quick scattering of waves can be simulated. It is also possible the radar target scatters the radiation nonlinearly but such situations are uncommon. Actually, the SEM was presented initially to explain the induced current on the surface of PEC targets in free space as a summation series of damped exponentials and an entire function in complex frequency Baum (1971). Subsequently, simulation of charge density and the scattering of energy from radar targets were also explained using SEM by Baum et al. (1991).

The concept of the scattering of electromagnetic radiation will be discussed here as a linear time invariant (LTI[1]) system, $x(t)$ and $y(t)$ will be taken as the input and output

[1] *The LTI assumption and the damped exponential model were proposed by Baum in the 1970s and it ~ applies for the late-time period. The impulse-like components in the early-time period corresponding specular reflections from the targets and the early-time response is considered to be time-varying in general. In light of the SEM, the target response in terms of the transfer function H(s) in the frequency domain is given by (Baum, 1971).*

function respectively, in the time domain with equivalent $X(s)$ and $Y(s)$ in the frequency domain. The incident magnetic current or electric field will be taken as the input of the radiation problem and the output will either be the induced current or the scattered (diverging) field. Then $h(t)$ (impulse response) will be the response of the target in this LTI system in the time domain or the corresponding transfer function H(s) in the frequency domain (Oppenheim et al., 1997).

$$\vec{H}(\vec{r},s) = \sum_{m=1}^{m} \tilde{\eta}_m(s,\vec{p})\,\vec{M}_m(\vec{r})(s-s_m)^{-n_m} + \vec{W}(\vec{r},s,\vec{p}) \qquad (2.5)$$

Where,

$\tilde{\eta}_m(s,\vec{p})$ is the coupling coefficient, ˜ denotes the two sided Laplace transform $\vec{M}_m(\vec{r})$, is natural mode, $s_m = \sigma_m \pm j\omega_m$ is the complex natural frequency CNR, σ_m and ω_m are resonance frequency and damping coefficients , m_m is multiplicity of the i^{th} pole and $\vec{W}(\vec{r},s,\vec{p})$ is the complete function.

The position vectors $\vec{r}$, $\vec{p}$ represent the target at which the transient response is measured and the polarization of the incident plane wave respectively (Baum, 1971;Taylor, 1995).

$\vec{M}_m(\vec{r})$ is the reaction of the system at s_m . It depends only on the position $\vec{r}$, on the structure of the object and parameters , $\tilde{\eta}_m(s,\vec{p})$ which is the coupling coefficient is the strength of the CNRs in terms of the target and incident wave characteristics such as the incident aspect angle and polarization angle, etc. and is unaffected by the target location.

Coupling coefficients can be categorized as class 1 and class 2. A class 1 coupling coefficient has a fixed value for each component,

$$\tilde{\eta}_m(s,\vec{p}) = \tilde{\eta}_m(s,\vec{p})|_{s=s_m} \tag{2.6}$$

This is known as class 1 coupling coefficient. If it is dependent on frequency, it is called class 2 coupling coefficient.

Class 1 coupling coefficient is of much more importance and the focus of most research and work over the years. It is because of its ability to model the late-time transient responses. Since the CNR is mainly dependent on the target geometry allows it to be a good tool for identifying and classifying radar targets by using one of extraction methods such as Prony's or E-pulse Baum (1991).

Richards (1994) has proposed that class 2 coupling coefficients be used for early time response modelling as opposed to late-time responses with class 1 coefficients.. It was a modification of the damped exponential model that used class 1 coupling coefficient but was much limited in terms of the information it provided. This was because the local aspect dependent scattering process of early time cannot be described on the resonance phenomena (Dudley and Morgan, 1985; Richards, 1994).

Applying inverse Laplace Transform to equation (2.6) and with class 1 coupling coefficient for late-time, the target response in time domain can be given by

$$\vec{h}(\vec{r},t) = \sum_{m=1}^{\infty} \tilde{\eta}_m(t,\vec{p})\, M_m(\vec{r}) e^{-s_m t} + \overrightarrow{W}(\vec{r},t) \tag{2.7}$$

By assigning values in the above equation, we get

$$\sum_{m=1}^{m} \tilde{\eta}_m(t, \vec{p})\, M_m(\vec{r}) = A_m(\vec{r}) = A_i \tag{2.8}$$

The LTR can be expressed as the sum of damped exponentials with constant residues by first removing the complete ETR function. It can be written as

$$r(t) = \sum_{m=1}^{M} \left[A_m e^{s_{m(t)}} + A_m^* e^{\dot{s}_{m(t)}}\right] = \sum_{m=1}^{M} a_m\, e^{-\sigma_m t} cos(\omega_m t + \emptyset_m), \tag{2.9}$$

$$t > T_L, \qquad A_m = a_m e^{j\emptyset_m} \tag{2.10}$$

Where M is the number of natural modes, T_m is the time at which late-time period begins, a_m and $\emptyset_m$ are the aspect dependent residues and phase of the m^{th} mode respectively, * denotes the complex conjugate.

Theoretically, there is infinite number of CNRs modes and the summation in equation (2.9) would give the result infinity. However the model order is replace the modal order by a finite number M in equation (2.10) because in reality, signals have a restricted frequency band and only a certain number of resonance modes can be excited, the CNRs or poles, are given by $s_m = \sigma_m \pm j\omega_m$ as explained before. Target response is given by $r(t)$ and it shouldn't not be confused with $\vec{r}$, which is a position vector indicating target position. The complete target response encompassing both early and late time responses is given by Morgan (1984).

$$r(\vec{r},t) = u(t-t_l)\sum_{m=1}^{m}\left[A_m e^{s_m t} + A_m^* e^{s_m^* t}\right] + \overrightarrow{W}(\vec{r},t)[u(t) - u(t-t_l)] \qquad (2.11)$$

$t_l = T_L$ which is the start of the late time response and u.is a unit step.

2.8 Matrix Pencil Method (MPM)

To achieve a better resonance extraction performance than the one obtained with Prony's method, researchers have been looking for an alternate method. According to Hua and Sarkar (1989) the MPM suggested by Jain, V. (1974) that originated from the pencil-of-function method turned out to be a good substitute Hua and Sarkar (1990). It is also known as Generalized Pencil of function (GPOF) (Ross, et al.,1988; Sarkar et al., 1989; Sarker and Pereira. 1995).

The Pencil-of-Function method has been used for various purposes. In mid 1970s, the POF was used to filter analysis based problems (Jain, 1974), and subsequently for system identification (Sarkar et al., 1989) and for applications requiring a damped exponential model (Jain et al., 2003). In particular, the GPOF method has been found to almost reach the Cramer-Rao bound which specifies the "absolute" best results that any method or technique can achieve in the noisy environment, when the performance of this algorithm with a range of different pencil parameters was checked using perturbation analysis (Hua and Sarkar, 1991).

Linear prediction (LP) and SVD, is one of the various versions available of the Pencil-of-Function method that can be found in the literature. It is useful because SVD helps in noise elimination from the test data and predict the value of mode order M i.e., the

number of poles required (Kumaresan and Tufts; 1982). The LTR, using equation (2.8) is given by:

$$y(t) = r(t) + n(t) = \sum_{m=1}^{M} A_m \, e^{s_m t} + n(t) \tag{2.12}$$

Where

$y(t)$ is the observed time response in Nano seconds

$n(t)$ is the system noise in Volts/Hz

$r(t)$ is LTR scattered from the target Also, $A_m = a_m e^{j\emptyset_m}$ and $s_m = \sigma_m \pm j\omega_m$, M is model order, a_m are the amplitude of complex exponential and $\emptyset_m$ are sinusoidal initial phase in radians, σ_m is damping factors and ω_m is natural resonant frequencies in rad/s.

The sampled version of equation (2.12) can be written as

$$y(kT_s) = x(kT_s) + n(kT_s) = \sum_{m=1}^{M} A_m \, z_m^k + n(kT_s) \,, \quad for\ k = 0,1,2\,..N-1 \tag{2.13}$$

Where

$$z_m = e^{s_m T_s}$$

N is number of samples in discrete time domain and T_s is sampling interval.

The following matrix is considered first

$$[Y] = \begin{bmatrix} y(0) & y(1) & \ldots. & y(L) \\ y(1) & y(2) & \ldots. & y(L+1) \\ \vdots & \vdots & & \vdots \\ y(N-L-1) & y(N-L) & \ldots. & y(N-1) \end{bmatrix} \quad (2.14)$$

Where, L represents the pencil parameter (Sarkar and Pereira, 1995; Hua and Sarkar, 1990). Noise in the MPM can be significantly reduced using the pencil parameter L. The value of L is chosen to be $N/2$ so that there is minimum inconsistency in parameters z_m due to noise. This value was chosen after a perturbation analysis was done on the performance of MPM by Hua and Sarkar (1989). The value of L can also be chosen between $N/3 \leq L < N/2$. This was suggested after further analysis in Hua and Sarkar (1990, 1995) when SVD applied to Y

$$[Y] = [U][\sum][V]^T \quad (2.15)$$

Where

$[U]$ and $[V]$ is unitary matrices, $[U]$ is composed of the eigenvectors of $[Y][Y]^H$, $[V]$ is composed of eigenvectors $[Y]^H[Y]$ and $[\sum]$ (diagonal) contains singular values of $[Y]$, i.e.

$$[U]^H[Y][V] = [\sum] \quad (2.16)$$

H, denotes the conjugate transpose.

Singular values $\sigma\ s$ are compared to find the model order M. A singular value σ_c is such that

$$\sigma_c/\sigma_{max} \approx 10^{-p} \quad (2.17)$$

Where

p = number of significant decimal digits in the data.

Noise singular values for which the ratio in the equation is below 10^{-3} should not be included in data reconstruction and this is applicable only if the data accuracy is up to three significant digits.

Generally in reconstruction of the first M singular values with $\sigma \geq 10^{-p}\sigma_{max}$ are considered and smaller singular values indicated by $M + 1\ to\ L$ are neglected, (Sarkar and Pereira, 2002) .

Only M dominant left singular vectors of $[V]$ are included in the 'filtered' matrix $[V]$ which is written as

$$[V'] = [v_1 v_2 \dots \dots \dots v_M] \quad (2.18)$$

Construction of matrices $[Y_1]$ and $[Y_2]$ is then done according to the following

$$[Y_1] = [U][\sum'][V_1]^T \quad (2.19)$$

$$[Y_2] = [U][\sum'][V_2]^T \quad (2.20)$$

Where

$[V_1']$ =$[V']$ with the last row of $[V']$ deleted

$[V_2']$ =$[V']$ with first row of $[V']$ omitted

$[\sum']$ is based on M dominant singular values, obtained from the M columns of $[\sum]$

By solving the following Eigen value problem, CNRs can then be established as,

$$\{[Y_1]^+ [Y_2] - \lambda[I]\} = 0 \tag{2.21}$$

where

$$\lambda_m = Z_m = e^{s_m T_s}$$

and

$$s_i = \frac{ln(z_m)}{T_s}$$

$[Y_1]^+$ is the Moor-Penrose pseudo inverse of $[Y_1]$ defined by Golub and Van Loan (1996) as

$$[Y_1]^+ = \{[Y_1]^H [Y_1]\}^{-1} [Y_1]^H \tag{2.22}$$

By solving the following system of matrices the residues can be found,

$$\begin{bmatrix} y(0) \\ y(1) \\ \cdot \\ \cdot \\ y(N-1) \end{bmatrix} = \begin{bmatrix} 1 & 1 & . & . & 1 \\ z_1 & z_2 & \cdot & \cdot & z_{2M} \\ \cdot & \cdot & . & . & \cdot \\ \cdot & \cdot & . & . & \cdot \\ z_1^{N-1} & z_2^{N-2} & . & . & z_{2M}^{N-2} \end{bmatrix} \begin{bmatrix} A_1 \\ A_2 \\ \cdot \\ \cdot \\ A_{2M} \end{bmatrix} \tag{2.23}$$

This explanation comprehensively covers the Generalized Pencil of Function method. In chapter 5 comparison between the GPOF and CWT methods will be made and resonance based target identification scheme will also be discussed.

2.9 Background subtraction

In order to obtain only the backscattered frequency domain data of the object being detected, the frequency domain response when the target not present is subtracted from the background frequency domain response obtained when the target is present. This cancels out most of the effects of the surroundings. Further treatment to correct the lack of non-uniformity in the response of the transmitting and receiving antenna is achieved by dividing the obtained response by the magnitude of the antenna response at the given frequency (Foo and Defence, 2004).

2.10 Antenna deconvolution

Transmitting and receiving antenna response need to be deconvolved from $h(t)$ to identify the target response from the antenna errors. For this purpose the cross-polarized transmitting and receiving antenna are placed facing each other at 1.0 m distance, and the antenna transient response S_{21} is captured with the help of vector network analyser VNA 3863B. Deconvolution was applied to the frequency domain backscattered data $S(t)$ with

the antenna response $E(t)$ in Equation (4.1), this should be non-zero to be effective (Muqaibel et al., 2002; Tseng and Sarkar, 1987).

Numerical instabilities will be induced in direct inversion of the convolution operator which is related to the noise present in the backscattered data. The conjugate gradient method is an iterative technique. In each iteration seeks the solution in the direction of the Eigen vector corresponding to the largest of the remaining Eigen values. To determine the appropriate stopping criterion of the iterative method the process can be terminated before the solution gets contaminated by the eigenvectors corresponding to the noise Eigen values. The conjugate gradient method has been previously applied successfully to the solution of various ill-posed problems, more details could be found in (Sarkar et al., 1988; Rothwell and Sun,1990 ; Rahman and Sarkar,1995).

Consider a concealed target excited by a causal time domain input signal $E\ (t)$, in which the recorded output is y (t). In the case of discrete convolution, they are related by,

$$y[n] = \sum_{k=0}^{k} a[k]\, E[n-k] = a[n] \otimes x[n] \tag{2.24}$$

From the given equation the deconvolution nature could be represented in form of matrix operator as $y = AE$ where A is the revolved Toeplitz matrix created from the system function $a[k]$ as follows:

$$A=\begin{bmatrix} a[K] & a[K-1] & . & . & a[3] & a[2] & a[1] \\ a[K-1] & a[K-2] & . & . & a[2] & a[1] & 0 \\ a[K-2] & a[K-3] & . & . & a[1] & 0 & 0 \\ . & . & . & . & . & . & . \\ . & . & . & . & . & . & . \\ a[2] & a[1] & . & . & 0 & 0 & 0 \\ a[1] & 0 & . & . & 0 & 0 & 0 \end{bmatrix} \tag{2.25}$$

where K is the used waveform sample number. Suppose system function and output is already known by which the input signal could be determined and the problem will be simplified to the inverse problem by determining $E = A^{-1}y$. The principle viewpoint of the conjugate gradient method is that to minimize the function, $F(x) = (AE - y)$ by searching cross a set of direction vectors p_k instead of workout the inverse problem directly. An initial estimation for $E = E_0$ is selected and the primary error remaining $r_0 = y - AE_0$ is produced. The early examination direction vector is given by $p_0 = A^H r_0$ where the subscript $(^H)$ denotes the complex conjugate transpose. The approximation updates are found by the following:

$$t = -\frac{\|A^H r_k\|^2}{\|Sp_k\|^2} \tag{2.26}$$

$$E_{k+1} = E_k + tp_k \tag{2.27}$$

$$E_{k+1} = y - AE_k = r_k - tAp_k \tag{2.28}$$

$$b = \frac{\|A^H|r_{k+1}|\|^2}{\|A^H r_k\|^2} \tag{2.29}$$

$$p_{k+1} = A^H r_{k+1} - bp_k \tag{2.30}$$

The repetition paused when the error excess $\|r_k\|$ falls below a predetermined value, however, in no case will it needs more repetitions than the dimension of *A* in the lack of round-off errors. Details of the procedure can be found in Sarkar et al., (1988), Rothwell and Sun (1990), and Rahman and Sarkar (1995). In Equation (2.24) it is shown that the output response seen at the recipient is formed by the convolution of the transmitter, the receiver, input characteristics and the target. There for utilizing the conjugate slope method $s = A^{-1}E$ is obtained by de-convolution where *A* is the system characteristics represented by $E(t) \otimes h(t)$, *s* is the output given by $s(t)$, and h is the target scattering response given by $E \otimes h$. Thus the target response $h(t)$ for an input of *E* is given by de-convolution of $E(t) \otimes Y(t)$.

2.11 Summary

Different aspects of resonance based radar target identification have been discussed in this chapter. Literature pertaining to SEM, which is the foundation of resonance based-target recognition has been provided along with information about resonance of targets in free space, ETR/LTR, electromagnetic scattering and its transient nature. Modern techniques for detection of concealed weapons at a standoff distance, such as resonance extraction procedures have been discussed to address problems encountered in application of target recognition schemes. In a nutshell, everything has been discussed including the antennae needed for the application of concealed weapons detection.

It is found that most of studies concentrated on the application of available technology in radar systems, landmine detection, cancer detection and imaging security systems. Several of the researchers focused in how to detect concealed objects at standoff distance by the use of one of the available filtering methods such as E-pulse or GPOF. However detection of onbody concealed objects by the use of continues wavelet transform is not widely reported. One of the objectives of this thesis is the use of continues wavelet transform for concealed weapons detection by extract and represent the LTR of the target in the time-frequency domain to overcome the disadvantages of the available filtering methods such as prony's, GPOF and E-pulse. In addition, it was found that most of the developed antennas suffering from LTR ringing and pulse distortion which makes them not suitable for the applications of concealed weapons detection at standoff distance in which antenna gain and antenna ringing have significant impact. The other objective of

this thesis was to study, develop and design antenna with distortionless and flat gain as much as possible to minimize the LTR ringing. These factors are the key role to overcome the mask of the LTR related to onbody concealed objects.

Different Tapered slot antenna parameters of the proposed antenna will be discussed and presented in the next chapter. Simulation and measurement results will be discussed as well. Time - frequency analysis will be discussed by use of the CWT for TF analysis in chapter 5.

Chapter 3

Tapered Slot Antenna Characteristics and Design

3.1 Introduction

This Chapter will focus on the first core element of this thesis in which different design regimes of the antenna parameters are considered and discussed. Results of the simulated and purpose built antenna module are presented.

A tapered slot antenna (TSA) was developed and optimized for operation between 0.25 and 3 GHz with a flat gain over the bandwidth. The TSA was chosen due to its simplicity and successful application in many types of radar systems. The TSA presented here will be used for concealed onbody object detection. The detection system includes identical TSA antennas, one used to transmit a sharp UWB pulse or frequency sweep while the other receives the back scattered signal. The design methodology is based on decreasing the reflection in every part of the antenna. The chosen antenna is a Strip Line Fed Vivaldi antenna because much research has been conducted on its development and optimization, (Robert, 2000). Furthermore, designs, plans and blueprints of TSAs are mainly based upon empirical studies such as the relation between the parameters of the antenna components and its performance which is not well understood (Gazit, 2005). It has been observed in many studies that the TSAs perform very well when the antennas dimensions cover almost a wavelength distance and the size of aperture is more than half of the wavelength, (Shin and Schaubert, 2002). Details of the principle of operation and the effect of different antenna parameters can be found in Milligan and Wiley (1985),

Janaswamy and Schaubert (1987), Shuppert (1988), Schaubert (1989), Lee (1991), Lee and Chen (1997), and Garg (2001).

3.2 Design objectives and specifications

Developing an UWB antenna that has a non-resonant identifiable gain that can be observed and distinguished throughout different frequencies in the required frequency range is critical in detecting onbody concealed objects such as knives and guns, (Mehdipour et al., 2007). In fact, to attain an impulse response for onbody concealed objects (weapons in this case) the objects need to be illuminated in the Far-field region by a very narrow pulse which is equivalent to a UWB frequency sweep. As the pulse propagates through the concealed objects, Omni-directional reflections and scattering occur at the interfaces (Pozar and Schaubert, 1995).

The aspect free resonances and their associated damping are of particular significance. These can be detected and measured using an UWB antenna. The phase and amplitude of this kind of backscatter is aspect reliant comparative to the linear polarisation. In order to have an efficient detection system with high quality and standardized resolution, the UWB antenna must be able to produce flat gain to cover the full frequency bandwidth with pulse transmission which is distortion free and should be directive in terms of high-radiation efficiency.

A voltage standing wave ratio (VSWR) around unity and a flat gain directional antenna is particularly advantageous for radar systems required to detect concealed weapons on the human body under clothing or hidden in bags or placed in some sort of covering. A

VSWR of around unity is required for efficient deconvolution of the response of the antenna signal which has been received from a scattered response as this enables the system to efficiently and exactly extract the CNR modes. If the antenna response does not meet these requirements, it may lead to an ambiguous resonance being detected by the system as any of the antenna resonances could hide or supersede the backscattered response of the concealed weapons or other threat objects. The bandwidth should be sufficiently broad to encompass all of the fundamental frequencies of the CNR frequencies scattered from the majority of common firearms. Because an antenna with these specifications is not currently available in the commercial market, a compact UWB exponentially tapered slot antenna having an operating frequency of 0.25 to 3 GHz will be developed here. This bandwidth is selected to cover the fundamental modes of CNR modes, to decrease the clutter from live subjects such as humans and other objects in the vicinity and to provide sufficient time resolution to resolve these CNR (Thiele and Taflove, 2002).

3.2.1 Vivaldi antenna configuration

Figure 3-1 illustrates the antenna configuration. The parameters shown are determined using the given values for the thickness of substrate board, dielectric constant, frequency band and antenna dimension which is a function of operating frequency band.

In the given work plan the antenna is supposed to be made up of a radial stub and a circular cavity. In some studies the method of moments (MoM) was used for the calculation of different antenna parameters but in this case, the closed form equations

have been used, (K. Gupta et al., 2007). The design plan and the calculations are presented in the following sections.

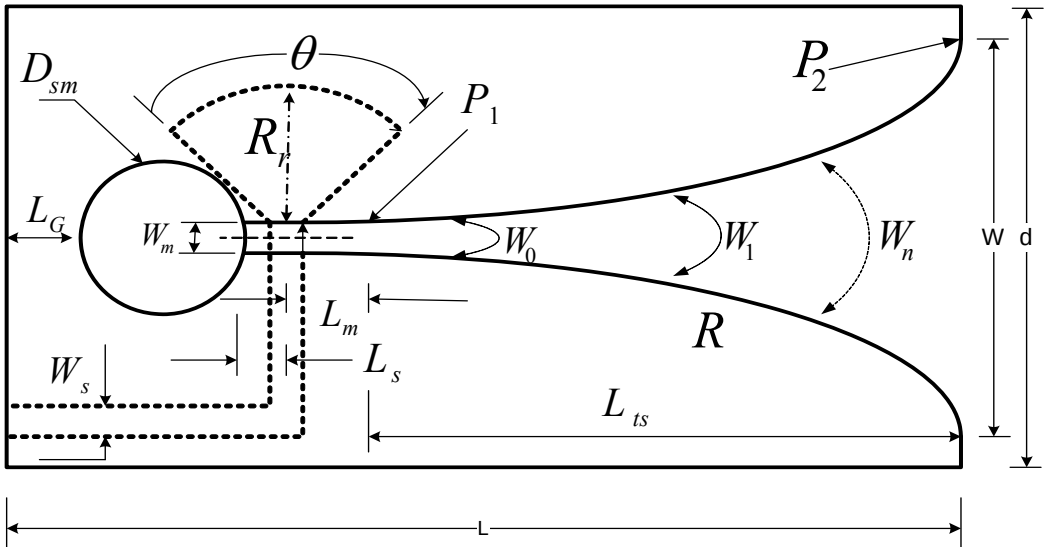

Figure 3-1 Tapered slot antenna parameters

3.3 Design methodology

For an efficient parametric design the methodology is of crucial importance. The flowchart given in figure 3-2 and guidelines provide an easy and efficient approach to the problem, (Gupta et al., 2007).

The antenna components should be aligned and combined in a certain critical order which is not dependent on the full final design. Design should be based on the importance and critical nature of components, complicated activities should be separated from simpler ones to avoid clutter. Critical components should be finalized first e.g. the transition must

be included in the design at the end. In order to achieve this, the different design steps were arranged as shown in Figure 3-2.

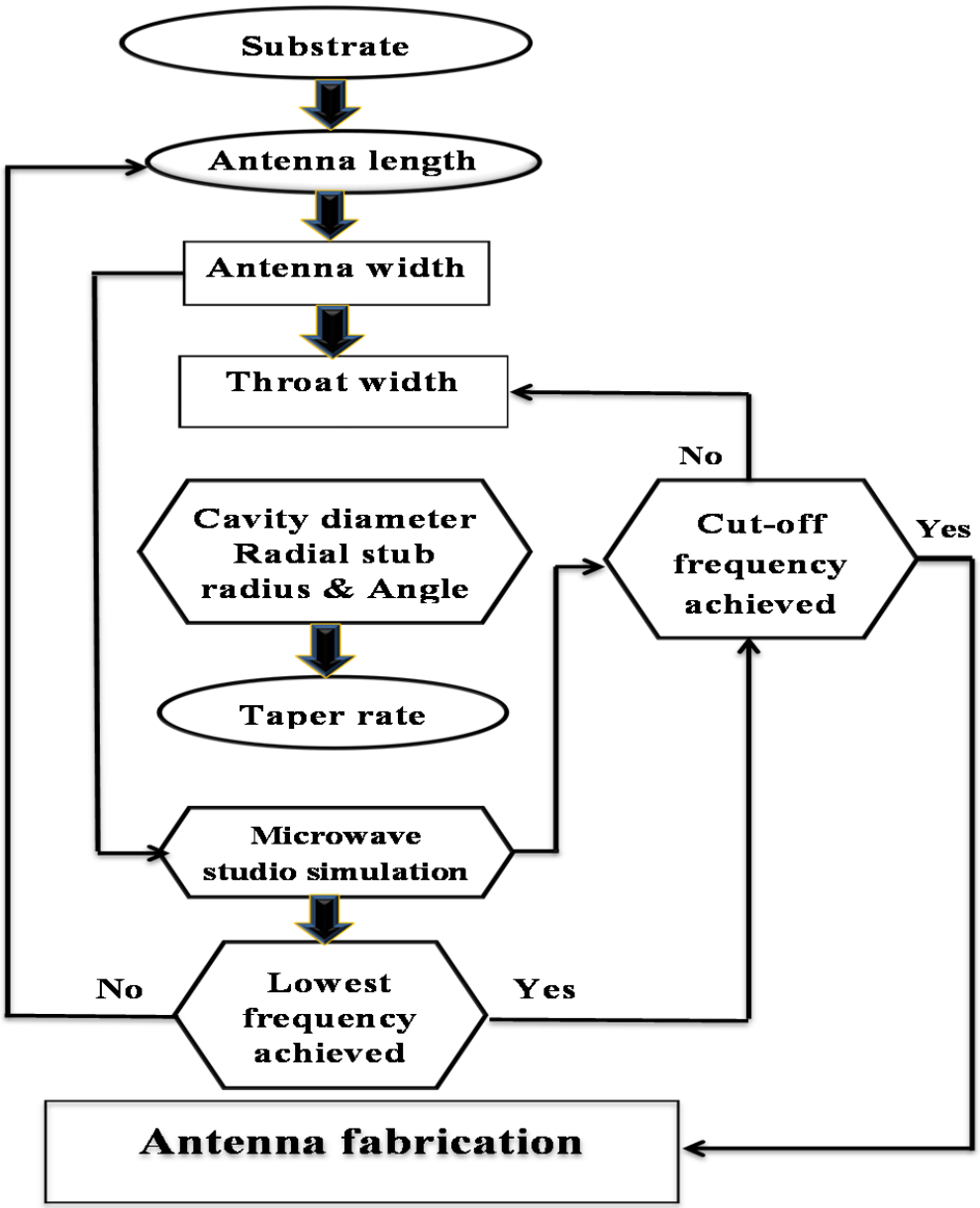

Figure 3-2 Design methodology flowchart

3.4 Substrate dimensions

As the first step in the design and plan process the parameters selected were thickness and the dielectric constant of the substrate to be used in the construction of the antenna. The optimum value for substrate board length should be more than the wavelength in free space of the lowest frequency of the radiation travelling mode (Sutinjo and Tung, 2004) and width should be larger than one half of this wavelength (Gupta et al., 1996) which means that.

$$L > \lambda \tag{3.1}$$

$$W > \lambda/2 \tag{3.2}$$

Where,

λ = free space wavelength at the lowest possible frequency of interest.

W = width of antenna

The selection of the dielectric substrate plays a major part in the development and simulation of transmission lines and the antennas. Some important parameters of the substrate are:

- Dielectric constant.
- The copper surface thickness.
- Coefficient of thermal Expansion.
- Dielectric conductivity.
- Cost effectiveness.
- Ease of construction or development.

A good number of substrates are available which can be utilized in the antenna design. Their characteristics vary significantly. A relative dielectric constant of $\varepsilon_r \sim 2.2$ gives good efficiency and a relatively wider bandwidth, substrates with relatively greater dielectric constants lead to smaller antenna dimensions and performance of such antenna will have very poor efficiency and bandwidth. This is tricky situation where design and performance cannot feature in the same model (Gazit, 1988).

Two main types of losses occur in the micro strip transmission line, dielectric losses and conductor losses. These losses are frequency dependent; the conductor losses are more significant at lower frequencies while at higher frequency the dielectric losses are prominent. The dielectric loss is due to the fact that the dielectric contains polarized molecules which show movement in electromagnetic fields. The heat energy dissipated is directly related to the speed of oscillation of these polar molecules, and at the high frequencies used is very rapid and as a result they heat up the dielectric. The heat energy generated due to the signal increases with frequency and is directly proportional to the frequency of the signal, the dielectric consequently loses functionality and shows erratic readings (Guillanton et al. 1998).

To keep the dielectric losses low at the given operating frequency FR4, a substrate material with low relative dielectric constant ($\varepsilon_r = 2.33$) and constant low loss tangent (0.025), was selected for the proposed design. The thickness chosen was 0.125 cm. The main properties of the material are given in table 3-1

Table 3-1 Substrate properties (FR 4 board)

Characteristic	Value
Dielectric thickness (h)	0.125 cm
Conductor thickness (t)	1 oz/ft^2 = 0.035 cm (0.305 kg of copper per m^2)
Coefficient of thermal expansion ($^oC^{-1}$)	-125x10^{-6} /°C (This material shrinks as it gets hotter)
Thermal conductivity (k)	0.30 W/m · K
Relative dielectric constant, ε_r	2.33

3.5 Micro-strip design

Figure 3-3 shows the parameters of the microstrip line to slot line transition:

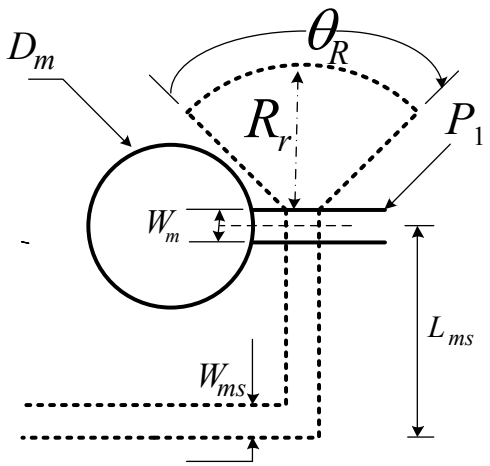

Figure 3-3 Parameters of the micro strip line to slot line transition

W_{ms} is the microstrip line width, W_m is the slot line width, R_r is radial stub radius, θ_r is the radial stub angle, D_{sm} is cavity diameter and L_{ms} is the length of microstripe line. Determination of W_{ms} requires slot-line impedance at the transition point, where slot-line impedance is calculated by the use of closed form of the formula given in Wadell (1991) and Gupta et al. (2007). The width of the FR4 board was 40 cm which is more than $\lambda_o/2$. It was chosen to have a value less than the resultant slot line impedance Z_{os} for simplicity of transition to the microstrip input section while being broad enough for precise production by means of standard PCB protocols.

The value of Z_{os} was determined using the given formulas which can be applied when the non-conducting board fulfils the given condition (Gazit, 1988);

$$\begin{gathered} 2.2 \leq \varepsilon_r = 2.33 \leq 9.8 \\ 0.0015 \leq (wsl / \lambda_o) = 0.0033 \leq 0.075 \\ 0.006 \leq h/\lambda_o = 0.008 \leq 0.06 \end{gathered} \tag{3.3}$$

Applying these conditions to the slot-line impedance equation, the value according to Gazit (1988) will be,

$$Z_{os} = \left[60 + 3.69\sin\left[\frac{(\varepsilon_r - 2.33)\pi}{2.36}\right] + 133.5\ ln(10\varepsilon_r)\sqrt{\frac{w_{sl}}{\lambda_o}}\right.$$

$$+ 2.8\ [1 - 0.011\varepsilon_r(4.48 + \ln\varepsilon_r)]\left(\frac{w_{sl}}{h}\right)\ln\left(100\ \frac{h}{\lambda_o}\right)\ \sqrt{\frac{h}{\lambda_o}} \tag{3.4}$$

$$\left. + 12.48\ (1 + 0.18ln\varepsilon_r)\frac{w_{sl}}{h\sqrt{\varepsilon_r - 2.06 + 0.85(w_{sl}/h)^2}}\right]$$

This is a closed form solution between the slot-line wavelength formula and free space wavelength. λ_0 is the free space wave length analogous to the centre frequency f_0 . The calculated value of Z_{os} is 71 Ω for this particular antenna. As stated previously, in order to have an ideal impedance match for greatest power transition, the micro strip stub reactance and the slot line cavity must be related as:

$$Z_{om} = n^2 Z_{os} \tag{3.5}$$

Where,

$$n = cos2\pi\frac{h}{\lambda_o}u - cot(q_o)sin2\pi\frac{h}{\lambda_o}u \tag{3.6}$$

Where,

$$q_o = 2\pi\frac{\mathrm{h}}{\lambda_o}\mathrm{u} + \mathrm{tg}^{-1}\left(\frac{\mathrm{u}}{\mathrm{v}}\right) \tag{3.7}$$

Substituting q_0 in the above equation we have,

$$n = cos2\pi\frac{h}{\lambda_o}u - \cot[2\pi\frac{h}{\lambda_o}u + tg^{-1}\left(\frac{u}{v}\right)]sin2\pi\frac{h}{\lambda_o}u \quad (3.8)$$

Given the values of u and v respectively we will now derive the wavelength for slot line following, (James et al., 1981):

$$u = \sqrt{\left[\varepsilon_r - \left(\frac{\lambda_0}{\lambda_s}\right)^2\right]} \quad (3.9)$$

$$v = \sqrt{\left[\left(\frac{\lambda_0}{\lambda_s}\right)^2 - 1\right]} \quad (3.10)$$

So,

$$\lambda_s = \lambda_o\left(1.045 - 0.365\ln\varepsilon_r + \frac{6.3\left(\frac{w_{sl}}{h}\right)\varepsilon_r^{0.945}}{238.64+\frac{100w_{sl}}{h}} - \ln\left(\frac{h}{\lambda_o}\right)\left[0.148 - \frac{8.81(\varepsilon_r+0.95)}{100\varepsilon_r}\right]\right) \quad (3.11)$$

Where,

λ_s, is the slot line wavelength at centre frequency f_0.

Here the determined values are $u = 0.99$, $v = 0.47$, $q = 1.17$, $n = 0.9813$ and the characteristic impedance of the micro strip at the cross plane $Z_{ms} = 84.46\ \Omega$, related to a micro strip line width $w_{ms} = 0.11\ cm$ calculated according to Equation number (3.12) (James et al., 1981). In Equation 3.12 the only unknown factor is the microstrip line width after inserting the relevant values of the dielectric constant and impedance.

$$Z_{ms} = \frac{120\pi}{\sqrt{\varepsilon_{eff}}}\left[\frac{w_{ms}}{h} + 1.95\left(\frac{w_{ms}}{h}\right)^{0.172}\right]^{-1} \quad (3.12)$$

And,

$$\varepsilon_{\text{eff}} = 1 + \frac{\varepsilon_r - 1}{2}\left[1 + \frac{1}{\sqrt{1+10\text{h}/\text{w}_{\text{ms}}}}\right] \quad (3.13)$$

3.6 Antenna taper design

Different methods have been utilized for the tapered designs. Most of these are based on the hit and trial method for the calculation of the exponential rate. Here a new method for the design of TSA is presented given by Gupta et al., (2007). The method comes from the equations of the closed form where the slot line is modelled by quarter wave transformation segments. The step impedances are determined using Chebychev transformer design equations. The exponential curve is then fitted into the steps.

A complete precise design which was based upon stepped approximations in combination with the numerical electromagnetic simulations was presented in Oraizi and Jam (2003) but the method needs a good deal of computational effort to achieve impedance step matching. An alternative to this method is a new design of slot line tapered profile to provide the required size and centre frequency is used here. The basis of this method is the plan of the slot line stepped transformer obtained by using the closed formulae for the amalgamation of the required steps and the resulting relatively easy exponential curves fit well into the plan. As a result of this we get more than three octaves impedance bandwidth.

The plan starts by considering a multi-section quarter-wave transformer design, as shown in Figure 3-4.

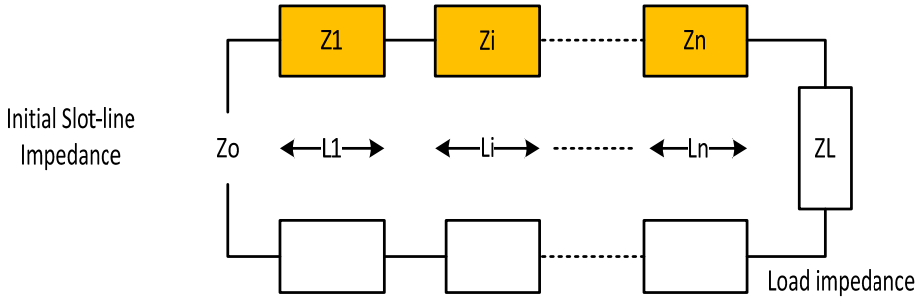

Figure 3-4 Multi-section transmission line

The length of each section is $L_i = \lambda/4$ and the characteristic impedances Z_i follow the rule:

$$Z_i Z_{N+1-i} = Z_o Z_L \tag{3.14}$$

$i = 1,2,\ldots N$. N is the number of section and Z_0 is the primary slot line impedance at each section. The load impedance Z_L is considered to be increasing to infinity ($Z_L \rightarrow \infty$). This corresponds to infinite width of slot line section. The intermediate characteristic impedance is calculated using Chebyshev transformer methods. This characteristic impedance is then used for the determination of the width of the slot by the use of standardized formulas for the slot line impedance. For fine results much of the work used is from the previous research in order to fit in the exponential tapered slot curve, to the computed steps of the formulas used for the slot line impedance.

3.6.1 Step impedance calculation

The parametric dimensions for the design are demonstrated in Figure 3-4. The specifications for the input are: specified antenna length, L (mm), the width, W (mm) and the proposed centre frequency f_0 (GHz). As described previously the length and the width are limited by the minimum frequency and they must be larger than λ_o and $\lambda_o/2$ of the smallest frequency in free space. The TSA Vivaldi antenna is modelled by the N-steps in the slot line portion. The characteristic impedance is chosen for easing the design and fabrication and the micro strip to slot line transition design, as shown in figure 3-5.

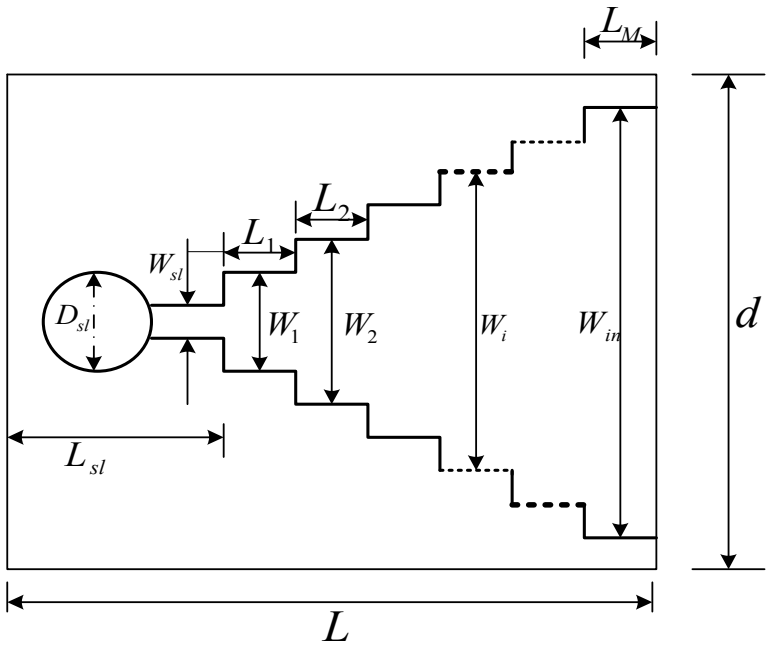

Figure 3-5 TSA step wise model

As every single step is $1/4$ guide wavelength, the number of steps is determined from the length L by the following formula:

$$N = 4(L - L_{sl})/\lambda_s \tag{3.15}$$

Where,

λ_s = slot-line guide wavelength;

L_{sl} = the distance from the board edge to the first step;

$L - L_{sl} = L_{ts}$ which is the taper length (as given in figure 3-5);

L_{sl} is set to $\lambda_o/4$ so as to provide space for the circular terminating cavity and some margin between the board edge and the cavity. The guide wavelength is dependent on the slot width. The slot width changes at every step and is primarily not known. For the computation of N as an initial estimate, this can be assumed as a guide wavelength for the initial step. For the succeeding steps the characteristic impedance is set by the use of following procedure Gupta et al., (2007)

$$\mathrm{T_N(x_o)} = \left(\frac{\mathrm{Z_L - Z_0}}{\mathrm{Z_L + Z_0}}\right)\frac{1}{\Gamma_m} \tag{3.16}$$

Where, $T_N(x_o)$ is the N^{th} order Chebychev polynomial and Γ_m is the maximum tolerable backscattered response in the pass band.

$$x_{\mathrm{o}} = \cosh\left[\frac{1}{N}\cosh^{-1}\left(T_n(x_{\mathrm{o}})\right)\right] \tag{3.17}$$

and

$$x_n = \cos\left((2n-1)\frac{\pi}{2N}\right) \; for \; n = 1, \ldots, N \tag{3.18}$$

From the $x_m$and x_o

$$\varphi_n = -2\cos^{-1}\left(\frac{x_n}{x_0}\right) \tag{3.19}$$

and

$$\omega_n = exp(j\varphi_n) \tag{3.20}$$

ω_n (rad/s) is then used for the formation of a polynomial equation in variable ω;

$$\sum_{n-o}^{N} \Gamma_n \, \omega^n = \Gamma_N \prod_{i=1}^{N} (\omega - \omega_n) \tag{3.21}$$

Where Γ_n represent reflection coefficient. These coefficients can be determined by matching powers of ω (rad/s). Each of them shows the coefficient of reflection at every step in the transformer. So the characteristic impedances for the steps are established recursively by use of,

$$Z_{i+1} = \frac{1+\Gamma_i}{1-\Gamma_i} Z_i \tag{3.22}$$

The width w_i at every stage is selected to give the characteristic impedance Z_i (Ω) by using empirical formulas such as found in Gupta et al., (2007).

3.6.2 Smoothing

The curvature effect was determined by Lee and Simons (2002) who showed that the curvature and the taper profile have great effect on the frequency bandwidth and antenna performance. The reduction in the curvature radius results in the increase in the half power beam width. In order to get a very smooth taper, exponential curves were fitted to the peaks, centres, and base points of the steps as shown in figure (3-6).

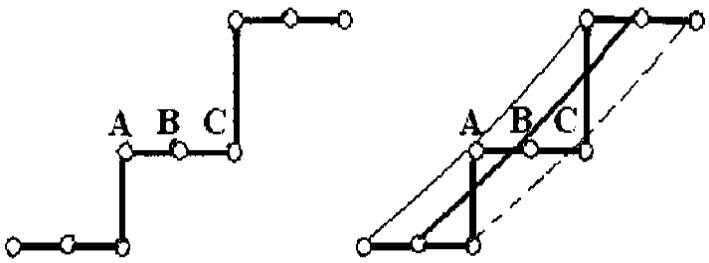

Figure 3-6 Curve fit points (A – peak, B – Centre point and C – base point)

The open mouth exponential taper of the antenna has already been used in some previous studies and designs (Oraizi, 2003). The procedure here can be represented as taking an average of the open mouth taper rate R_a when selecting taper results in a required centre frequency and total dimension. The overt formula for the curve is:

$$y = c_1 e^{Rx} + c_2 \tag{3.22}$$

Where,

$$c_1 = \frac{y_2 - y_1}{e^{Rx_2} - e^{Rx_1}} \tag{3.23}$$

$$c_2 = \frac{y_1 e^{Rx_2} - y_2 e^{Rx_1}}{e^{Rx_2} - e^{Rx_1}} \tag{3.24}$$

c_1 , c_2 are constants, *(y_i, x_i)* and *(y_2, x_2)* are the coordinates of the origin and ending of flare curve respectively, and the taper length $L = x_2 - x_1$. The taper is optimized to make the antenna impedance equal to that of free space (377 Ω).

Based on the parameter study performed Janaswamy and Schaubert (2002), the resistance in the antenna input frequency increases with the rate of opening (R_a), as shown in Figure 3-6, in which three dissimilar values of R_a = 0.1, 0.2 and 0.3 (mm) have been used. The other parameters are considered as constant.

3.7 Antenna configurations

The final design of the TSA is optimized to achieve frequency band 0.25 to 3.0 GHz at centre frequency of $f_o = 1.5$ GHz. To achieve the objective of a broadband antenna in both gain- and impedance, the TSA scheme is shown in Figure 3-7.

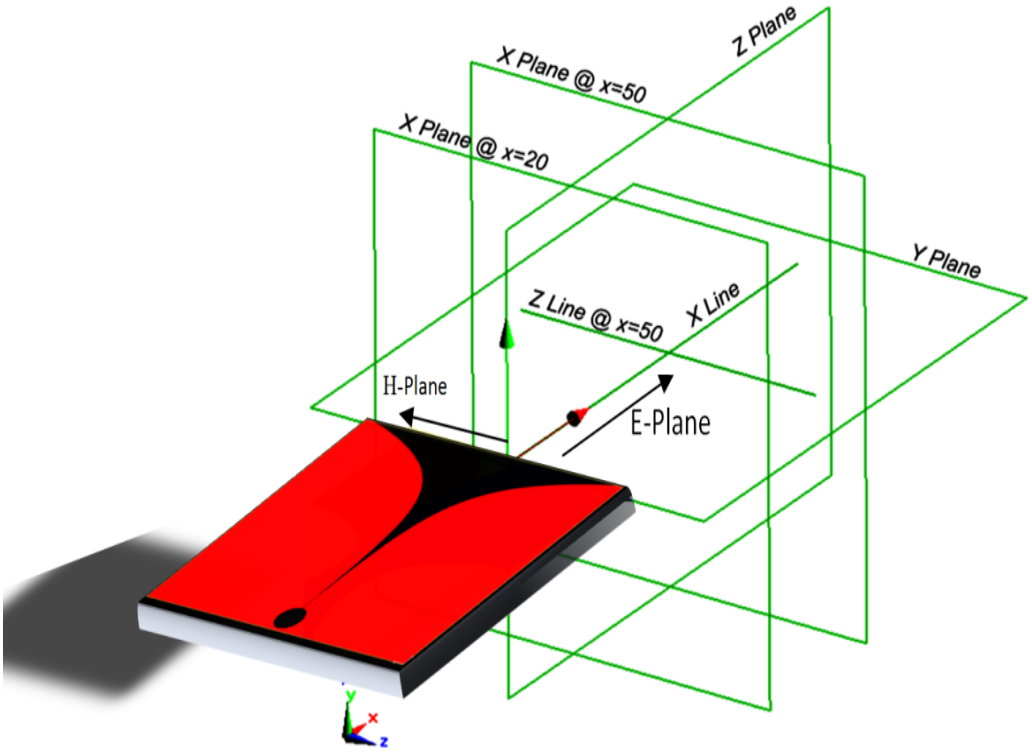

Figure 3-7 Schematic of the TSA E and H planes

The parameters for antenna are chosen bearing in mind several factors, which encompass the newly gained knowledge and fabrication requirements. It is manufactured on the FR4 substrate having $\varepsilon_r = 2.33$, and thickness $h = 1.25mm$. The overall size of the Vivaldi antenna is *L=510 mm*, width, *W= 400 mm*, W_{ms}*=100 mm*, L_s*=200 mm,* and D_s *= 38 mm* which relates to the resonant frequency of the slot line cavity at 1.5 GHz. The rate of opening $R = 0.018mm$, this was a trade-off between antenna bandwidth and reflection coefficient. $R_{rad} = 7\ mm$, which is the radius of the radial stripline stub sector and its related to the resonant frequency of the micro strip stub at 3 GHz.

3.8 Simulation setup

The parameters of the antenna that need to be adjusted to obtain an optimum antenna design and minimise ringing of the antenna are:

- Cavity radius.
- Flare angle.
- Throat width.

These factors are the most sensitive elements that give great influence on the efficiency of the antenna and must be carefully optimized figure 3-8 explained the process.

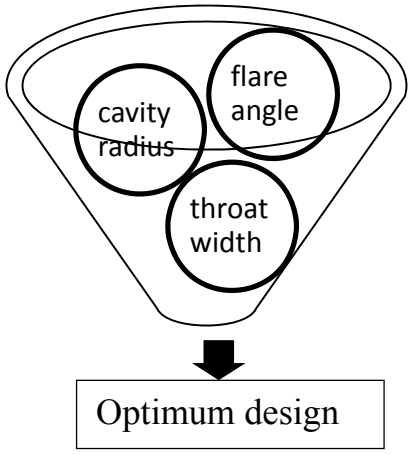

Figure 3-8 Optimum antenna design parameters

Keeping in mind these factors helps achieve an optimum antenna design which reduces the ringing of the antenna as much as possible. Final antenna parameters are presented in table 3-2.

Table 3-2 Tapered slot antenna parameters

PARAMETR	VALUE (mm)
Length L	400
Width d	510
Mouth opening W	480
Taper Length L_{ts}	320.075
Taper rate R	1.80
Cavity diameter D_{sm}	45
Throat length w_m	29.25
Throat width l_m	1.1
Back wall offset L_G	5
Radial stub radius R_r	70
Radial stub angle θ^0	105^o
Connector type	SMA

CST Microwave Studio based on *transient Solver* mode was used to validate the proposed design procedure. The antenna is located in the *x-y* plane, the E-plane of the antenna is in the *x-z* plane($\varphi = 0^o$) and *H*-plane is in the y-z plane ($\varphi = 90^o$).

The antenna is excited with a Gaussian monocycle pulse in the time domain and is optimized and simulated using the *electromagnetic FTD solver of the CST Microwave Studio Transient Solver mode*. This helped to reveal the most critical antenna areas in which to reduce cavity resonance and to ameliorate their related transmitted and received amplitudes. The excited monocycle pulse has maximum amplitude at a frequency 0.75 GHz, which was carefully selected to excite basic CNR of most common firearms (Harmer et al.,2010). Figure 3-9 illustrates the antenna model.

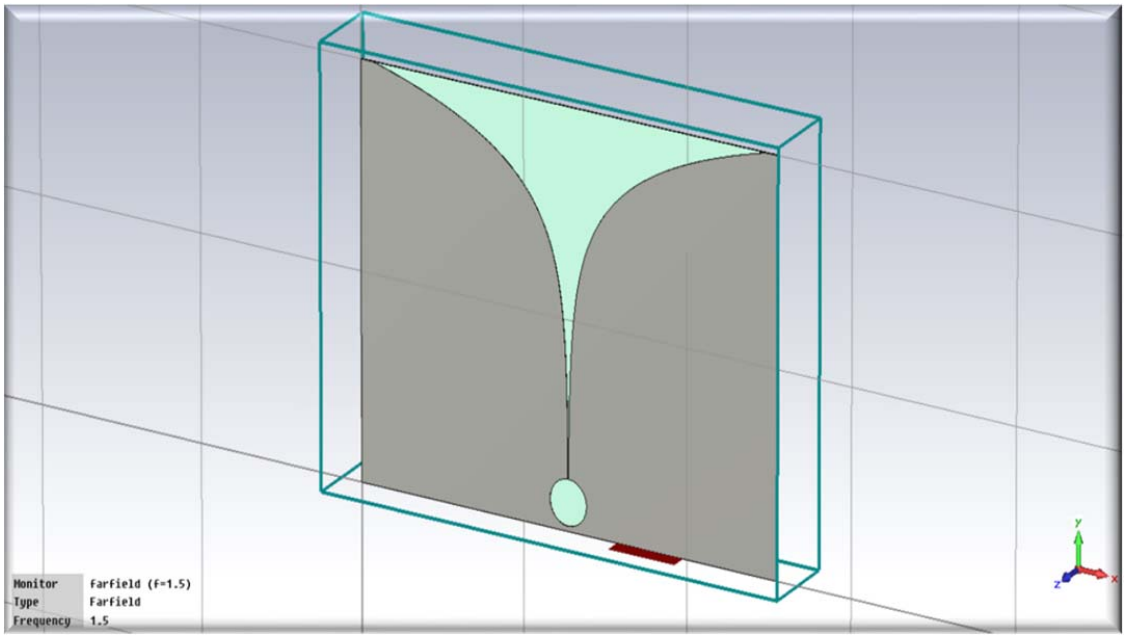

Figure 3-9 Antenna CST model

3.9 Tapered slot antenna measurements

A plan view of the fabricated antenna is shown in figure 3-10. To control surrounding atmospheric interference, the antenna test was done within an anechoic compartment which has the walls covered with RF absorbers. The walls offer a reflection coefficient of about - 40 to - 42 dB at lower frequencies such as 250 MHz

Agilent Network Analyser AN8336 which has the frequency range of 50 MHz to 40 GHz was used to make the antenna measurements.

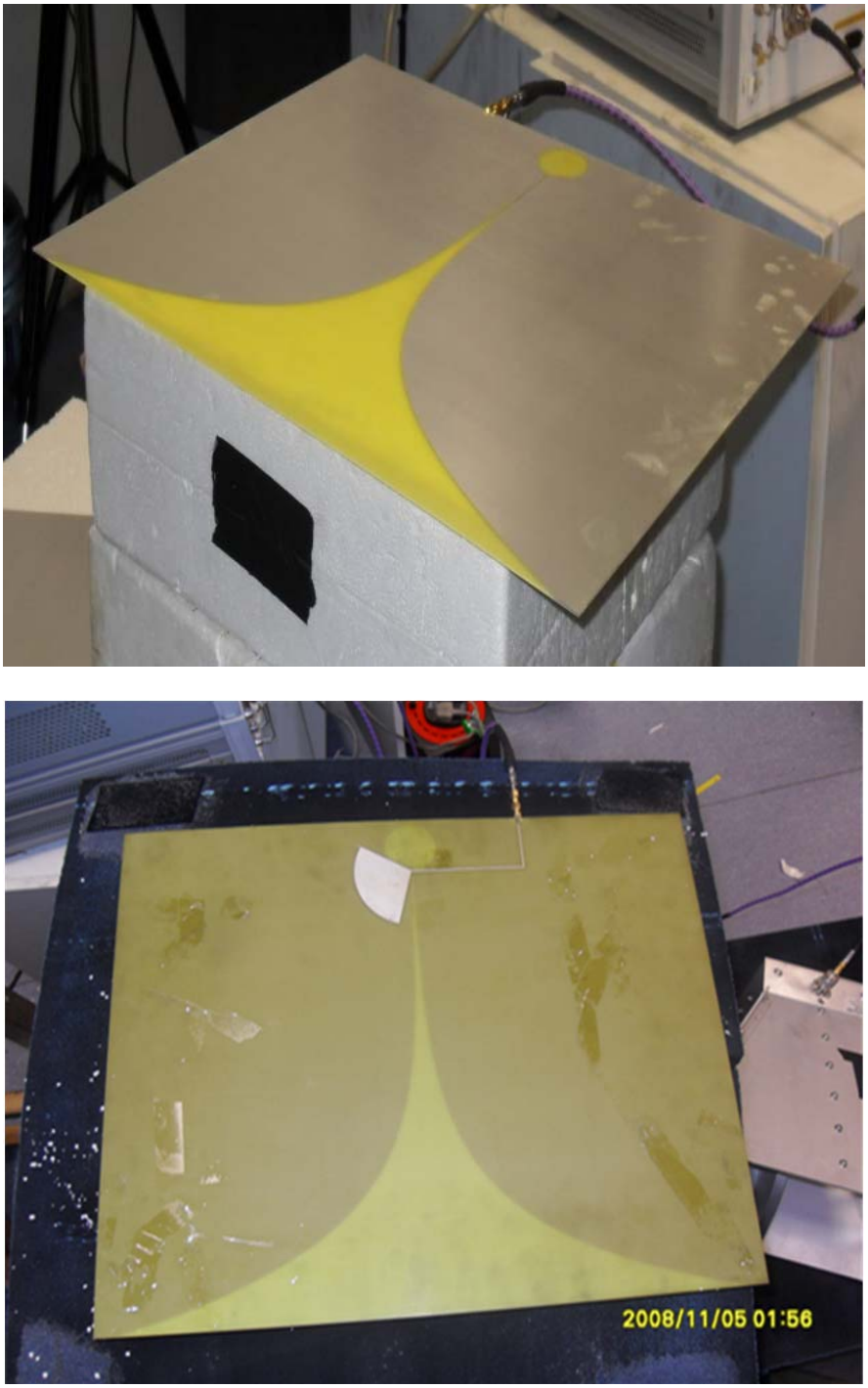

Figure 3-10 Top and bottom fabricated TSA antenna.

3.9.1 Impedance bandwidth

The antenna return loss S_{11} is taken in provisions of the -10dB. The backscattered port of the VNA network analyser, port 1, was calibrated to the input of the antenna over the 0 to 3 GHz frequency band. The antenna was tested in the anechoic chamber and the reflections of the transmitted sweep frequency obtained from 0 to 3 GHz were recorded and plotted against the simulated results as shown in figure 3-11. The results show that about 80% of the objective is achieved, simulation results closely resemble to the measured results which confirm the design procedure of the antenna over the objective bandwidth of 0.25 to more than 3 GHz.

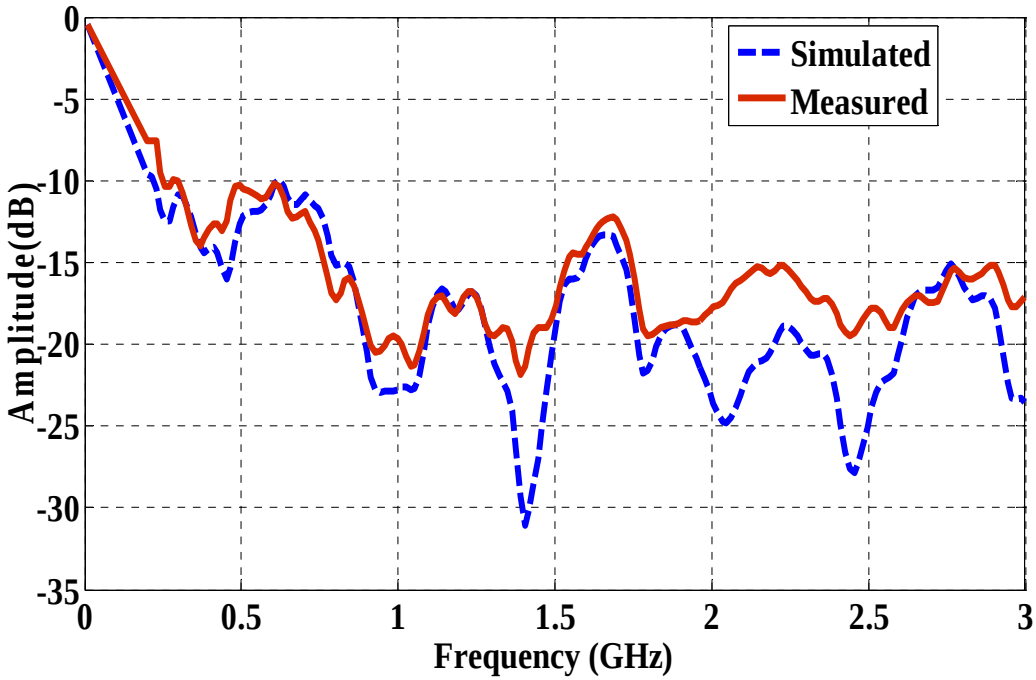

Figure 3-11 Measured and simulated S_{11} return loss.

Both the measured and simulated figures show that the antenna gain of the designed antenna achieves the requirements of flatness and VSWR around unity for frequency desired frequency band as shown in figure 3-12. The difference between the measured and simulated result is around 5% which related to the hardware fabrication of the antenna.

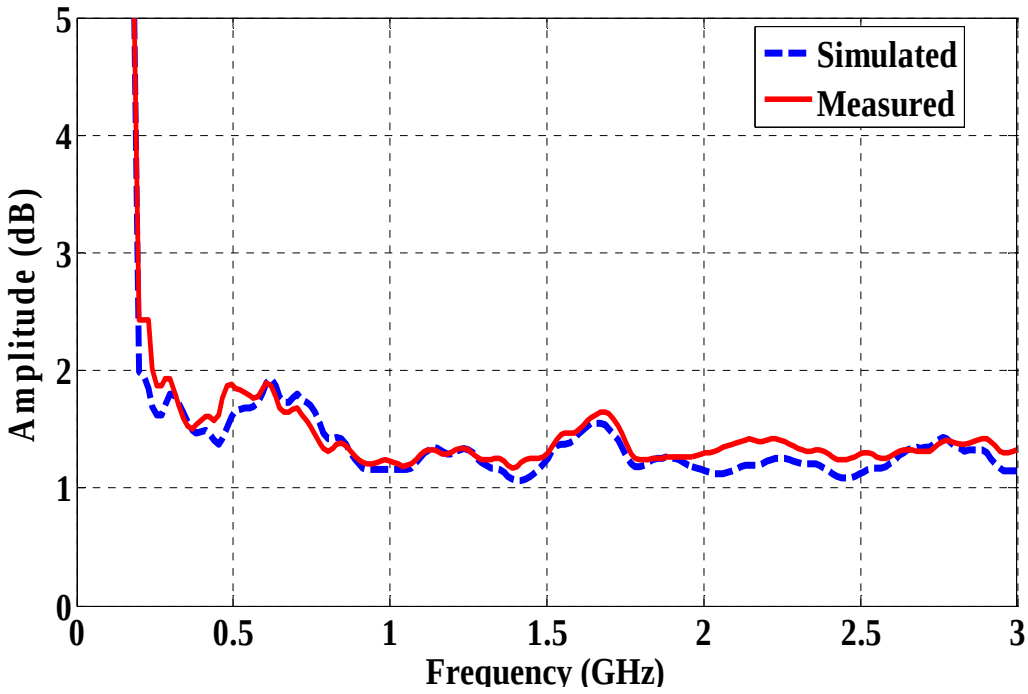

Figure 3-12 Measured and simulated VSWR standing voltage wave ratio.

3.9.2 Far-field radiation pattern

The far-field radiation patterns of the antenna were again calculated using CST Microwave Studio software. These far-field results are presented in figure 3-13 for the

frequencies 0.7 GHz and 1.5 GHz. The antenna achieves directive properties with an average front-to-back ratio which is greater than 6 dB across the whole band, making it convenient for standoff detection application.

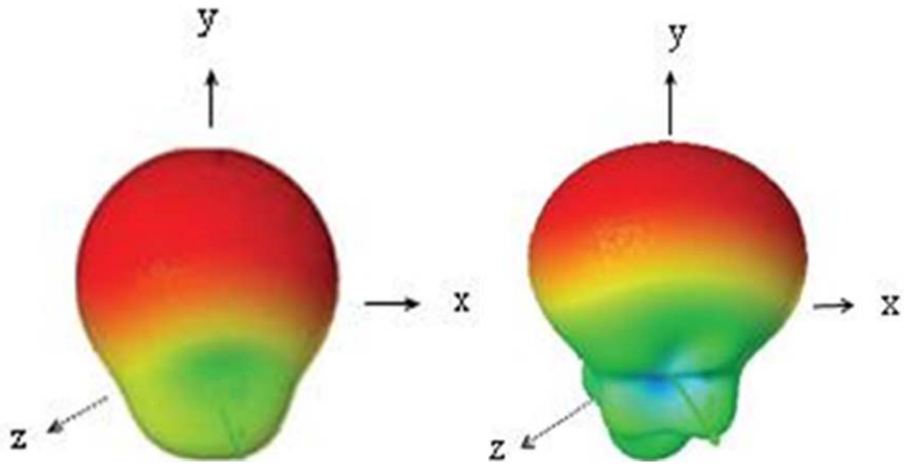

(a) - 0.7 GHz **(b) - 1.5GHz**

Figure 3-13 Simulated three dimensional far field radiation pattern (a) - 0.7 GHz and (b) - 1.5 GHz.

3.9.3 Gain bandwidth

To accurately determine gain bandwidth, we plot the maximum gain pattern in all the directions and the gain at the direction of $\theta = 90^0 \; and \; \emptyset = \; 0^0$, for the frequency range 0.25 – 3 GHz. Figure 3-14 shows the entire absolute antenna gain in dB Clearly the gain is a function of frequency range in the working bandwidth. It's quite clear that measured and simulated gain of the antenna in good agreement. The gain met or exceeded 6 dB at the range of 0.25 - 3.0 GHz, which illustrates there is no split cross the antenna

bandwidth however there is obverse different (about 10%) between the simulated and measured results which is happen because of the fabrication of the antenna.

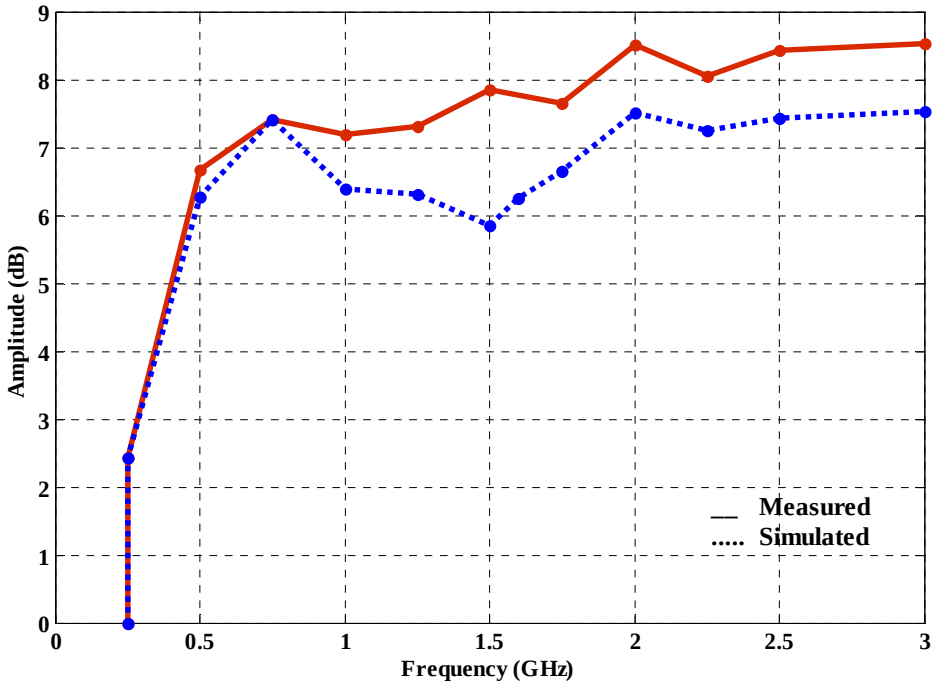

Figure 3-14 Simulated and measured of antenna.

3.9.4 Impulse response

The performance in the time domain was also measured. Two identical co-polarized antennas were set facing each other 50 cm apart. The least far-field space is obtained by Appel-Hansen (1981) and Mehdipour et al. (2007)

$$R \geq 2D^2/\lambda \tag{3.25}$$

Where

R = Range length in meter (distance between transmitter and receiver antennas)

D = length of the antenna aperture in millimetre.

λ= Measurement wavelength in millimetre

The measured results are presented in figure 3-15 which shows that the time pulse of the antenna is 0.7 nanoseconds. The results show that the optimized antenna provides a narrow pulse with distortionless which makes it an excellent radiator for the application of a detection system with low LTR ringing.

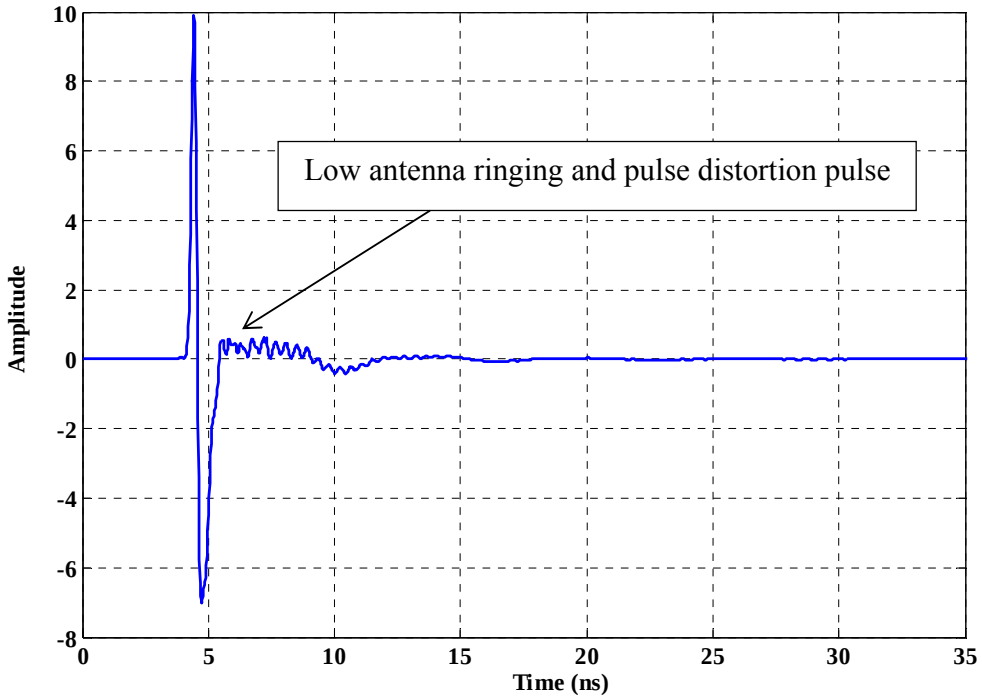

Figure 3-15 Antenna impulse response

3.10 Summary

An UWB TSA for use in concealed weapon detection has been designed and fabricated. Detection of concealed onbody weapons is limited by antenna response as any antenna ringing could mask important aspect independent scattering related to the concealed object signature. An approach is described based on an antenna with 80% flat gain across the operating bandwidth. Simulated and measured antenna characteristics illustrate that the developed antenna has relatively flat gain cross the proposed bandwidth from about 0.25 GHz to more than 3.0 GHz. The time domain of the antenna has been studied as well. It has been illustrated that the given antenna could send and receive very narrow pulses with less than 5% distortionless manner which meet the requirements of successful concealed weapon detection based on the LTR scattered from the illuminated objects. The different between the simulated and measured results are mainly related to the antenna fabrication. Performance of the proposed antenna in capturing the LTR of the illuminated target is described in chapter 4.

Chapter 4
Antenna Performance in Extracting Late Time Response

4.1 Introduction

The demand for quick and accurate identification of friends or foes at standoff distance is essential to most processes for screening people for concealed weapons and is urgently needed in, for example, screening at the entrances to public places such as airports and government buildings. Such a prevention technology is not currently available. The challenge is therefore, to develop some kind of non-imaging access system that avoids the risks and caveats associated with the wrong interpretation of the images and increase the possibility of detection and identification of concealed objects that pose a threat in real time at standoff distance. Detection using this method depends on exciting the complex natural resonance frequencies (CNRs) of the object being detected with short electromagnetic pulses of an appropriate frequency and extracting characteristics of the object independent of the aspect presented to the detector. These CNRs will be used to identify the object and whether it is a threat or not (Baum et al., 1991). Such an approach has, to date, only been successfully applied to landmine detection by ground penetrating radar, and for radar target recognition such as aircraft and many other objects (Yarovoy et al., 2000). The reasons for this are simple: an airborne aircraft is isolated from other targets, is situated in nearly perfect anechoic conditions and presents a large surface area for induced electrical currents to persist and re-radiate after excitation by high power

electromagnetic interrogation pulses. None of these conditions can normally be met in the case of a human carrying a small metallic object and consequently the application of this well-known technique without high false alarm rates is considerably more difficult.

A hidden object in the far-field is irradiated with a radar signal which is sufficiently broadband to include the resonance region of the target. The scattered signal will include particular resonance frequencies. The time domain signal from a target consists of two parts which are sequential. The first part is the direct reflection of the incident wave by the object and is normally used to locate the position of a target, it is aspect dependent on the dimensions of the target, (Wang et al., 2000). The latter part occurs after the initial electromagnetic pulse and represents the decay of the response, and is the target's unique signature and is due to resonance phenomena within the target. These resonances have two sources , (i) so-called "external resonances" which correspond to surface waves: with a perfectly conducting target only external resonances would occur, and (ii) internal resonances which relate to cavities existing within the object (Baum, 1971). The resonant behaviour during the late time is characteristic of the studied target and can be used to define a method of identification. The above scattering description is the basis for the antenna design. In the previous chapter, a design, simulation and measurements of a flat gain UWB tapered slot antenna was presented. This chapter provides details of the performance of the designed and fabricated antenna to capture the back scattered LTR of different objects. Measurement and data analysis is given and discussed in the following sections of this chapter.

4.2 Theory

When an object is irradiated with a sweep frequency or short electromagnetic pulse, currents will be induced in its surface which will propagate across the surface in all directions until eventually they strike the physical limits. At these boundaries they are reflected, and bounce back and forth across the object's physical geometry. Provided that the band of frequency of the short electromagnetic pulse covers the range of about 0.4 to 4 wavelengths of the target size, global full body resonances (known as CNRs) related to the resonant behaviour of the entire object will be established. These resonances are aspect independent and provide a unique signature of the object being detected, (Morgan, 2005).

According to the singularity expansion method (SEM), modelling of the ETR can be extracted from the exponentially damped models applicable to the LTR by introducing frequency dependent coupling coefficients, (Richards, 1994). Richards demonstrated the feasibility of this method and good numerical results were achieved for wire scatters. However, as Dudley and Morgan pointed out, using the global resonance model with a frequency dependent coupling coefficient does not provide any new physical insight into the local scattering phenomena, as the resonant modes have to be established from the LTR to be applied to the ETR (Dudley and Morgan, 1985).

Compared to the complicated ETR modelling, modelling LTR is much simpler. This is because the scattering phenomenon in the late time period is dominant by global resonances and theoretically such global phenomena are purely target dependent and

aspect independent. In practice some of the resonance modes cannot be extracted at particular aspects because they are not well excited (with relatively low values of residues) at those aspects. Late-time scattering can be fully described by the SEM, which describes the LTR by a sum of damped exponentially decaying sinusoids model using CNRs. This approach is similar to acquiring the transient response of any LCR circuit or linear time invariant system in the Laplace domain and then inferring from the transient response the physical properties of the circuit. The back-scattered signal in the time domain can be described as a convolution process between the emitted signal and scattered impulse response of the object as illustrated in Equation (4.1) linear time-invariant system**.**

$$S(t) = E(t) \otimes h(t) \tag{4.1}$$

Where

$S(t)$ Radiation backscattered electromagnetic signal in time domain.

$E(t)$ Emitted electromagnetic signal in time domain.

$h(t)$, Object impulse response.

If the object being detected is excited with a sharp pulse (delta function) then Equation (4.1) could be approximated by

$$S(t) = \delta(t) \otimes h(t) \approx h(t) \tag{4.2}$$

$\delta(t)$ is the impulse function.

$$S(t) = h(t) \tag{4.3}$$

Equation (4.3) illustrates that, if the duration of the excitation signals is short enough the back-scattered response of the object that approaches a unique LTR signature for the object to be detected which is aspect independent. This late-time scattering response can be fully describe by the SEM as illustrated earlier by Equation (2.1)

$$h(t) = \sum_{m=1}^{M} A_m \, e^{-\sigma_m t} cos(\omega_m t + \varphi_m) \tag{4.4}$$

$$t \geq T_l \tag{4.5}$$

$$A_m = a_m e^{j\emptyset_m} \tag{4.6}$$

$$cos(w_m t) = cos(2\pi v_m t) \tag{4.7}$$

Where

$h(t)$ Late time scatter response is sum of M exponentially damped modes.

M Is the number of natural modes.

A_m Residue, aspect dependent complex amplitude of the m^{th} mode.

$w_m = 2\pi v_m$, harmonic frequencies, aspect independent.

(φ_m) Relative phase of the m^{th} mode, aspect dependent.

$(-\alpha_m t)$ Damping factor, independent of target aspects.

T_L , Starting point of the LTR.

Determining the start of the late-time period is generally difficult. For the usual case of backscattering measurements, this time is given by Mooney et al. (1998) as already given in equation (2.2) in which the number of CNRs theoretically tends to infinity. In practice, however, because real signals are band limited only a finite number of resonant modes will be excited and the number of useful modes can be said to be a finite number, *M*. The presence, or otherwise, of these modes useful could be used to detect and identify an object by comparing the given signature to a library data base.

Usually, *M* is unknown at the start of any particular examination and will depend on the bandwidth of the signal used, the target geometry and the electromagnetic characteristics of the material of the target (Harmer et al., 2010). Harmer et al. (2009) found that in practice, only the first few CNRs are sufficiently excited to be observable, so the modal order need only include these lower-order modes to give a good measure of LTR. The modal amplitudes A_m (equation 4.6) depend mostly on the form of the irradiating pulse and the aspect of target on which they are incident, but the re-radiated modal frequencies, v_m, and their rates of decay, α_m^{-1}, are independent of target aspect and, provided the excitation pulse is of short enough duration, independent of the excitation wave form (e.g. its temporal development or wave front shape). This fact has proved immensely useful in radar identification of aircraft where suitable mathematical techniques have been developed to extract CNRs from the measured LTR of the target (Chamberlain et al., 1991). Of course, any noise contributing to the LTR will not form part of the signal re-radiated by the surface currents excited on the target.

4.3 Methodology

The block diagram of the proposed standoff concealed weapon detection system is illustrated in Figure (4-1).

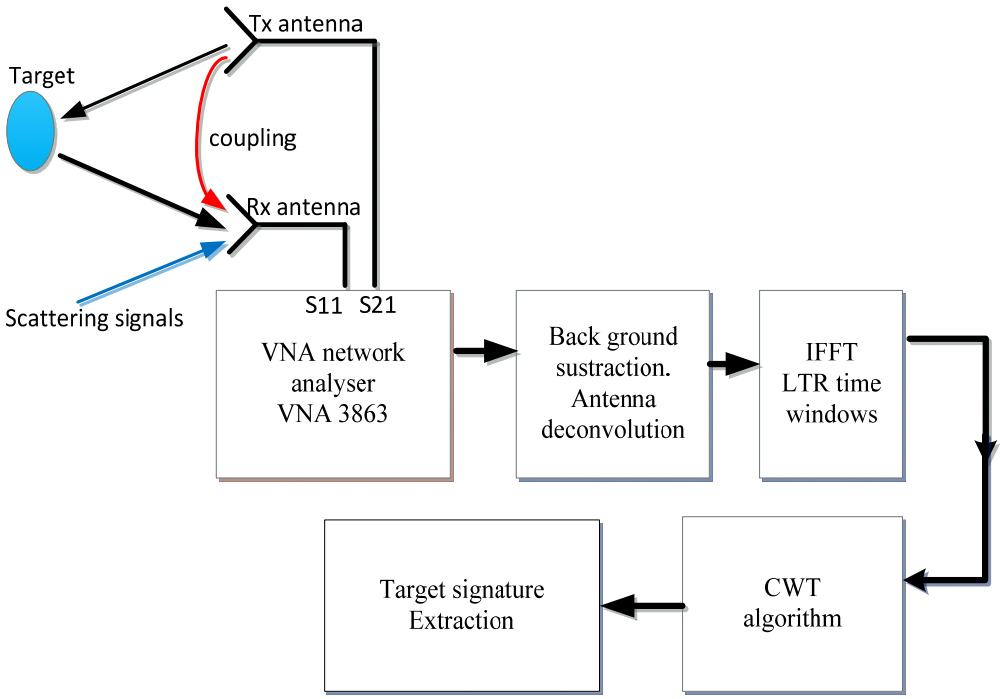

Figure 4-1 Standoff concealed weapon detection system.

The target illuminated by a short UWB pulse (practically 0.25 GHz - 3 GHz) using the fabricated directional TSA. The UWB pulse bandwidth includes frequencies and harmonics of the naturally occurring resonances within the target, this leads to good time resolution, with an LTR which is easily separable from the more complex and aspect dependent ETR.

Two identical TSAs were used to transmit a sharp pulse and to collect the backscattering data. Cross-polarized transmission and reception were used to give enhance discrimination between ETR and LTR.

The receive antenna was connected to Vector Network Analyses Agilent VNA 3863 to capture the re-radiated signal that contains amplitude and phase information of the back scattered electromagnetic field. The captured data will contain the complex frequency domain scattered signals both for object to be detected and identified and for the background (no target). Background parameters should be constant and their measurement can be used to mitigate the effects of drift in the measuring equipment.

With the LTR extraction algorithms data will be extracted using only fixed time duration windows (around 10ns), and passed through a relevant filtering algorithm to extract a unique object signature to be used for identification and classification. LTR will be extracted according to the following procedure.

A strong forced ETR signal can masks the LTR radiation related to target features in the co-polarization measurements. In contrast, the forced ETR signal is suppressed in the cross-polarization measurements and the LTR reflection signal is relatively enhanced following the direct wave. Cross-polarization measurements can provide significant improvements in antenna resolution and minimize antenna interference and clutter. Comparative measurements illustrate that the direct-wave isolation between the transmitting and the receiving antenna is significantly improved with the use of cross polarization (Sato et al., 1995).

4.3.1 Inverse Fast Fourier Transform (IFFT)

An IFFT was applied to the object back-scattered response to yield the time domain signal. The resulting time domain is then windowed to split the time response signal into four separate and sequential sections; time period before the illumination, time period during the forced target response, time period after the forced target radiation when the object is fully energized and radiates omni-directionally, and the time interval after the object has stopped radiating and which tends to background noise.

The sampling to obtain the time response was divided into four parts, and an FFT was applied to each of these to obtain frequency domain information and find out the start and end of the stronger ETR and the beginning of the weaker LTR.

A MATLAB program was written to read in complex data, achieve background subtraction, antenna convolution and do the IFFT of the data to produce the time domain data used for time windowing (gating). The data was stored to a file for subsequent data processing. Many different filtering techniques such as E-pulse, GPOF have been described by different authors to extract the unique object signature (Ilavarasan et al.,2002; Ye and Jin, 2010; Harmer et al., 2010). A new approach to extract the target signature from the captured LTR will be presented on the next Chapter.

4.3.2 Experimental setup

Before presenting the analysis the experimental setup is described. The experiments are carried out in the Millimetre Wave Laboratory of the School of Engineering, Manchester Metropolitan University. Figure 4-2 shows the lay-out of the equipment for the

experimental detection of concealed objects at standoff distances the picture taken from inside the chamber room, figure 4-3 shows the experimental environment in which the object are stands inside the camber room. Important are two identical TSAs which were designed and successfully built especially for this project. These have a lower cut-off frequency of around 0.25 GHz by which the LTR fundamental frequency of the most firearms is covered.

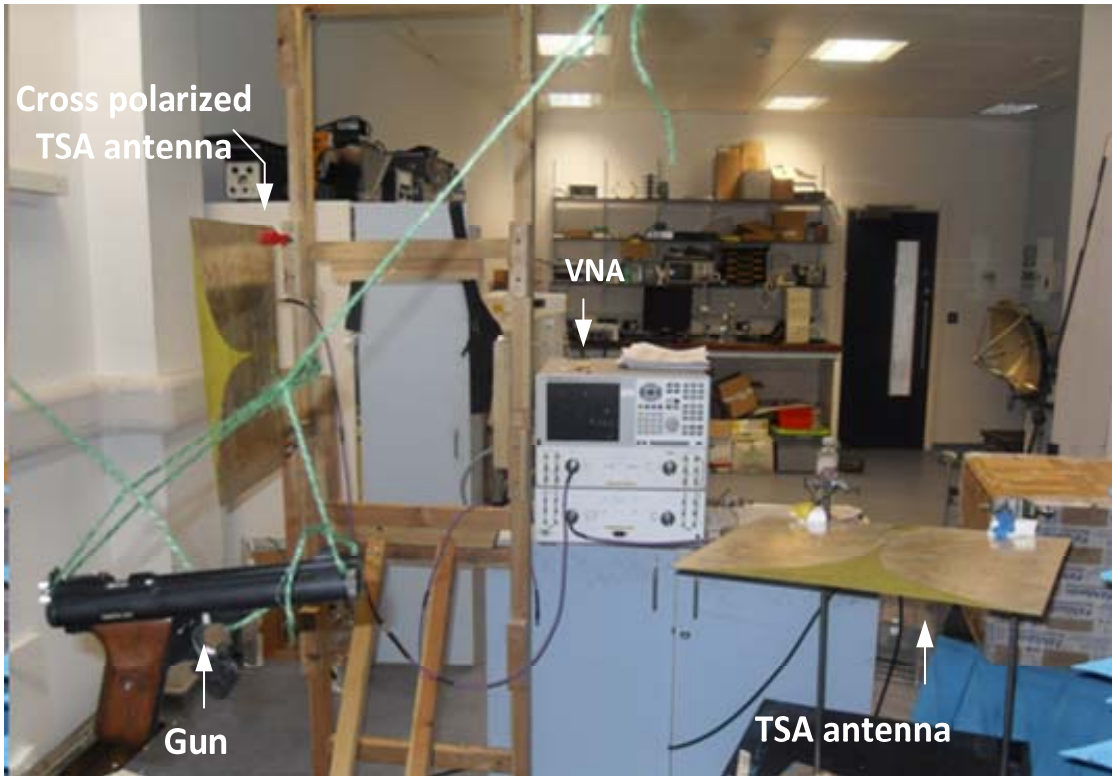

Figure 4-2 Experimental setup

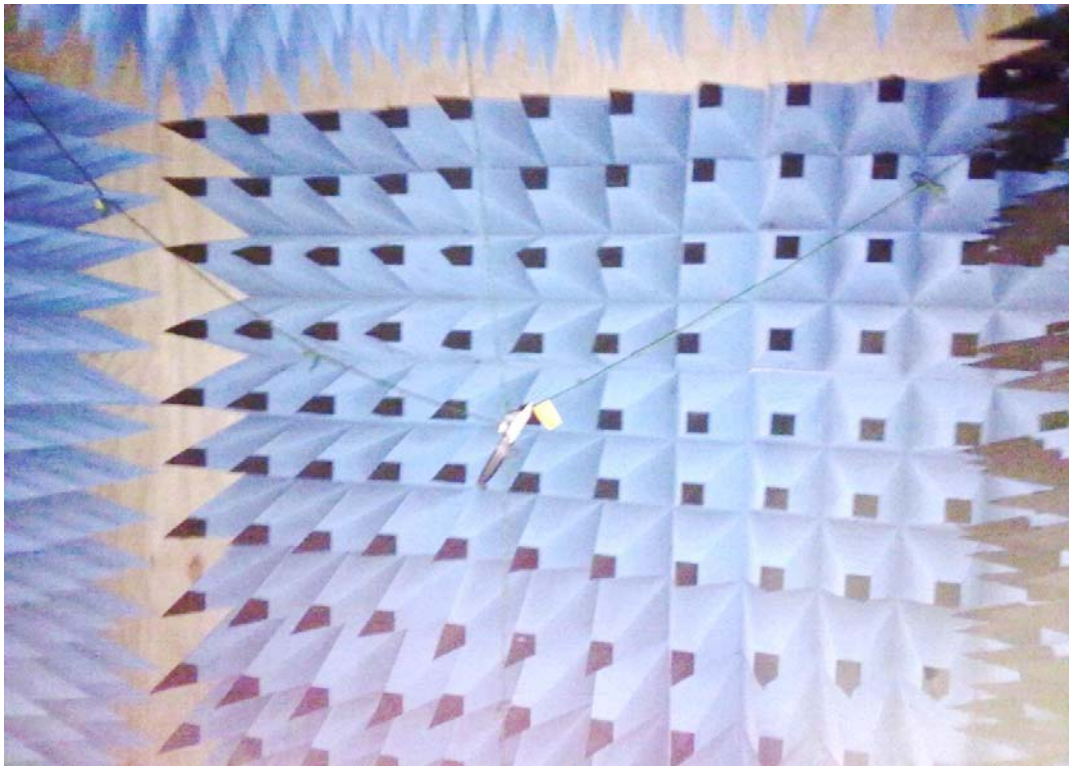

Figure 4-3 Experimental environment.

As shown in the figure 4-2 the two identical TSAs designed and made as part of this project, with cut off frequency around 0.25 -3.0 GHz. These antennas were used here as both transmitting/receiving antenna, the transmitting antenna was oriented in the direction of the illuminating radiation and the receiving antenna at 90^{o} (cross-polarized) to give better discrimination between the early and LTR. To illuminate the target the vector network analyser VNA E8363B was adapted to effectively generate a sweep frequency of bandwidth 0.25-3.0 GHz, which is transmitted by the transmitting antenna. The tested target placed in the camper room and its orientation was 45^{o} as shown in figure 4-3,

The backscattered radiation was collected by the receiving TSA and applied to the second port of the VNA to digitally collect measured data S_{21}. 801 data points were collected and recorded. Figure 4-3 shows the backscattering diagram.

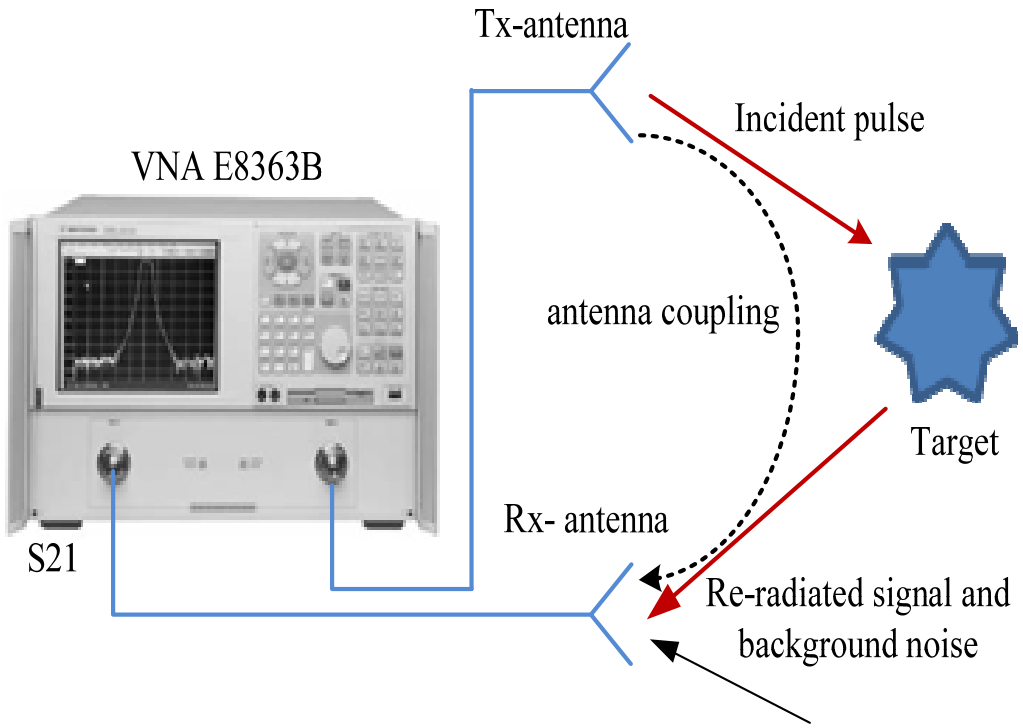

Figure 4-4 Schematic arrangement for transmission excitation signal and measurements of backscattered response with interference.

The VNA drives the transmitting antenna which converts the transmitted signal into incident field and captures the backscattered data from the receiving antenna.

To obtain the LTR of the object, the target measurements are processed to reduce or eliminate undesired parameters such as the antennas coupling field, background noise, unwanted reflections (known as the clutter field) and the antennas response. Elimination of these fields from the measured S_{21} gives the frequency response of the object. The elimination of undesired background noise and antenna coupling and errors will be treated first by background subtraction and antenna deconvolution as these parameters are common in all of the proposed objects measurements.

Many experiments were conducted using different objects from simple to complicated, a 10 cm, 21.5 cm wires, knife and handgun, to demonstrate the effect of the object geometry on the back-scattered LTR. The results of these experiments are discussed in the next section.

The back scattering impulse response S_{21} was measured by VNA and separately analysed by MATLAB code. The object background is subtracted, and the antenna response is convolved and normalized. The collected data was transformed into time domain by applying the IFFT on this frequency response produce the object's impulse response. From this impulse response, the object's LTR can be extracted.

4.4 Results and discussions

All of the experiments focus on the collection of radiation response of different objects mentioned above and the collected LTR response. Frequency domain scattered field data is digitally captured from VNA for the required bandwidth 0.25 - 3.0 GHz. This data was then treated as described above. Firstly, the background noise data is measured as

presented in figure 4-4. This data is common in all of the following experimental measurements.

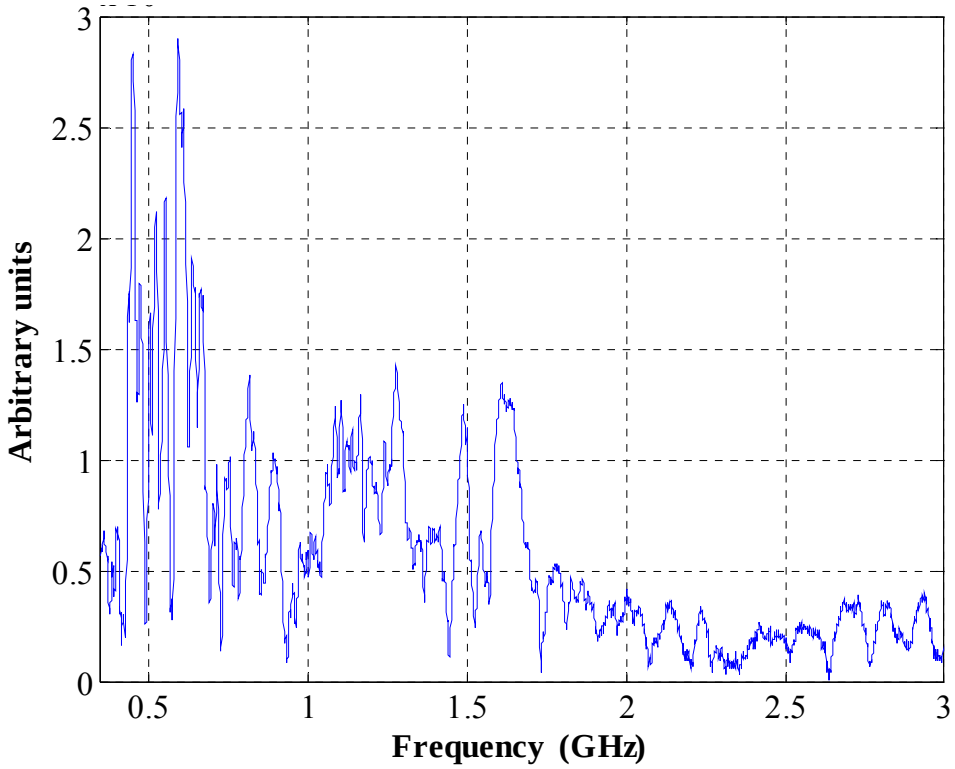

Figure 4-5 Captured background data.

Both figures 4-4 and 4-5 are for no target present and are used to "clean" the target response in the frequency domain to give a better target response for signal processing.

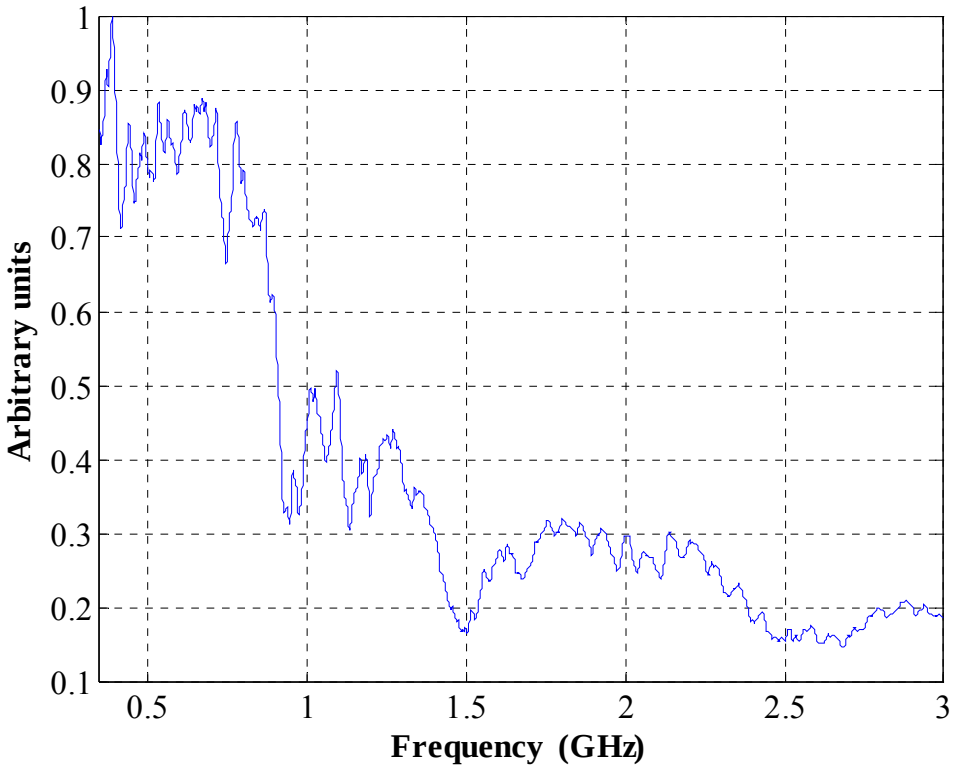

Figure 4-6 Antenna response

After measuring the antenna and target backscattering response, the antenna response was convoluted to identify the target response from the antenna errors that might be present. The system is now in place to introduce the different simple and complex experimental targets; first the simple objects are presented followed by complex objects.

4.5 Simple objects

The target time response is directly dependent on the target geometry including size, which is clearly illustrated by the test objects, where the target time response of simple objects is very short compared to that of complex objects such as handguns.

4.5.1 Wire of 10 cm Length

The first simple perfect electric conductor (PEC) target was a 10 cm length and diameter of 0.4 cm placed 1.5 m from the transmitting/receiving cross-polarized antennas. The orientation angle of the wire was 45^0 which represented the incident angle of the transmitted sweep frequency and this was fixed for all of the following experimental work hence the LTR is independent on angle of incident, (Hamer et al, 2009). The scattered field was measured for the 0.25 – 3.0 GHz frequency band. The reason for selecting this particular target was because theoretically the reflected waves can be precisely calculated and by comparison, the validity of the measured results (appendix C) can be confirmed. Once its validity had been verified, the same measurement procedure could be extended to more complex objects.

Cross-polarization was used to minimize the direct reflection from the object being detected and hence maximize the relative amplitude of the LTR. Figure 4-6 shows the initial response of the wire after background was subtracted and antenna deconvolved. These processes are very helpful to minimize interference and to identify pure target response.

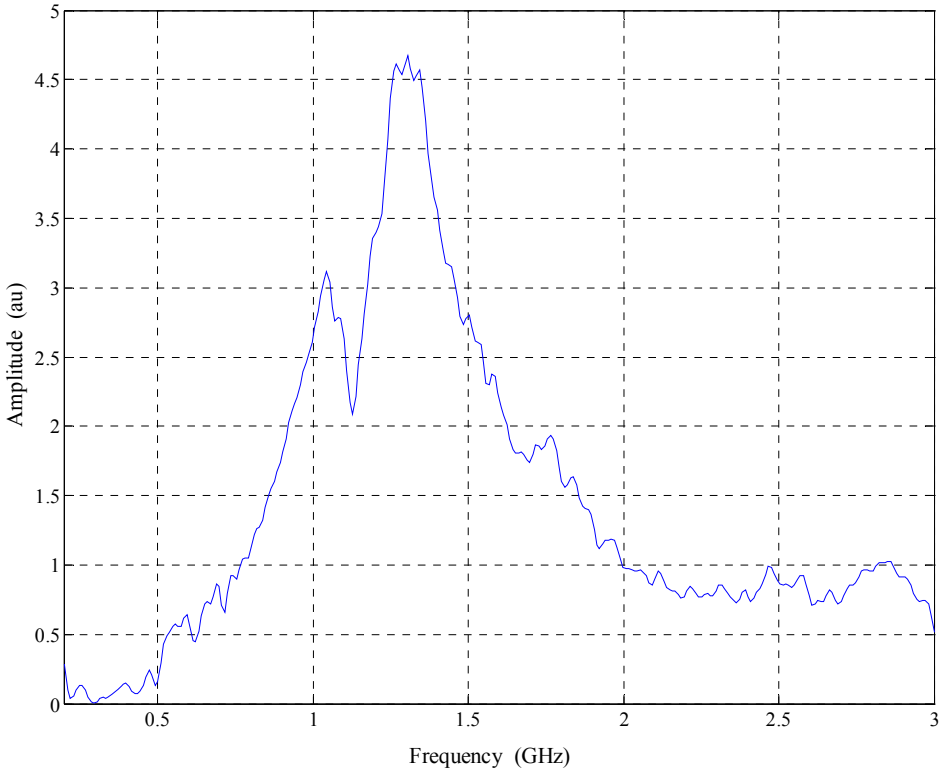

Figure 4-7 Frequency response of wire (L = 10 cm, d = 0.4 cm).

Time domain signals were obtained by taking the IFFT of the windowed back-scattered frequency response. Figure 4-7 shows the time domain of CNR frequency related to the target (wire), from which LTR is extracted and presented in figure 4-8. The life time of this LTR is around 6ns after this time the response is due to background noise and error effects as stated in the SEM. The 6 ns LTR life time is sufficiently large enough for target identification. However this is not constant and could be less or even more according to the extracting filtering techniques to be used for the identification of a target signature.

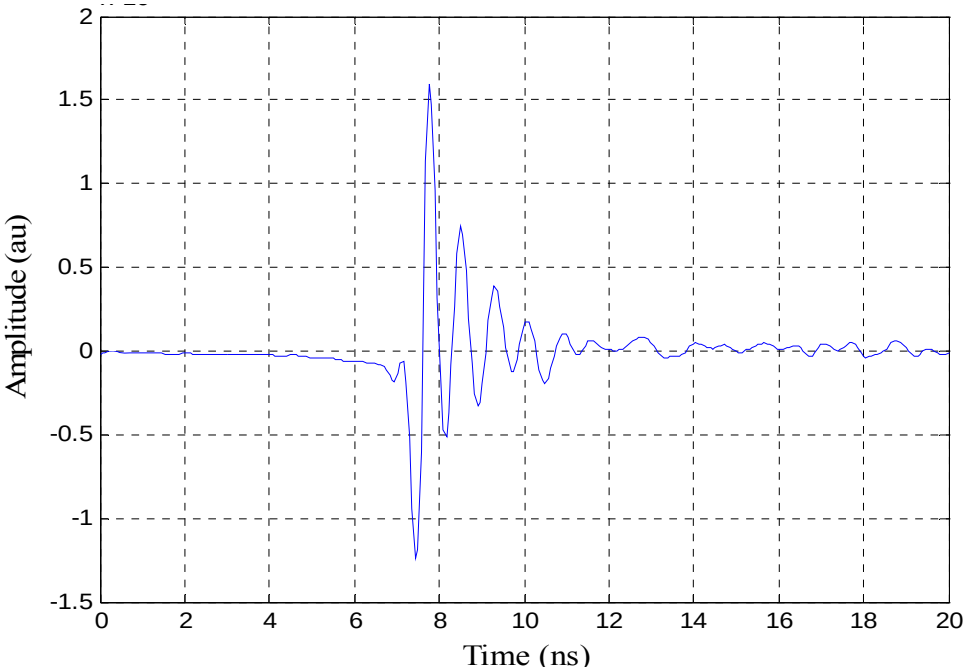

Figure 4-8 CNR frequency of simple wire (L=10 cm, d=0.4 cm).

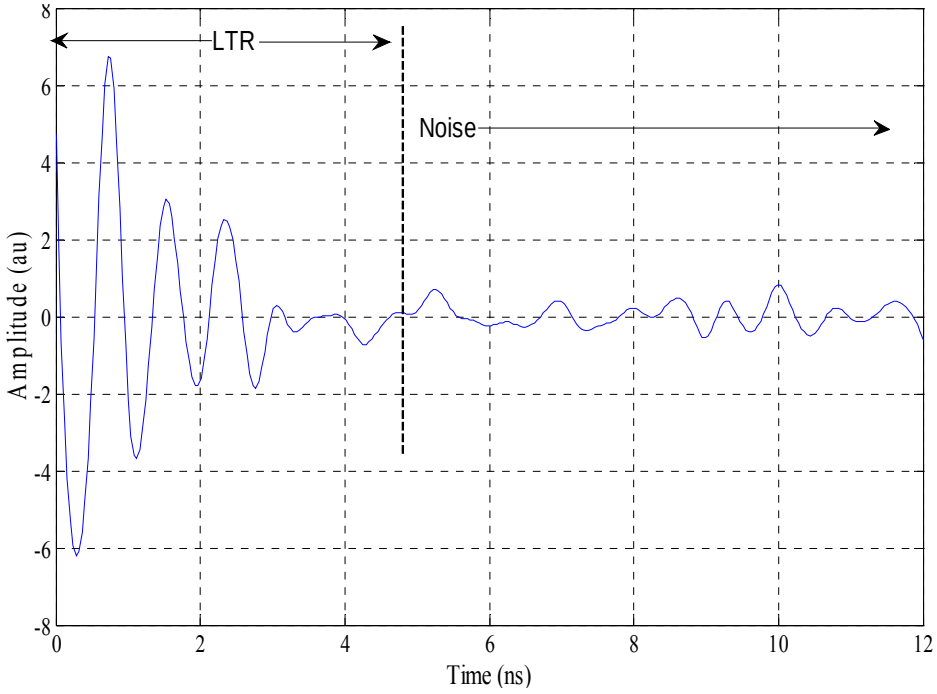

Figure 4-9 LTR of simple wire (L=10 cm, d = 0.4 cm)

The scattered field was measured in the 0.25 – 3.0 GHz frequency band, which includes the object's main resonant frequency region back-scatter where the fundamental resonance at approximately 1.4 GHz. The LTR of the proposed target obtained by convolution of the antenna response with back scattered response, the starting of the LTR determined according to Equation 2.1, LTR is clearly longer than the forced response ETR but it's much weaker.

4.5.2 Wire of 20 cm length

A wire of length L = 20 cm and diameter of d = 0.4 cm was the second simple target to be tested. Again the wire placed 1.5 m far from the antennas and its orientation was 45^{o}. The response of this target could be easily seen, the co-polarization yields smaller amplitudes and low interference could be masked by noise. Thus changing the polarization of the interrogating signal increase the LTR tail and give more confident in the results extracted. Figure 4-10 to figure 4-12 illustrate the object initial response, CNR frequency response and its extracted LTR respectively.

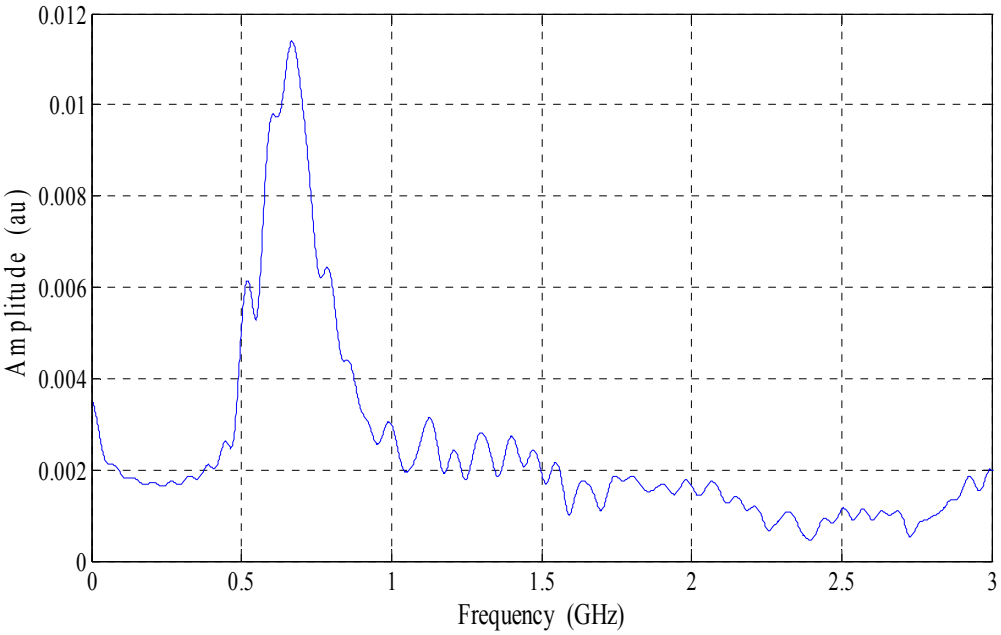

Figure 4-10 Frequency response of wire (L = 20 cm, d = 0.4 cm)

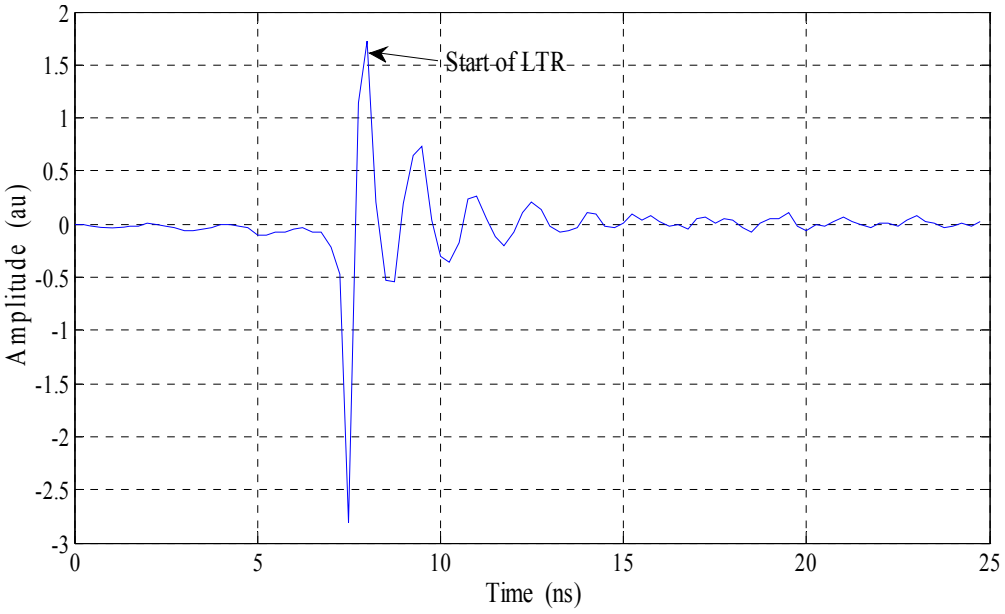

Figure 4-11 CNR frequency response of wire (L= 20 cm, d = 0.4 cm).

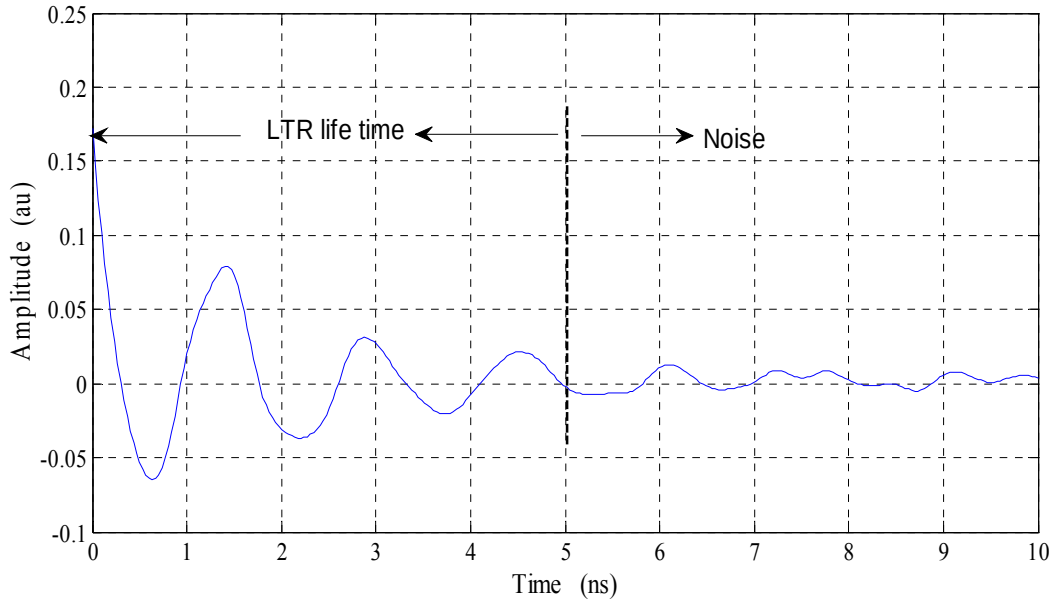

Figure 4-12 LTR of wire (L= 20 cm, d = 0.4 cm).

As can be seen from these figures the natural frequency response of a larger object has its first natural resonance at a lower frequency than corresponding smaller objects. The transient time and consequently the starting of LTR for each object is a function of aspect angle. The maximum transient time of the target being detected should be used to calculate the starting of the LTR since the aspect angle will be unknown in a real situation.

4.6 Complex objects

For most irregular objects such as guns and knives, there are no exact solutions of the theoretical impulse response and frequency CNR It must rely on measured results. The accuracy of the proposed approach is verified by taking the measurements many times, so

that the results can be trusted when applied to other objects. Many incident angles of the interrogating pulse have to be tried in order to extract all the CNR modes.

The performance of the manufactured TSA has been tested to capture back scattering from complex objects such as knifes and handguns. The captured data is recorded by VNA and numerically treated to deconvolution the antenna response from the impulse response and then extract the LTR.

4.6.1 Knife

Figure 4-13 illustrate the tested knife,

Figure 4-13 Tested knife.

The knife's axis was oriented perpendicular to the incident electric field. The dimensions of the knife were length L = 12 cm and the width of the PEC part is $d_1 = 0.11$ cm, the width of the dielectric part is $d_2 = 0.14\ cm$. The initial frequency response for the knife is shown in figures 4-14 to 4-16.

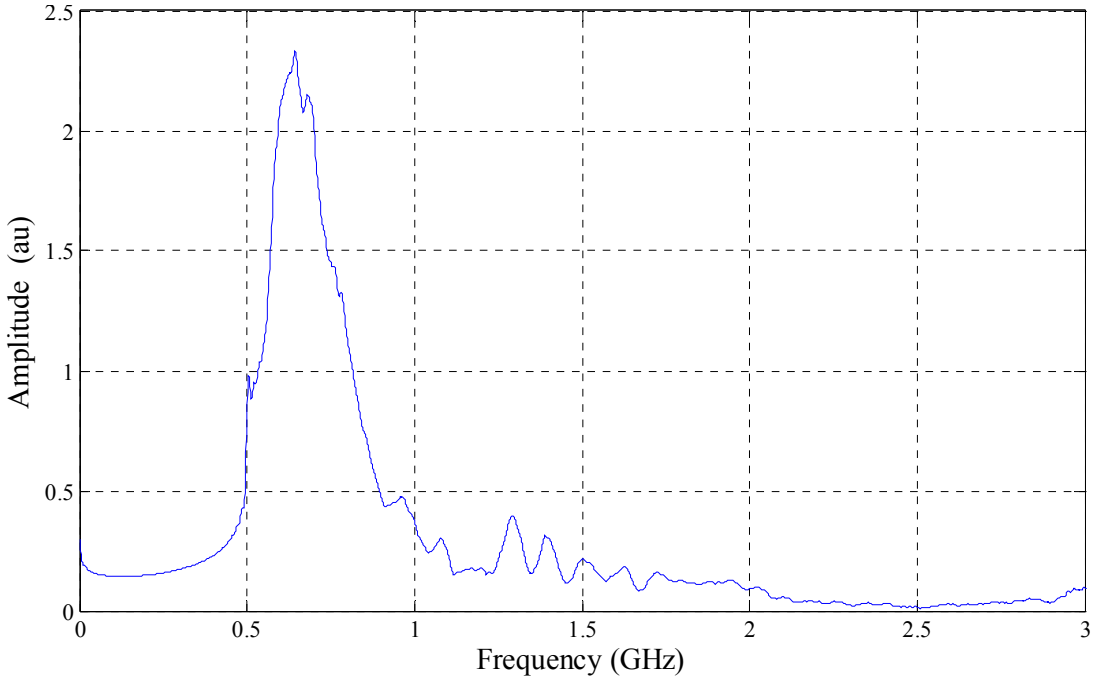

Figure 4-14 Frequency response of a knife.

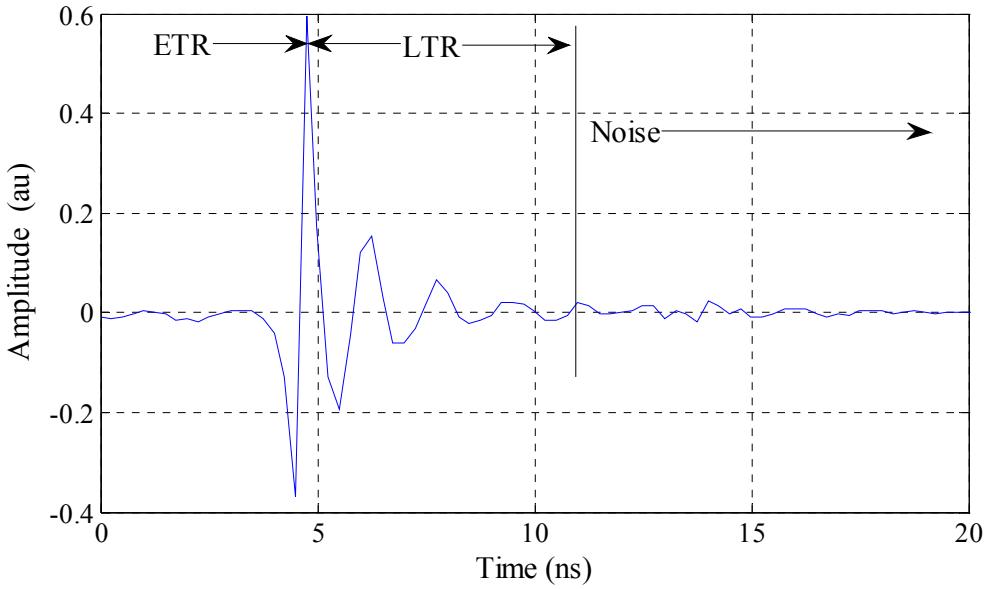

Figure 4-15 CNR of a knife.

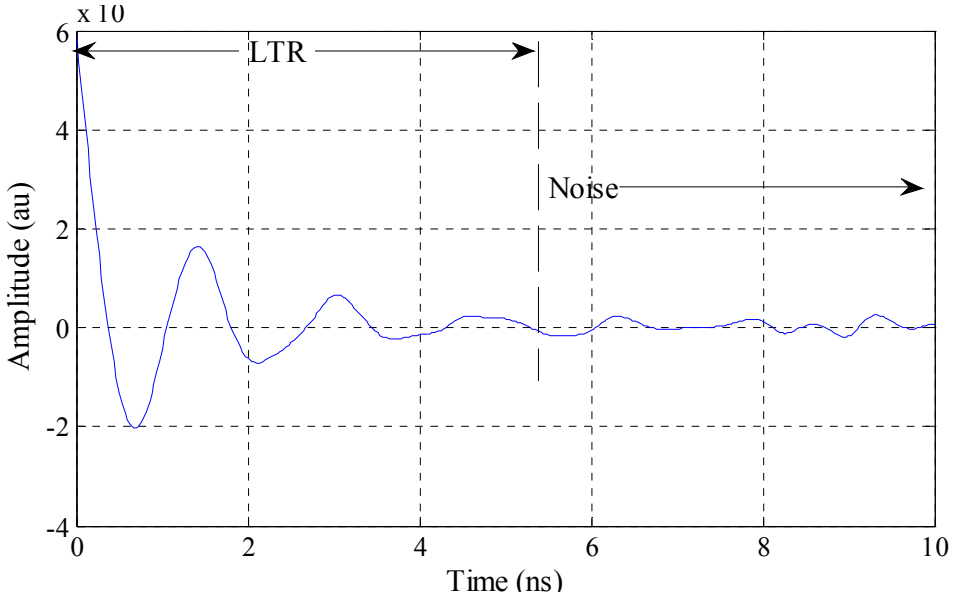

Figure 4-16 LTR of a knife.

The backscattered signal of complex object shape such as knifes and handguns are different from those scattered from simple objects, where they represent the complicated object geometry which sometimes contains dielectric and PEC materials properties, therefore the life time of these signals are sometimes longer**.** This is quite clear in figure 4-16, where the LTR lifetime is less than *6 ns* before it tends to noise.

4.6.2 Small handgun

Handgun with length of L = 16 cm was the next complex object as shown in figure 4- 17 Its aspect for the test was $\varphi = 45^0$ and the backscattered impulse response captured and recorded by the VNA. The transmitter and receiver antennas were again placed for cross-polarized detection.

Figure 4-17 Tested small handgun

Figures 4-18 to figure 4-20, present the responses obtained. The gun is more complex and generally complex geometry object than the simple wire and knife, so its LTR lifetime is more complicated and has more modes. The first fundamental resonance frequency of this handgun is appearing at 0.61 GHz as shown in figure 4-17. It's quite clear that the LTR of the gun is more complex and it has more resonance modes than simple objects.

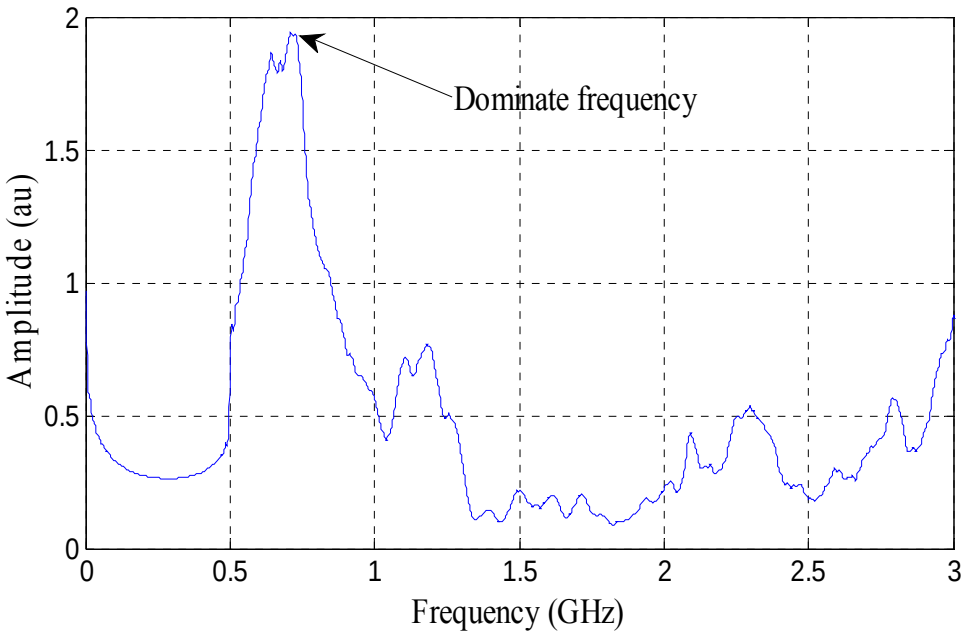

Figure 4-18 Frequency response of small handgun.

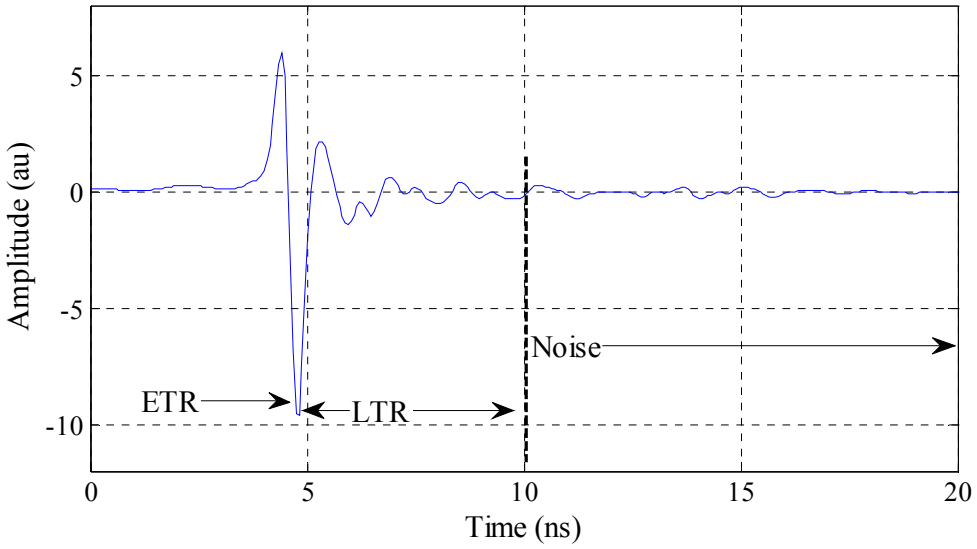

Figure 4-19 CNR of small handgun.

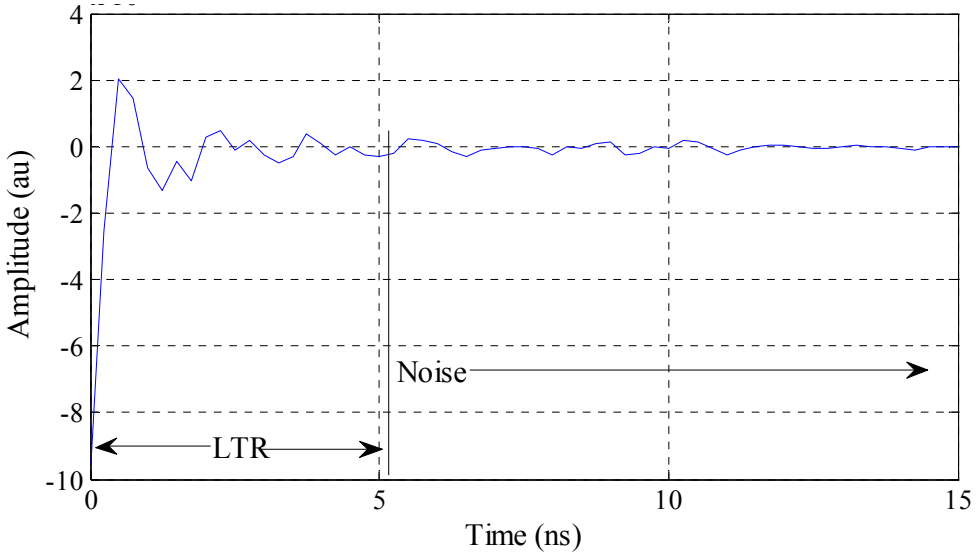

Figure 4-20 LTR response of small handgun.

The LTR of the handgun is clearly visible as the damped oscillations after the reflection of the excitation pulse (sharp peak). Complexity of the LTR related to the multi target edges, in other words the LTR modes are clearly dependent on the target geometry.

4.7 Discussion

In order to test the performance of the designed antenna and capture the backscattered target response a series of experimental measurements were carried out with simple and complex objects. It's found that the LTR ringing of the proposed antenna is very low and the antenna has the ability to detect and capture the backscattered response of different objects. During the experimental target detection, it was found that the presence of background noise and the antenna coupling effects almost overshadowed the real target response leading to masking the LTR and unsuccessful or wrong target identifications. In this research the background and antenna coupling effects are largely eliminated by subtraction of the background when the target is not present from that when target is present. Cross-polarized antennas have great impact on the enhancing of the LTR since apart of the strong early target response is supressed. The captured backscattered target response contains the antenna response in addition to the target re-radiated response. To have purely target response the antenna response is deconvolved by the conjugate gradient method and the background noise is subtracted. An IFFT was used to transform the row data to time domain in order to extract the LTR of each target by the using of equation (2.1) by which the starting of LTR is determined.

For the four different objects examined it was found that the frequency response of the target depends mainly on the target geometry and the frequency response increased in complexity and the LTR had more resonant modes as the object geometry becomes more complex, hence the LTR of the handgun more complex than that of the wire.

4.8 Summary

The antennas designed and made to illuminate the target and collect the backscattered target response have been tested and performance validated. Simple and complex objects were illuminated and interrogated and their LTRs were captured.

The measurements were accomplished for the various targets in the frequency band 0.25 – 3 GHz. Distance between cross-polarized antennas was 1 m, distance between antenna and target was around 1.5 m. The captured raw data was treated by the MATLAB algorithm. The background was subtracted, the antenna response convolved then the data was subjected via an IFFT to the windowed backscattered response to extract the LTR for each target. In the next chapter a new approach to filtering the target LTR to extract its unique signature will be presented.

Chapter 5

Continuous Wavelet Transform (CWT) Analysis of Target Signature

5.1 Introduction

In chapter 4 response of the tested objects were analysed in the time domain signal to extract the starting of the LTR for the target detection and identification. In this chapter attention is focused on the second topic of the research in which, the target signature is extracted and represented by TFDs using the CWT, the time-frequency analysis method is described that will be applied to the target feature aspect independent backscattering LTR response. Continuous wavelet transforms (CWT) are applied to the experimental data of various wire dimensions, off and onbody threat objects such as knife and handgun in order to extract the LTR signature features.

5.2 Why joint time-frequency analysis?

The transient scattering returns of a radar target in free space was first modelled by SEM. In the given model late-time period of the target response was obtained as a sum of damped exponentials convolved with resonant frequencies and noise. This beneficial characteristic allows the resonances to be used for target identification. Widespread discussions took place in the mid 1980s to develope a model of the transient scattering behaviour and modelling for early time response, Dudley (1985, Felsen (1985). SEM model has neither been a true reflective nor there a nearby solution to this problem due to

the intricate nature of the process itself. As discussed previously in chapter 2, Prony's method suggests target resonance extraction to be directed upon the interval of late time response, if the nearby objects are included in the extraction, fairly accurate CNR extraction is achieved. Prony's method thus requires that accurate late time commencement evaluation is critical for the overall accuracy of target resonance extraction. Late time responses are target dependent and theoretically independent of polarization state and target orientations. However, practically the late time period cannot correctly extracted in some cases.

Knowledge of the model order is critical in the extraction process and in the subsequent calculations for poles and residues algorithms. If the model order is underestimated this can cause loss of poles in the calculations. Similarly, resonant modes are unlikely to be excited or weakly excited in all incident aspects and states of polarization due to a dependency on residues. It is apparent from the complexity of the methods and algorithms involved that another method is required for the extraction of the resonant modes. To increase further the physical insight of the problems connected to the authentic transient electromagnetic scattering procedure, one feasible approach is to examine the scattering phenomena analytically using electromagnetic theory. This has been extensively studied by Heyman and Felsen, (1985), Heyman et al., (1989), Heyman and Felsen (2002) and Shirai and Felsen (2002). It is well recognized fact that analytical solutions to transient electromagnetic problem involve huge mathematical calculations and are imperfect for some canonical problems. An alternative choice, stemming from a

signal processing perspective is to apply Joint TF analysis and this chapter discusses the various possibilities. In this chapter the discussion upon the various distributions for TF analysis is presented.

The joint time-frequency analysis has been commonly applied in many engineering applications such as signal processing in bio-medical data, speech processing, wireless communication, radar imaging and sonar applications. With radar applications in particular substantial work has been carried out on stationary targets using frequencies in the low GHz frequency region i.e. up to 2 GHz. For UWB radar a substantial amount work on feature extraction has been done by Ling and Kim (1992) and Chen and Ling (2002) on TF analysis of backscattered signals including the range of the profiles for the stationary targets.

These later applications frequency of operation is in the quasi-optional regions. GTD in the electromagnetic context describes that quasi-optional regions lie outside the essential resonant modes and high frequency scattering portents such as edges and corners diffraction, Balanis (1989). The particular focusing in this research is on the late-time resonant that are observed in the SEM and to study the scattering phenomena of the objects using TFDs which is the second core of this research. As TFDs are of a complex nature, studies of TFDs on the objects response will be considered first as these version has its specific pluses and minuses. The doubts around various TFDs are explained.

The Wavelet transform is introduced as alterative approach to overcome the STFT resolution limitation, a detailed explanation of the wavelet theory could be found in

Moghaddar and Walton (1991), Hwil and Walnut (1989). Particularly, the wavelet transform utilizes the wavelet as a 'window' and also as a fundamental for the analysis of multi resolution, (Kaiser, 1994). To provide good time resolution (small scales) at high frequencies the 'mother' wavelet is compressed so that the wavelet of the time response provide effective resolution in detecting the presence of high frequencies. To have a good frequency resolution at low frequencies the mother wavelet is expanded (large scales), by which the wavelet transform has effective resolution in frequency domain in detecting the appearance of the low frequencies. In fact, in this research the CWT approach is proposed to extract the target signature and represent the LTR in time frequency domain. A Morlet wavelet is used as the mother wavelet within the CWT algorithm because it is simple and well suited for time frequency localization and resolution for concealed weapon application. The CWT provides coefficients in which the degree of correlation is proportional to the peaks or amplitude. Another perspective is that the analysed signal decomposes into a superposition of scaled mother wavelets by the wavelet transform.

The scattered response of the concealed weapons involves a forced (direct) return response from an early time event which aspect target dependent and resonance at the late time event which is aspect independent to the target. In order to extract the target signature that appears in the late time response it is desirable to use good time resolution in the ETR and good frequency resolution in the LTR, a CWT with a 'Morlet' wavelet mother is used for this purposes.

The aim of this study is to examine TFDs to represents electromagnetic scattering though extracting the LTR which is very useful for object identification and classification. Different simple and complex targets signatures are studied. Instead of new approaches of extracting resonance parameters directly or development of existing methods, the role of the study is for novel development of object recognition algorithms using the CWT.

5.3 Linear class of time-frequency transform

Standard Fourier analysis takes the whole interval of the signal in time and then takes the transforms when compared with STFT in which the signal is first windows with a time-limited window then transform the frequency domain via Fourier transform. The STFT was the first tool used for studying time varying signals. The STFT considers the spectrum of frequency for a signal for a short period of time. The STFT of a time domain signal can be mathematically described as

$$F_s(t,f) = \int_{-\infty}^{+\infty} x(\tau)h(\tau - t)e^{-j2\pi f\tau}\, d\tau \tag{5.1}$$

Here, the signal is *x(t)* while the window function or basis function in the time domain is represented as *h(t)*. If the signal *x(t)* is a linear grouping of some specific signals components then the STFT of the signal *x (t)* is the linear sum of each of the signal components (Hlawatsch and Boudreaux-Bartels, 1992). The STFT satisfies the linearity principle. If

$$x(t) = c_1x_1(t) + c_2x_2(t), \tag{5.2}$$

Then, $$F_x(t,f) = c_1 F_{x_1}(t,f) + c_2 F_{x2}(t,f) \quad (5.3)$$

The subsequent transform is known as the power spectrum TF.$|F_x(t,f)|^2$ the resultant transom is considered and it is known as SP. The limitation of the STFT is that due to the constraint of the uncertainty principle, it is not possible to get accurate time and frequency resolution simultaneously i.e. to obtain fine resolution in the frequency domain the resolution in the time domain will degraded and vice versa (Cohen, 1995 and 2002; Percival and Walden, 2006). Mathematically this can be expressed as

$$\Delta t \Delta f \geq \frac{1}{4\pi} \quad (5.4)$$

Here, Δt is known as the duration and Δf is the bandwidth of the signals (Cohen ,2002). For attaining adequate resolution in the time domain a small value of Δt is essential. This means Δf has to be larger due to the limitation imposed by the uncertainty principle, see Equation (5.3). Similarly for adequate resolution is required in frequency domain. By applying TFDs under the bilinear class, such limitations can be controlled, see the next section. The fundamental idea here is to substitute the frequency shifting or time shifting operation that occurs in the STFT by a time or frequency scaling operation respectively (Kim and Ling, 1992 and 2008; Rioul and Flandrin, 2002; Hlawatsch and Boudreaux-Bartels, 1992; Chen and Hao, 1999; Sadiku et al., 2005; Rioul and Vetterli, 1991).

5.4 Continuous wavelet transform

In the application of detecting the response of concealed onbody weapons, powerful signal processing algorithms that accurately extract the target signature is needed. In this

section CWT time frequency analysis method is used for analysis and extracts the target signature from the backscattering response. Hence the wavelet transform is a powerful TF analysis and it has a multi resolution capability which is not available in WVD and STFT. The basic variable of Fourier Transforms, the frequency, is not possible directly with wavelet transforms instead a new term called "scale" is used and the wavelet transform introduces time-scale representation (Young, 1992).

Many mother-wavelets are utilized for varies implementation and applications. The best known are Morlet, Daubechies and Haar wavelets. Also of great importance are the coiflet, symlet, Mexican Hat and biorthogonal wavelets. In signal analysis applications, it is usual to extract signal features with Fourier transformation, but only if the time domain transform has no time-frequency localization features. The theory of wavelet transformation was first proposed in the field of multi-resolution analysis; among others, it has been applied to image and signal processing. A CWT can analyse a signal into a set of limited basis functions, which can uncover transient features in the signal. Wavelet analysis is the contravention up of a signal into dilated and translated versions of the original mother wavelet. The wavelet should be oscillatory, have amplitudes that speedily tends its decay to zero, and has at least one vanishing moment, (Young, 1994; Torrence and Compo, 1998).

In the wavelet theory many wavelet mother functions have been considered because every wavelet mother has its suitable application. In this work, the chosen mother is Morlet wavelet because of its advantages and features such as, it's fine tuning to the

desired frequency band, good resolution and localization in time and frequency domain, capability of detection and extraction oriented features Torrence and Compo (1998). Morlet wavelet mother is a sinusoidal signal modulated by a Gaussian wave. Its offers higher spectral resolution compared with Mexican Hat, this is because of the narrow frequency response. This wavelet is particularly useful for filtering out the background noise of the target response.

The CWT is the member of the linear class of TFDs. The prime definition of the CWT is,

$$CWT_x(t,\alpha,h) = \frac{1}{\sqrt{\alpha}}\int_{-\infty}^{+\infty} x(\tau)h\left(\frac{t-\tau}{\alpha}\right)d\tau \tag{5.5}$$

Here the mother wavelet is known as *h(t)* and is localized in time, the continuously varying scaling parameter is *a.* The CWT transforms a one dimension time domain signal *x(t)* is plotted into a two dimensional space across scale a and time scale t. The CWT can be considered a member of Time-Scale Distribution (TSD) series. This section contains the details of TSD. If we compare the STFT with the CWT, then CWT is different from STFT as it can longer be adapted to modulation or frequency shifts as it now created by scaling factor a though the price paid is that the CWT gives a time-scale representation of the signal rather than a time- frequency representation. if we set $\alpha = \frac{f_o}{f}$ where f_o centre frequency of $h(t)$, for the TF analysis application, the subsequent distribution can be written as (Rioul and Flandrin, 2002; Hlawatsch and Boudreaux-Bartels, 1992)

$$CWT_x(t,f,h) = \sqrt{\frac{f}{f_0}}\int_{-\infty}^{\infty} x(t)h\left(\frac{t-\tau}{f_0}\right)d\tau \tag{5.6}$$

The magnitude of the CWT is called as the Scalogram (SC) and is similar of the SP.

$$|CWT_X(T,F,H)|^2$$

The mother wavelet needs to satisfy certain mathematical criterion. A complex or real-value function *h(t)* is defined as a wavelet if,

$$\int_{-\infty}^{\infty} h(t)dt = 0 \tag{5.7}$$

This shows that a wavelet must have a zero dc component i.e zero average value in the time domain. This indicates that in the frequency domain the signal must be oscillatory. Admission Condition is another condition that a wavelet has to mollify, which is given by Rioul and Flandrin (2002) as:

$$\int_{-\infty}^{\infty} |H(f)|^2 \frac{df}{|f|} = 1 \tag{5.8}$$

Here

$H(f)$ = is the Fourier Transform of $h(t)$.

It can be shown that the signal $x(t)$ can be recovered from the following equation Rioul and Flandrin (2002)

$$x(t) = \int_{-\infty}^{\infty}\int_{-\infty}^{\infty} CWT(\tau,\alpha,h)h\left(\frac{t-\tau}{a}\right)d\tau\frac{da}{a^2} \tag{5.9}$$

A large number of wavelets meet the Admission Condition only if $h(t)$ satisfies the Admission Condition. The Morlet wavelet is one of the most frequent used wavelets that does this and is given by Sadiku et al. (2005) as

$$h(t) = e^{jw_0 t} e^{-t^2/2} \tag{5.10}$$

It must be appreciated that individual wavelets have different characteristics so they are appropriate for different applications. To discover whether the multi-resolution property of the CWT is appropriate for investigating transient scattering consequently, it is necessary to decide which mother wavelet is selected. Expecting the result somewhat, in this thesis it is the multi-resolutions characteristics of the Morlet CWT that are examined to determine whether the CWT is a convenient method extracting the LTR of concealed weapons. TSD in the signal processing literature was first introduces with respect to the CWT and then later applied to TF analysis by Rioul and Flandrin (1992). CWT produces a fixed time and frequency resolution throughout the 2-D plot if compared to STFT; the CWT has a multi- resolution capability like TSD. The CWT gives a good time resolution but poor frequency resolution when a is small (high frequency as $a = f_o / f$), but good frequency and poor time resolution when a is large i.e. low frequency (Debnath, 2003). As shown in figure 5.1 (a), the SP TF tiling is assumed to be unchangeable in the whole time and frequency band, however in CWT the SP varies according to the time and frequency changes as shown in figure 5.1 (b).

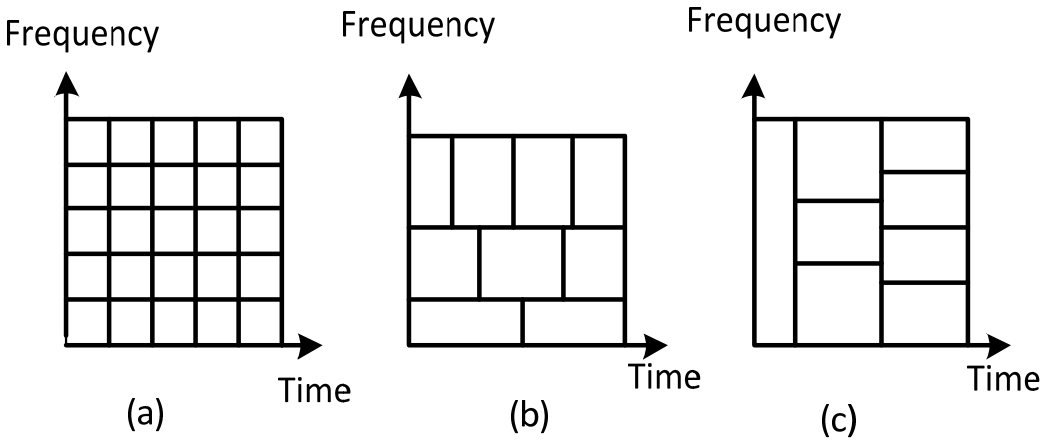

Figure 5-1 Comparison between TF tiling of (a) SP, (b and c) CWT

Time and frequency resolution at both high and low frequencies are essential in this thesis and thus a perfect solution for our application cannot be found using multi-resolution features (Auger et al., 1996). The multi-resolution features of the CWT offers another solution or it can be said, a substitute for TF analysis. In fact, the notion of time-scale has also been comprehensive and applied to other TFDs and these are collectively acknowledged as the time-scaled or affine class TFDs.

Ling and Kim (1992) have successful reported work on TF analysis for electromagnetic scattering using the SP and CWT. Although, the wavelet transform they used is unlike the standard explanation presented here were the wavelet transform is distinct in the frequency domain as an alternative of time domain and is given by Equation (5.9). The wavelet transform described by Kim and Ling (1993) was given as

$$CWT_x(\tau, \Omega, H) = \int_{-\infty}^{+\infty} X(\omega)\sqrt{\tau}H\big(\tau(\omega - \Omega)\big)d\omega \tag{5.11}$$

Where H(t) is the mother wavelet, X(ω) is the Fourier Transform of signal x(t). Equation (5.10) might be expressed as analysis of the frequency signal $X(\omega)$ to a set of dilated and shifted wavelets $H(\tau(\omega-\Omega))$. This wavelet fundamental function has changing width which is dependent on τ at every frequency Ω. $H(\tau(\omega-\Omega))$ is larger for small τ and smaller for bigger τ. accordingly; high time resolution is obtained in the ETR (small value of τ) and high resolution of frequency in the LTR (large values of τ).

In subsequent sections practical measurements will be reported for simple and complex targets of scattering phenomena and electromagnetic transients using the CWT. The main purpose of this chapter is to conduct an in-depth study of the experimental results of samples of different dimensions of simple and complex targets. The purpose of this study is to examine the LTR scattering phenomena for TFDs based on the CWT and analyse what possibilities and limitations are faced. This is to achieve a comprehensive understanding about scattering problems so as to highlight different types of scattering concepts, their existence and practical occurrence and how they interact with the TF domains of the targets.

The two dimensional TF plots for the test targets will be considered to obtain a better understanding of the applications of concealed weapons recognition and classification. The chapter will conclude by presenting practical and theoretical limitations of TFD.

The same experimental setup was used for these tests as described in chapter four unless otherwise stated. A Gaussian shaped window was used throughout and the frequency target response were subjected to background subtraction, deconvolution of the antenna

response and then an Inverse Fourier Transform was used for sample transformation into the time domain. The start of the LTR was determined using Equation 2.1.

5.5 Simple wire

Available literature shows that a huge amount of work has been carried out on the transient scattering phenomena (chapter two presented a literature review of such work). Similarly extensive research is available for the study of scattering and its behaviour using common wire as a target. To be more specific, the LTR behaviour of a wire target is a commonly studied in the SEM context. For obtaining an in-depth and better study, three different examples of a wire target have been used for TF analysis. In the first test the LTR resonance modes are extracted by the use of GPOF and the CWT was also used to obtain their behaviour in the TF domain.

The second test used different wire lengths and diameters to identify the CWT performance and its ability to represent and extract the LTR target signature in TFDs. In the third and final example, complex target such as a knife and gun were considered (on- and off-body) for CWT analysis. The purpose of conducting these tests was to study the occurrence and existence LTR resonance events in the TF domain.

5.5.1 Late time resonance modes extraction:

In the first experiment a wire with length L = 21 cm and diameter d = 4 mm with incident target orientation angle $\varphi = 45^{o}$ is considered. The same experimental setup described in Chapter Four is used here and for all of the subsequent experiments unless otherwise stated. A Gaussian shaped window was used after which the frequency target responses

were subject to background subtraction, deconvolution of the antenna response and then an Inverse Fourier Transform for transformation to the time domain. The start of the LTR is measured by the use of equation 2.1. In this experiment the forced ETR target response starting at 3 ns and thus $Tb = 3\ ns\ with\ Tp = 14\ ns, \varphi = 45^{o}$.

$$T_{tr} = \frac{L\ sin\ \varphi}{c} = 0.59\ ns$$

This provides that the late time life time to be around 10ns. LTR resonance modes are extracted by using the GPOF, (Harmer et al., 2009). Figure 6.1 shows the scattering poles of the wire of length 21cm extracted by the GPOF with estimated model order *M = 6*. It was stated previously that GPOF is very sensitive to the target model order which means that any bad estimation will lead to spurious poles and increase the error of target detection and identification.

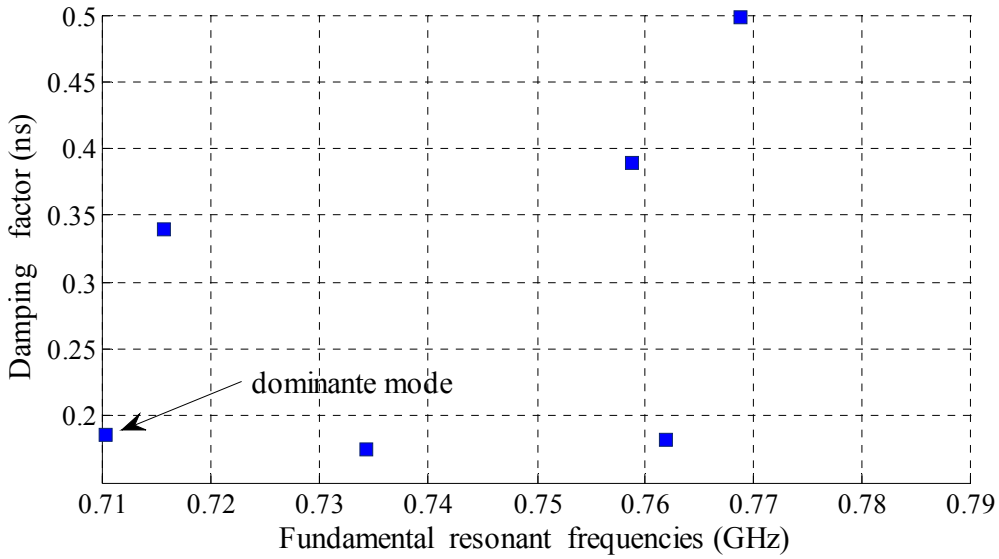

Figure 5-2 Poles of wire of length 21cm

From figure 6-1 it is seen that the dominant mode resonates frequency is close to the theoretical value $f_{res} = \frac{c}{2l} = 0.71GHz$ where c is speed of light and l is the target length, (Kraus, 1988). The lowest pole of the scattering has a similar resonant frequency of the LTR and can be used to reconstruct it by

$$f\big((n-1)\Delta t\big) = \sum_{m=1}^{N} c_m \, e^{s_m (n-1)\Delta t} \tag{5.12}$$

Where $s_m = \sigma_m + i\, w_m$ are the poles and c_m are the residues, σ_m is the damping factor and w_m is the resonant frequency (Chen and Geng (1999). the first three resonances values are for the 21cm wire are $1.5 - i2.2500, 3.0000 - i1.5000\ and - 4.5000 + i2.2500$ (imaginary parts in GHz and real parts inns^{-1}).

The frequency bands of interest of the particular target wire determined from the results of GPOF are considered as points of reference for the initial dominant modes of resonance. In this subsection a simple case of an idealized target response using the resonant modes is considered. The construction of these artificial responses is based on equation 2.6, using the resonant modes shown in figure 6-1. These resonance modes are different with respect to their resonant frequencies and damping factor, and therefore in the TF domain of CWT there should be significant separation for these resonant modes. From figure 6-2 the dominant resonant frequency can be calculated from consecutive peaks – these are about 1.5 ns apart corresponding to the dominant frequency mode of about 0.7 GHz. This is in agreement with figure 5-3. Figure 5-4 shows the frequency responses of the target backscattered data in which the dominant resonance frequencies are quite clear. Figure 6-3 shows the IFFT of the frequency response in which the

commencement of the stating of LTR is around 3*ns*. Figure 5-5, presents the CWT result in which all of resonance modes of the target signature are obvious in the 5 energy levels.

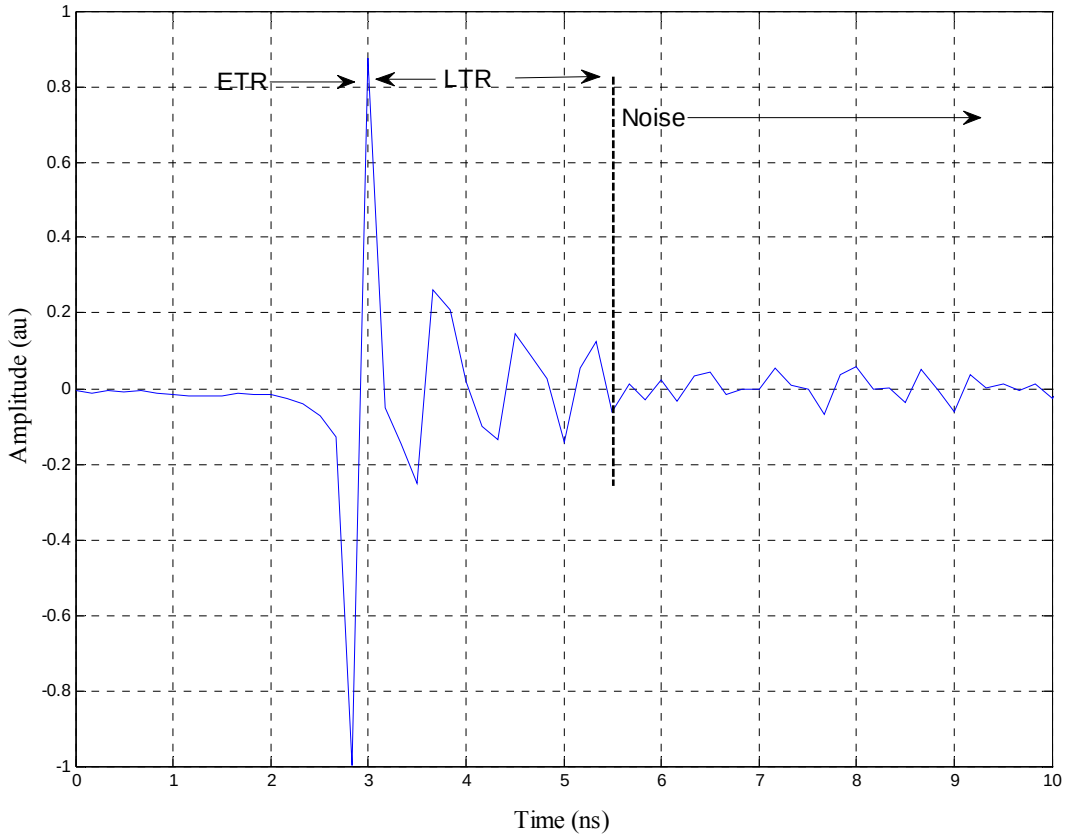

Figure 5-3 CNR wire of (L= 21cm, d = 0.4cm).

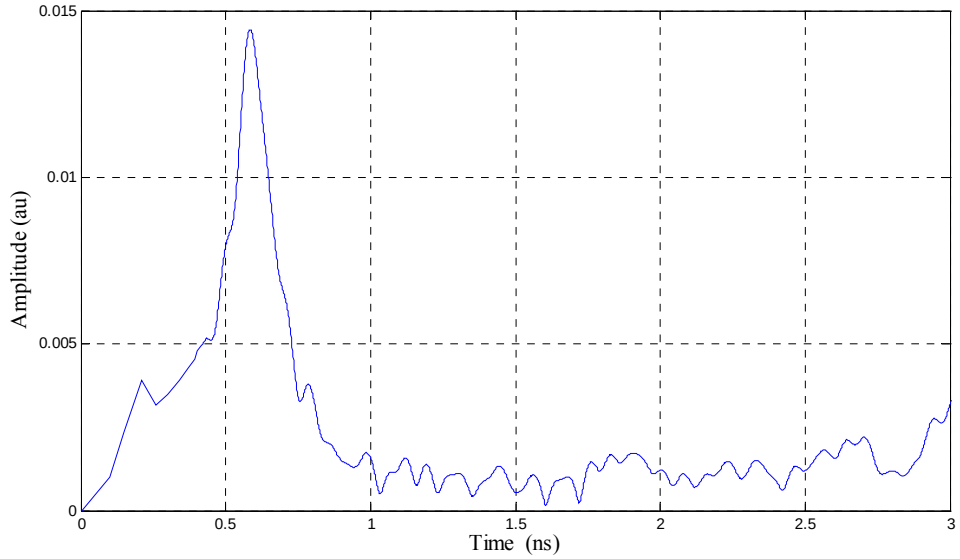

Figure 5-4 Frequency response of wire (L= 21cm, d = 0.4cm).

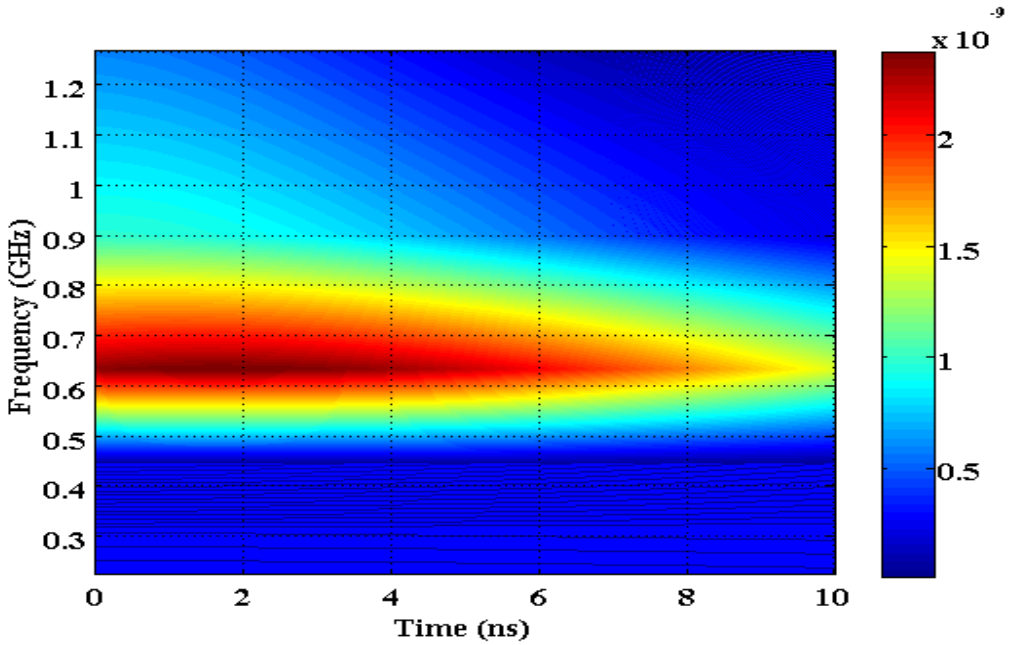

Figure 5-5 CWT of wire (L= 21cm, d = 0.4cm).

It is quite clear that the reconstructed signal of the TFDs which is computed using a CWT algorithm shows most of the dominant resonance frequencies according to energy levels. in which the dominate frequency mode has highest energy levels which labels by red colour, the other frequency modes have less energy level that labels with light red, yellow and ends with blue in which energy level is zero and it indicates the end of LTR life time. As the late time period of the signals is extracted, we choose to label the start of this period as 0, i.e. $t = 0\ s$ on the TF plots as in figure 6-4, which actually corresponds to the beginning of the late-time, i.e. 3 ns after the pulse is emitted from the antenna. The figure shows both the time and frequency domains of the signal.

For the TFDs a frequency of 0 to 1.3 GHz was chosen as the dominant resonance mode of this wire (~ 0.67 GHz) is included in this range. In figure 5- 5 all of the LTR resonant modes can be seen according to their energy levels, this makes the CWT convenient to extract the LTR target signature as it has good frequency resolution in the LTR period and good time resolution in the ETR period. It is observed that high energy levels are been observed at the frequencies that correspond to the frequency peaks for all the plots, providing the general conclusion in the scenario where $\sigma \ll \omega$ the relevant energy *E* of a single mode signal would be given by $E = \frac{Z^2}{\varepsilon}$ where *Z* is target impedance, ε is the target permittivity properties. The results show that the energy of the basic frequency of ~ 0.67 GHz is of higher energy level. The CWT shows an enhanced or a very good concentration of signal at the correct frequency after reassigning that is very clear on the

energy levels of the dominant frequency by which the dominant resonant frequencies have the higher energy levels.

5.6 CWT performance on wires of different dimensions

In this section four experiments were carried out to determine the entire response of four wires with different lengths and diameters, photos of these objects will be found in Appendix A. The aim here is to investigate CWT suitability to extract the LTR modes from different target signatures. For the first two experiments the wire diameter was constant and the length changed, and in the third and fourth experiments the wire length was kept fixed and the diameter changed.

5.6.1 PEC wire 1: length 20 cm and diameter 0.4 cm

In this experiment a PEC wire with length L = 20 cm and diameter d = 0.4 cm is tested and the backscattered response captured by the VNA via the receiving antenna. The LTR response of this wire is illustrated in figure 5-6. The figure clearly illustrate that the occurrence of the resonant modes in the scattered field can easily be identified. Furthermore, figure 5-7 shows the results arising from the application of CWT to the proposed target response. As mentioned before since only the LTR is considered in this section the time scale is shifted back to $t = 0s$, corresponding to the beginning of the LTR. This will be done in all the subsequent practical examples. The overall time limit of the signal is the LTR life time.

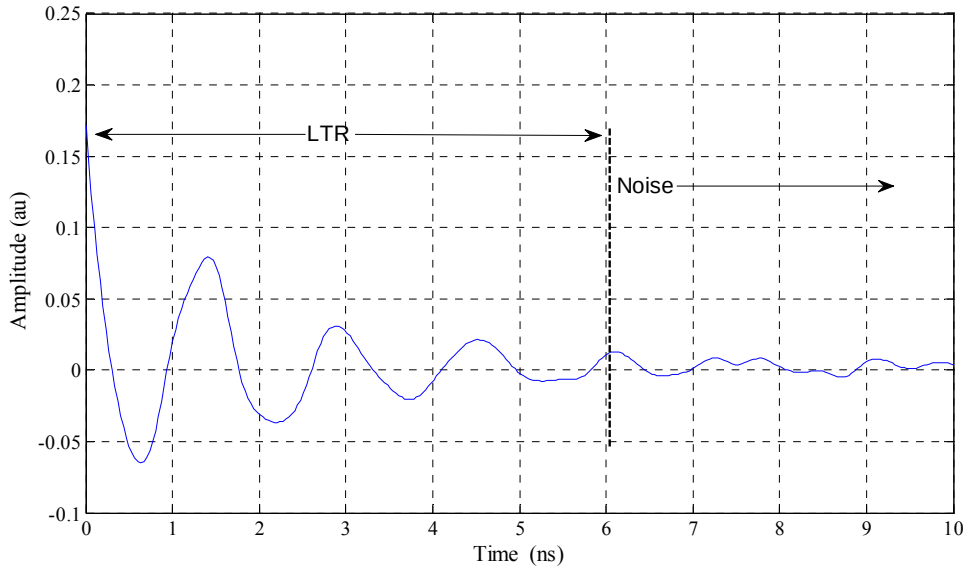

Figure 5-6 LTR of wire1 (L =20 cm and d = 0.4 cm).

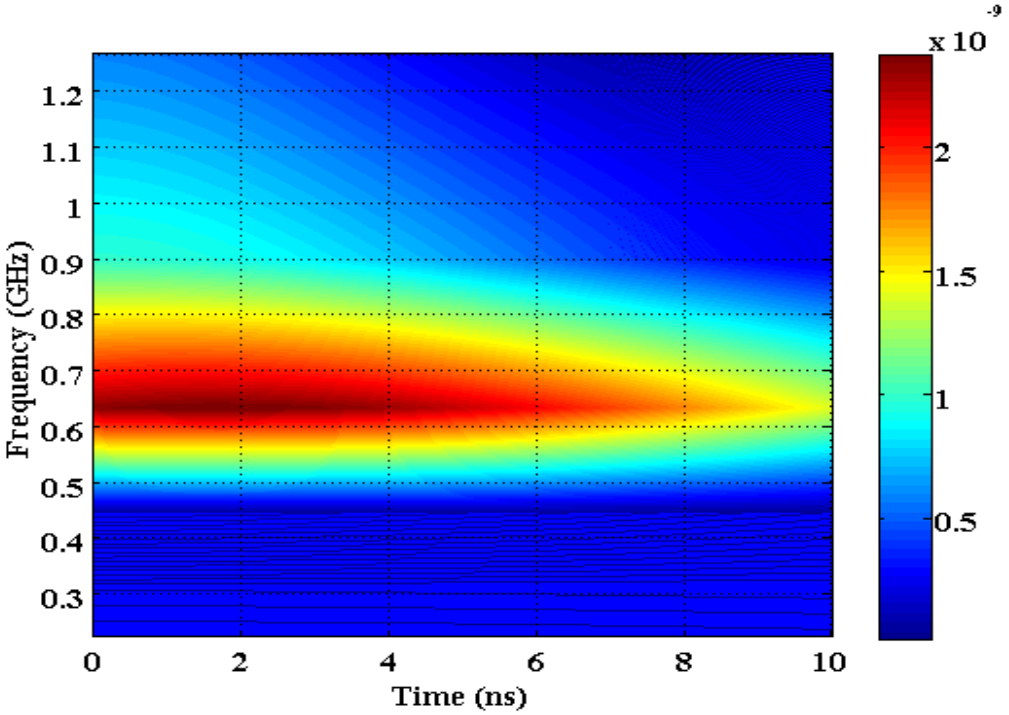

Figure 5-7 CWT of a wire 1 (L = 20 cm and d = 0.4 cm).

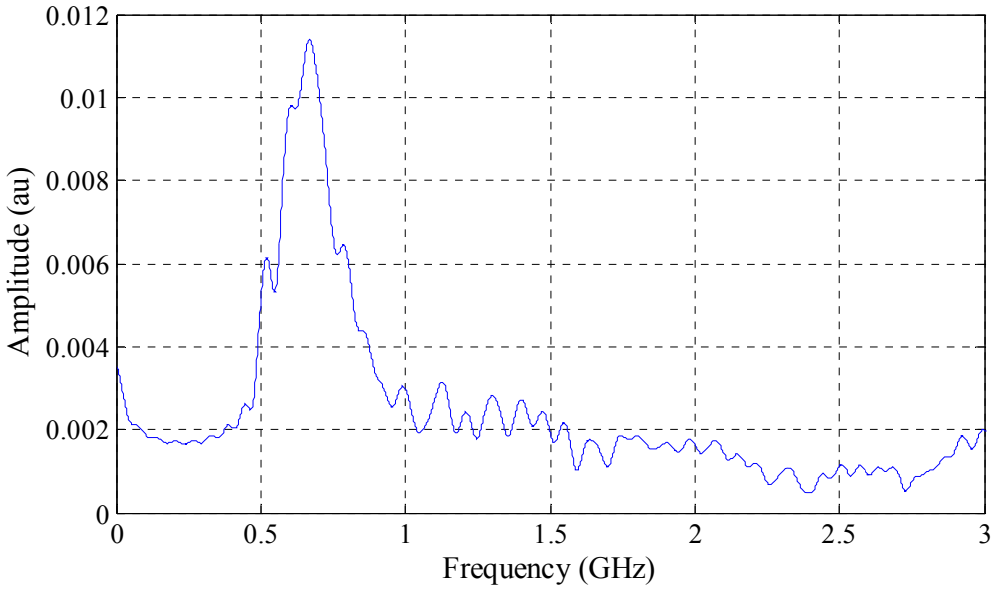

Figure 5-8 Frequency response of a wire 1 (L = 20 cm and d = 0.4 cm).

The results presented in figure 5-7 show that the dominant high energy LTR events can be clearly seen. The dominant resonant frequency of this object is appear at ~ 0.67 GHz which has the highest energy level, however, the rest of the target response spectrum has energy levels so low as shown in Figure 5-8. This result also confirms the decaying nature of the LTR.

5.6.2 PEC Wire 2: length 10 cm and diameter 0.4 cm

The second experiment was with a PEC wire of length L = 10 cm and diameter d = 0.4 cm. The object faced the transmitting and receiving antennas and the back scattered data was captured according to the procedure stated earlier. The purpose here is

to study the performance of the CWT when the length of the target is changed while the diameter was kept constant. Figure 5-9 presents the LTR life time of this target.

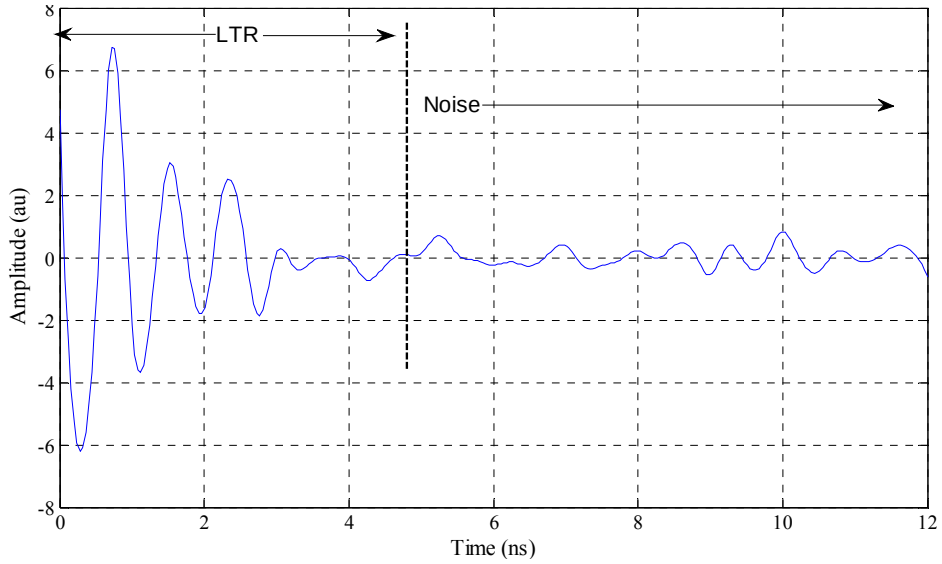

Figure 5-9 LTR of a wire 2 (L = 10 cm and d = 0.4 cm).

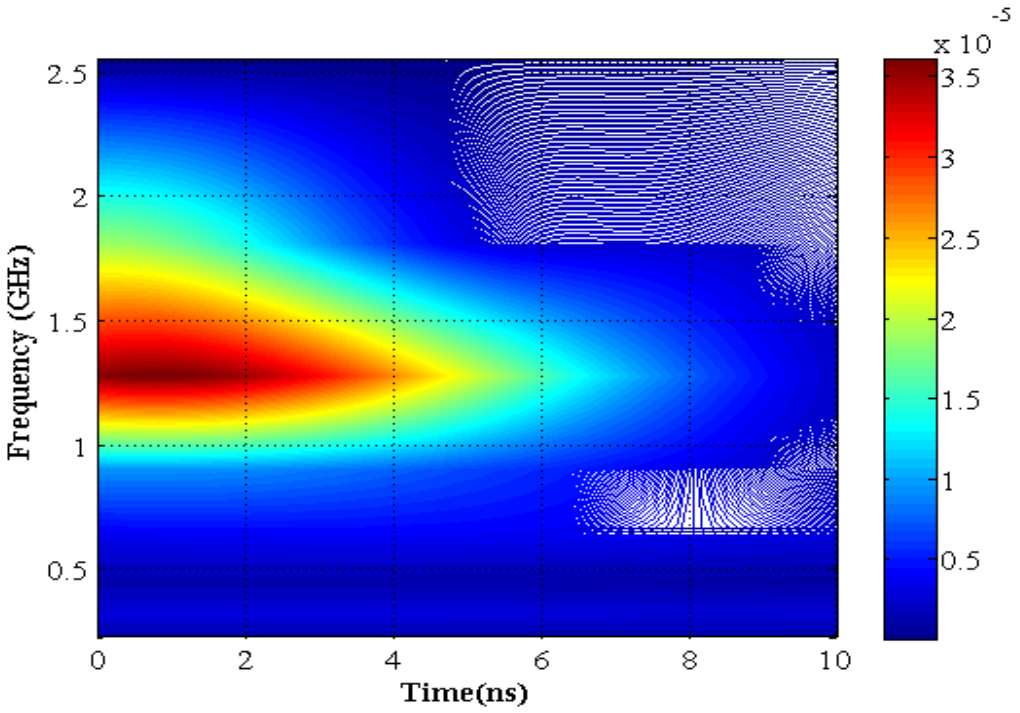

Figure 5-10 CWT of a wire 2 (L= 10 cm and d = 0.4cm).

Comparing the results of Figures 5-7 and 5-10, it is found that the target size (length) affected the lifetime of the LTR. In figure 5-10 for the 20 cm long wire the LTR life time is around 7 ns before it is lost in noise, while for the 10 cm long wire the life time of the LTR is around 4.0 ns as illustrated in figure 5-10.

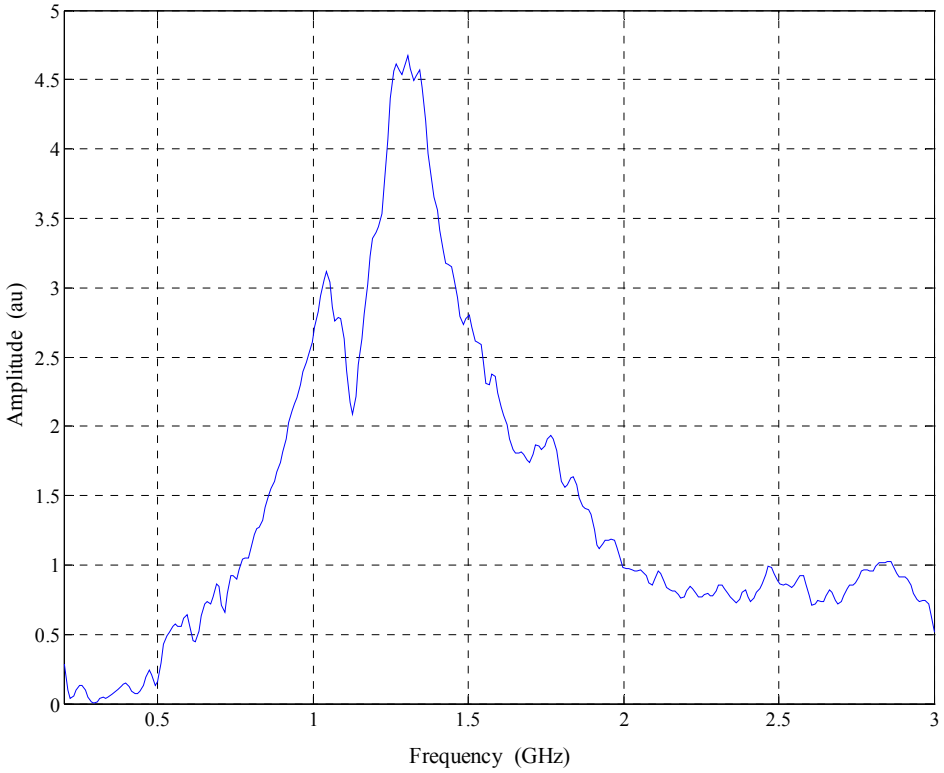

Figure 5-11 Frequency response of wire 2 (L= 10 cm and d = 0.4 cm).

Figure 5-10 and figure 5-11 show the CWT and the target spectrum respectively for the 10 cm long wire. It's very clear that all of the dominant high energy LTR modes can be distinguished.

5.6.3 PEC wire 3: length 15 cm and diameter 0.4 cm

Next, attention is paid toward the performance of the CWT when the diameter of the proposed target is varied and the length kept fixed. In the following two experiments the length is kept fixed at 15 cm while the diameter is changed as will be illustrated. In the

first example a PEC wire with length L = 15 cm and diameter d = 0.4 cm is considered. Figure 5-12 present the LTR of the target.

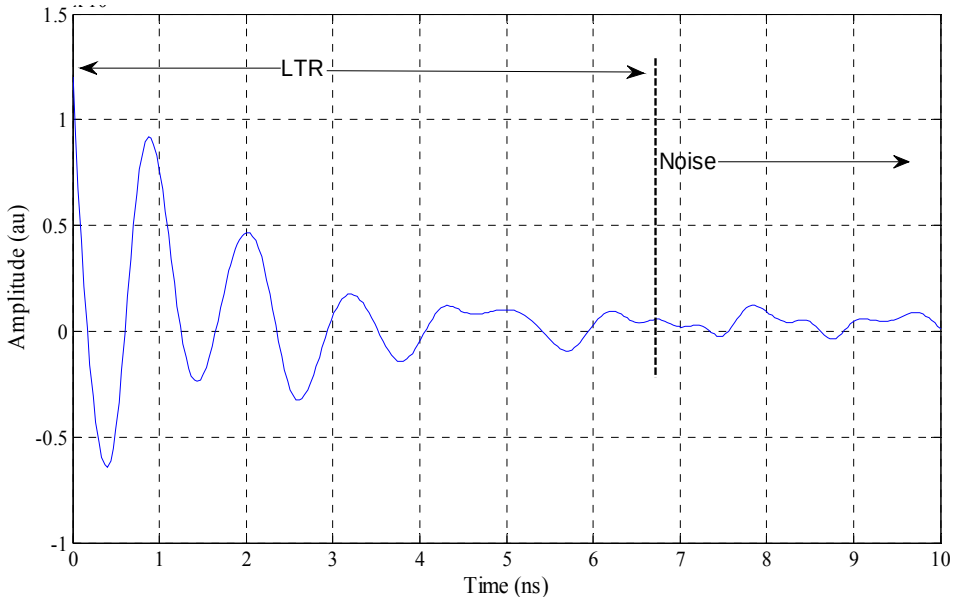

Figure 5-12 LTR of a wire 3 (L = 15 cm and d = 0.4 cm).

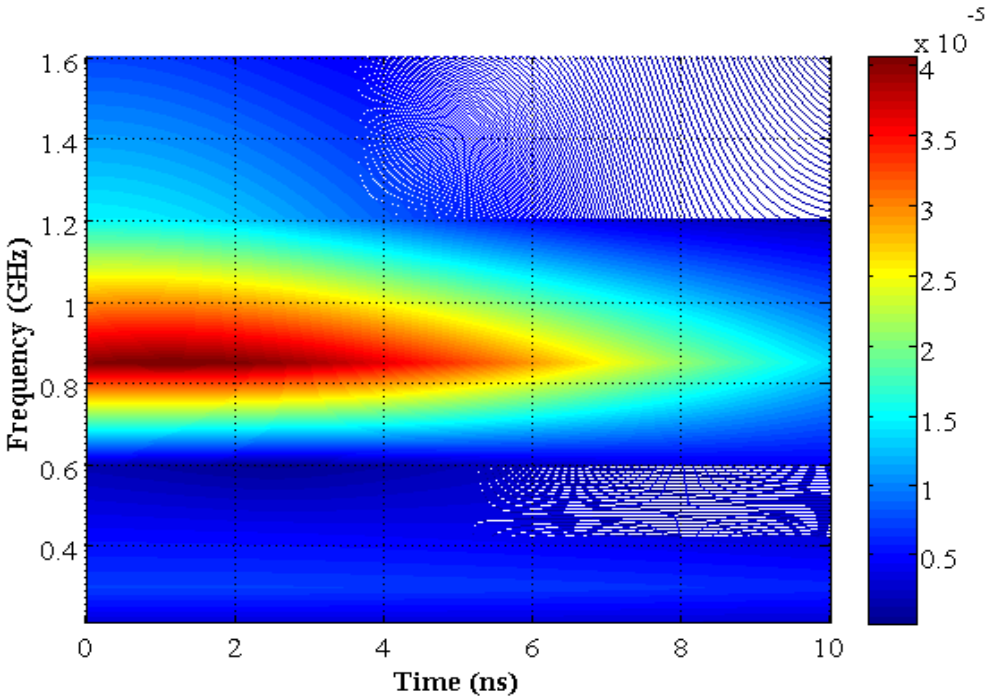

Figure 5-13 CWT of a wire 3 (L = 15 cm and d = 0.4 cm).

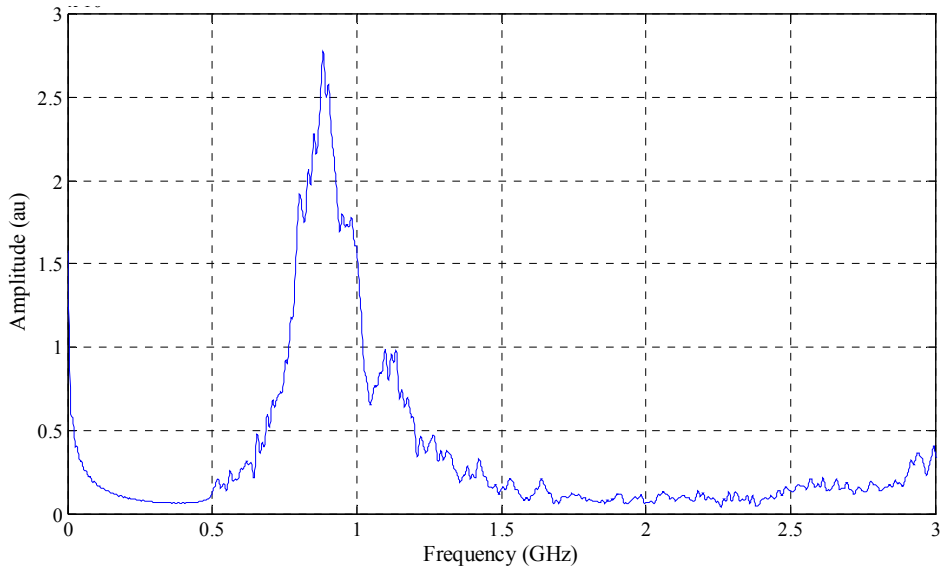

Figure 5-14 Frequency response of wire 3 (L= 15 cm and d = 0.4 cm).

Figure 5-13 shows that the re-radiated energy of this particular target is much less when compared with that in example 5.5.2. This is due to the reduction of the target diameter as a result of which the LTR life time will be also less.

5.6.4 PEC wire 4: length 15 cm and diameter 1.0 cm

The fourth target was a PEC wire 15 cm long (same as wire 3) but with diameter 1.0 cm. The objective here is to find out how well the CWT can represent the target energy when diameter of the simple target changed. Figure 5-15 shows the LTR time domain life time, it is very clear that the dominant mode of the resonant frequencies (the one with the highest energy level) lies between 0 to 4 ns. These energy levels are observed clearly in the time frequency domain by the use of CWT features as shown in figure 5-16. Power spectrum levels are presented in figure 5-17 in which the results completely match those obtained by CWT.

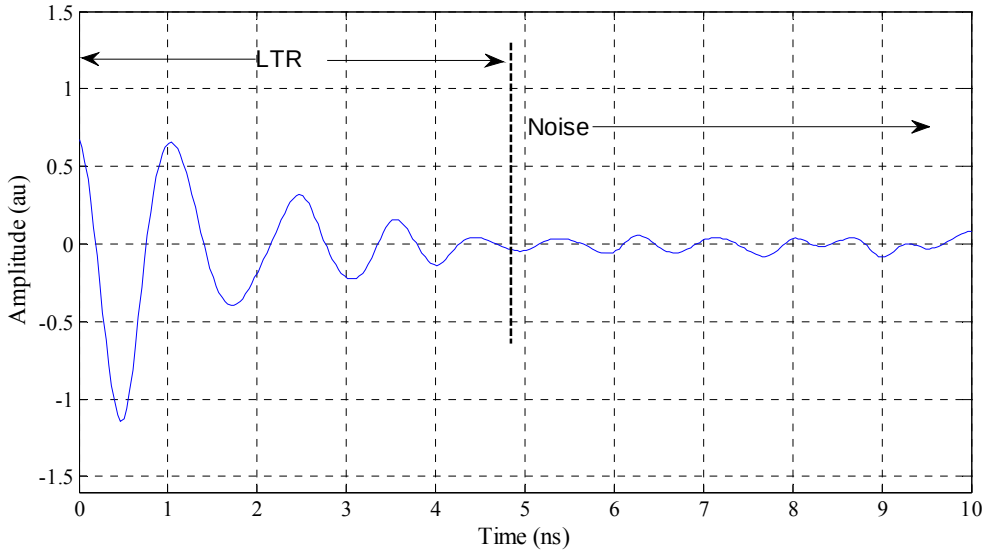

Figure 5-15 LTR of wire 4 (L= 15 cm d = 1.0 cm).

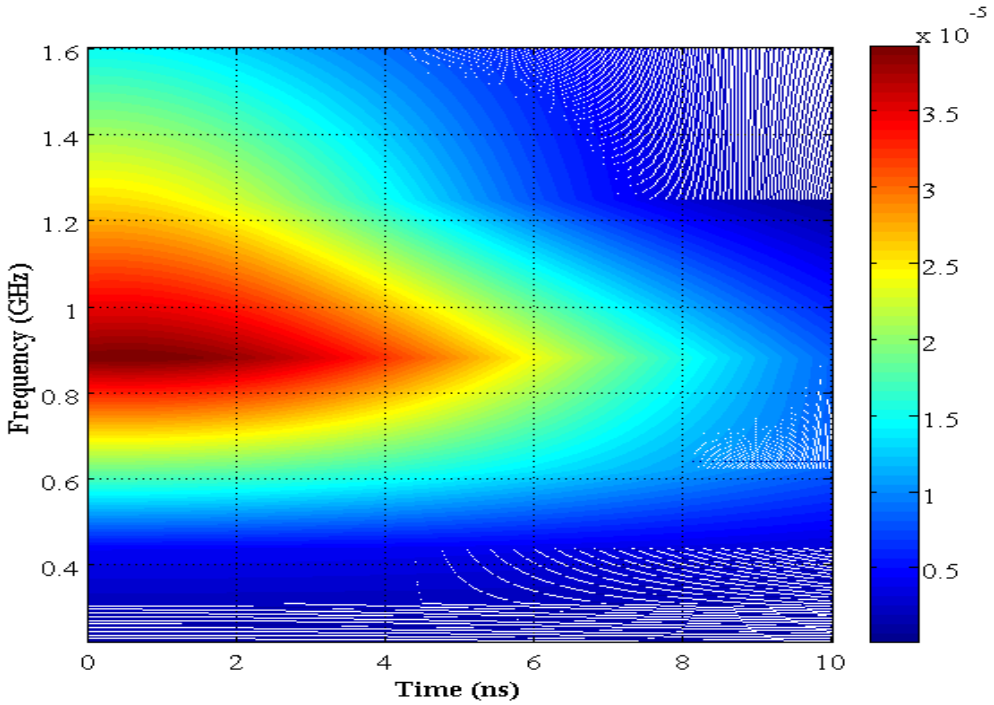

Figure 5-16 CWT of a wire 4 (L= 15 cm d = 1.0 cm).

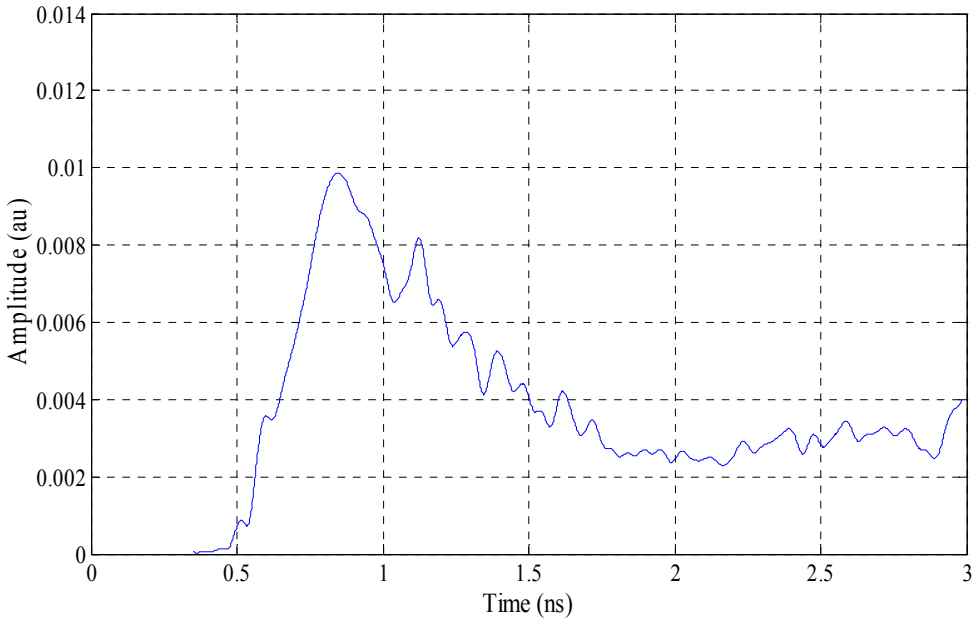

Figure 5-17 Frequency response of wire 4 (L= 15 cm d = 1.0 cm).

The results of different wire experiments that CWT can be used to extract the target signature based on the energy levels of each target in which the dominant fundamental frequencies of the LTR target signature are easily distinguishable, which make CWT a very promising technology in the field of concealed weapons detections.

It can be seen that from the results shown in figures 5-12 and 5-15 that the LTR re-radiated energy of wire 4 larger than that in wire 3 however the LTR life time is very similar. This result is clearly observed in the energy levels in figure 5-13 and 5-16 and also in the frequency response peaks (amplitude). The thicker target has higher energy levels with shorter life time while the bigger diameter has long energy life time with less amplitude.

5.7 Complex objects

In this section, TF analysis of the transient response for a real life example of a radar target is given. This section strengthens the theoretically based studies and their implications in standoff concealed weapons detections based on TF analysis. Two real target objects consisting of a small handgun and a kitchen knife, see Chapter 4, were chosen and tested.. The aim here is to further investigate the advantages, disadvantages and the limitation of using CWT analysis for more complicated targets.

5.7.1 Knife

First, a practical experiment was carried out using real knife with length of 12 cm and the width of PEC part was 1cm and the dielectric part was 1.5 cm, the depth of the dielectric

part was 0.5 cm and the PEC part was 0.1 cm. A picture of this target is shown chapter 4, section 4.6.1. The LTR of this target is plotted in Figure 5-18 in which the late time response life time is about 6 ns. This LTR represents all of the fundamental frequencies of the dominant LTR modes. Figure 5-19 and 5-20 show, the CWT and the spectrum respectively.

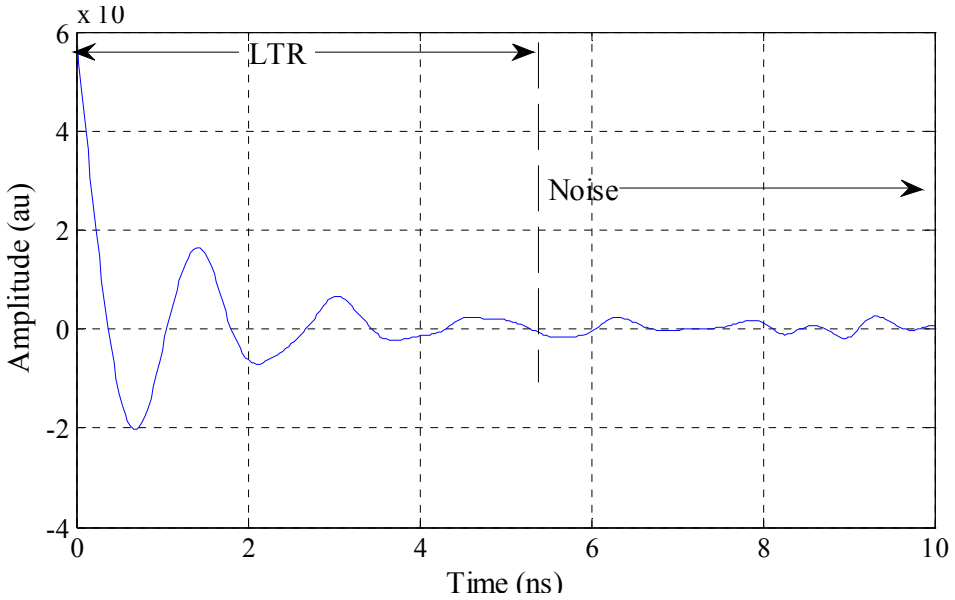

Figure 5-18 LTR of knife

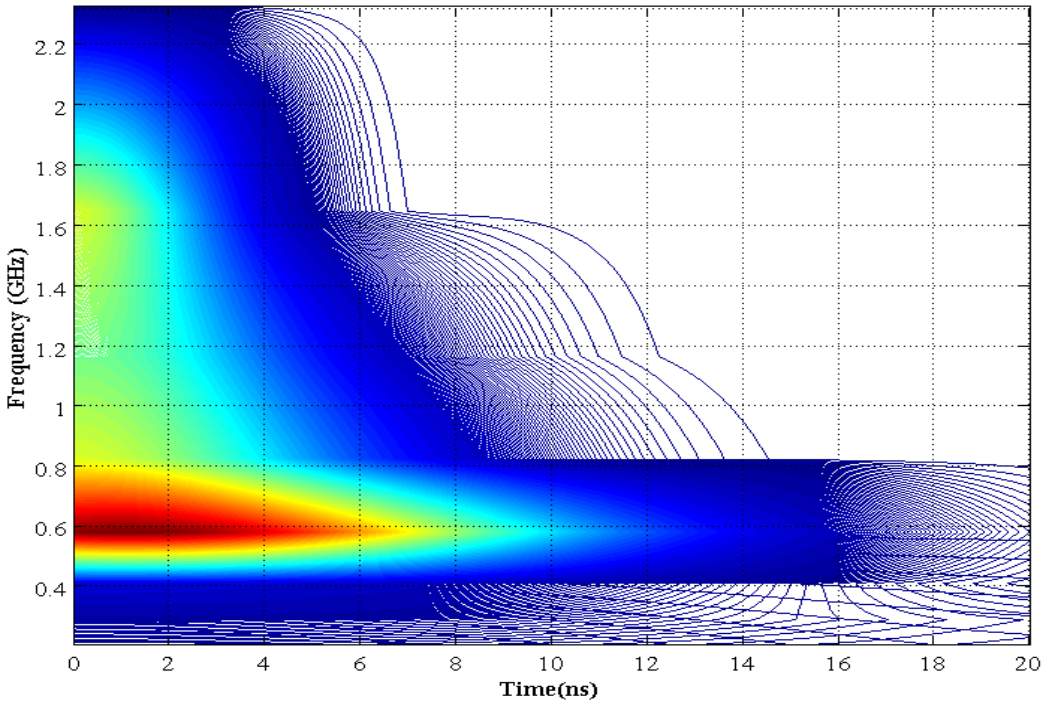

Figure 5-19 CWT of knife.

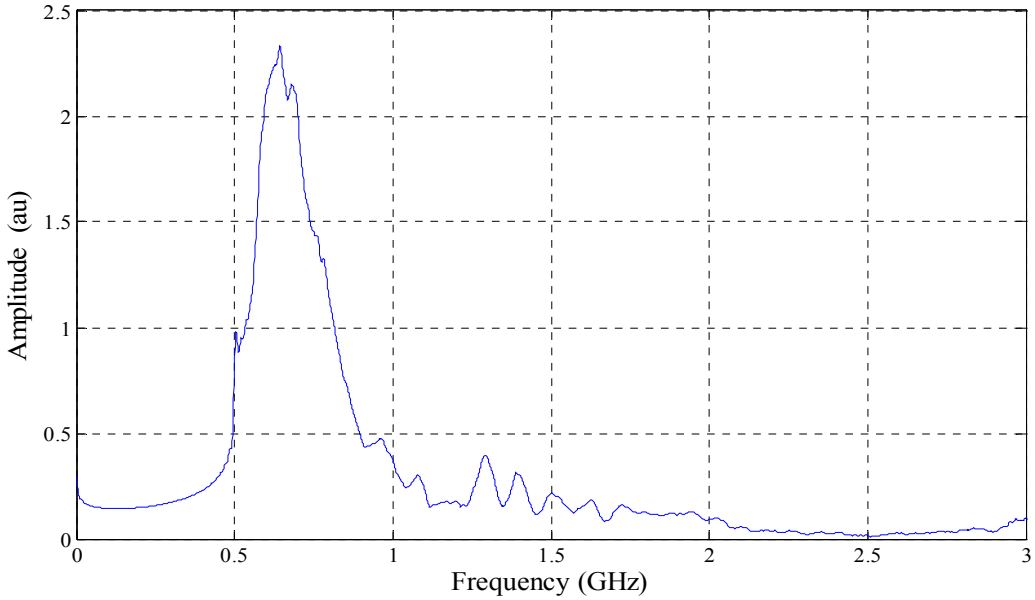

Figure 5-20 Frequency response of a knife.

The fundamental frequency and TFD modes lie between 0.5 and 1 GHz and those represents the unique signature of this target by which it could be identified. The observation shows the high energy levels of the PEC part of the knife and low energy levels corresponding to the dielectric part of this target. The energy levels represent the response of this target according to its reradiated energy corresponding to its LTR target signature.

5.7.2 Small handgun

The second complex object to be tested was a small handgun, an Olympus pistol that was used in chapter four where picture is shown in figure 4-16. The results for the LTR, CWT and frequency response can be seen in Figures 5-21, 5-22 and 5-23 respectively.

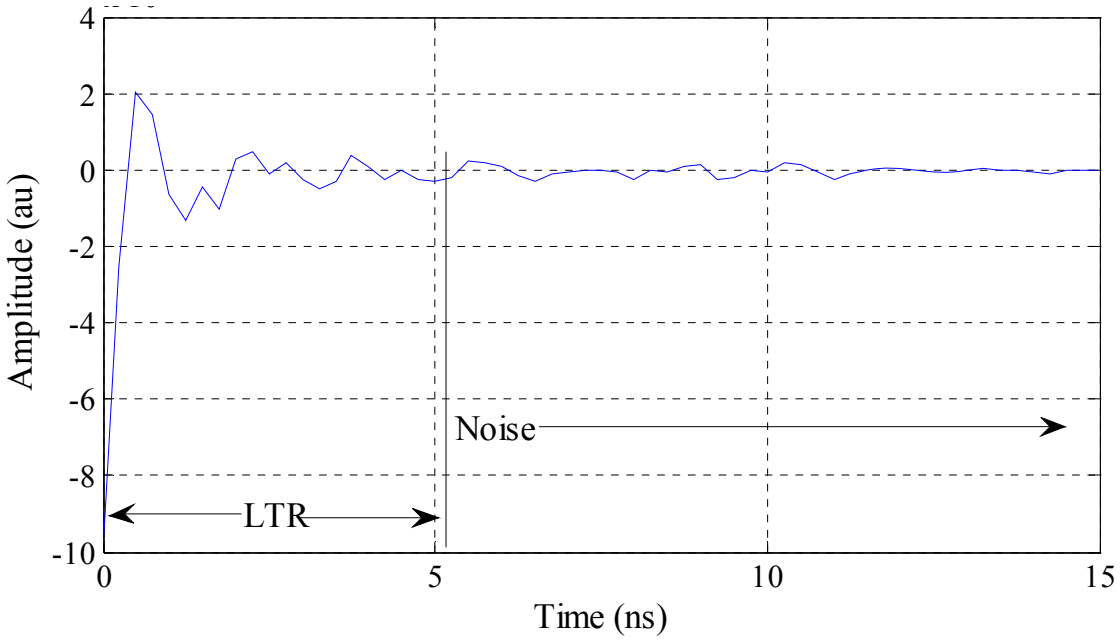

Figure 5-21 LTR of small handgun.

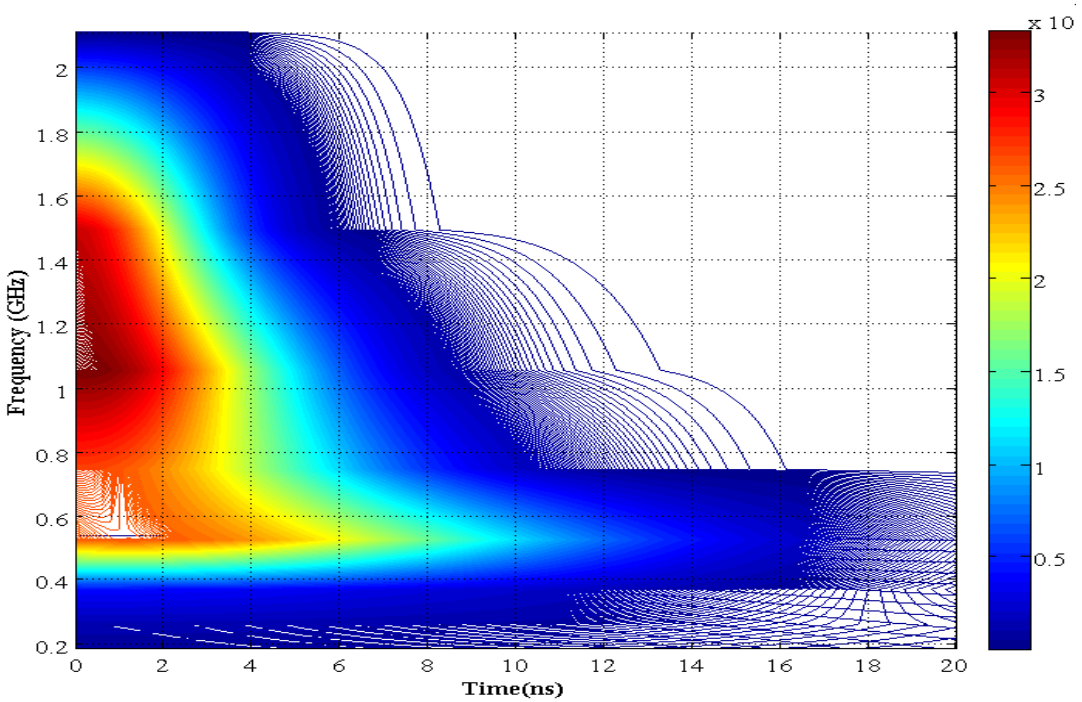

Figure 5-22 CWT of small handgun.

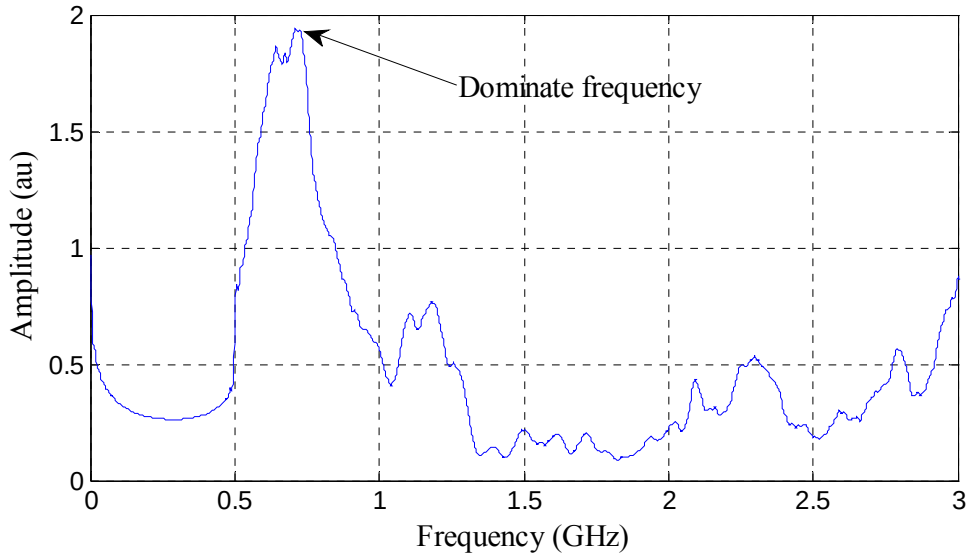

Figure 5-23 Frequency response of small handgun.

This practical example shows that the scattering from the gun is more intense than from the wire due to its shape geometry. Moreover, the results of the exponential model for the late-time period show similar results to the original SEM model. Nevertheless, the HWSEM model brings a more advanced and comprehensive approach for studying the transient scattering in comparison to the SEM model due to the extensive information it provides.

Figure 5-22 shows the target TFD response by CWT analysis, all of the LTR resonant frequencies could be clearly observed as discussed in the preceding practical examples. After observing the LTR global resonance frequency, it can be seen that the target does not have many resonance modes as the knife or wires, in other words the LTR life time of this target is shorter than a simple wire. In figure 5-22, representing the TF domain, this can be seen by the very short duration of the high energy frequencies. The activity corresponding to most intense resonance dies away much more rapidly that for, say the wire targets. Figure 5-23 show that only the resonant mode seems to be below 1GHz. This can be explained further as follows, previous studies have shown that layers of SEM poles exist in the S-Domain. When these layers are superimposed or added in any specific layer a wave front phenomenon is synthesized. Also, wave front phenomena can be found if SEM poles are summed up in a particular layer. The same has been found to be true for the convex targets where the wave front analysis has been described as a creeping wave (Le-Tien et al., 1997, Wei et al., 2010) with a GTD . Each GTD wave front events can be combined with numerous resonance modes by using the example of

flat strip target provided that the actual resonant modes utilized for each wave front is also included.

Although this theory is applicable for high scattering frequencies, studies have shown that the concept holds true for low frequency resonance region as well if the SEM poles are developed based on the superposition of wave fronts.

5.8 CWT performance of onbody concealed weapons.

In the last section, analyses of the response from wires of different dimensions have been presented using CWR time frequency analysis. The practical results show that CWT analysis is very promising and can be used as an alternative means for studying the transient scattering of onbody concealed weapons and to gain further physical insights into the process. In particular, the occurrences of LTR resonances are clearly observed in the TF domain.

In this section, transient re-radiating from real target objects such as knives or handguns sited beneath clothes covering the human body will be analysed and studied, and the different dielectric properties will be considered. The purpose here is to study the interaction between the target and the human body in the TF domain. The CWT time frequency domain analysis of scattering from the human body only, a concealed knife onbody and a concealed gun onbody are considered respectively. The aim is to study in the TF domain how the interactions between the target and the medium interface affect the LTR response.

5.8.1 Human body response in the TF domain

Backscatters from the human body will be analysed using the CWT. A real human body stood 2 m away from the transmitting and receiving antennas from which a sweep frequency of operating bandwidth is transmitted toward the human body and the backscatter data captured by the VNA via the receiving antenna (the experimental setup given in Chapter 4 is used). Figures 5-24 and 5-26 show the time domain response, CWT response and the frequency responses respectively of the human body only.

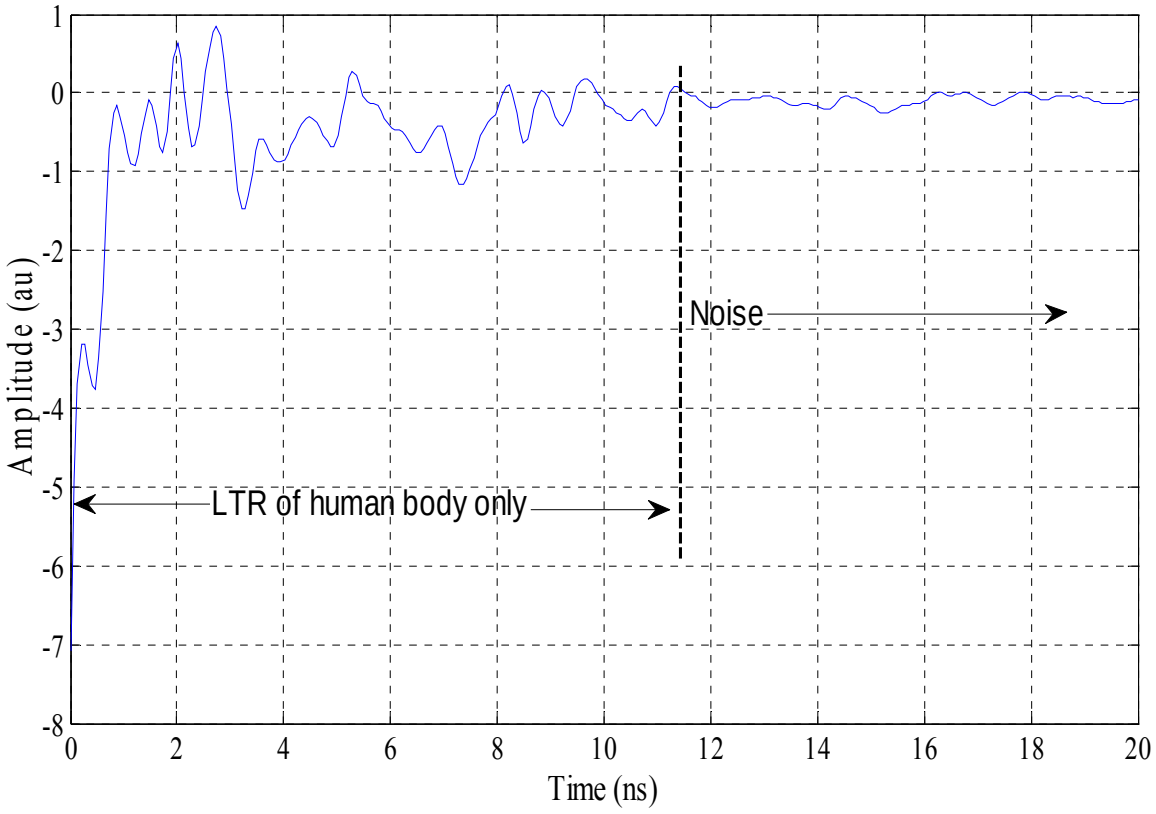

Figure 5-24 Response of human body only.

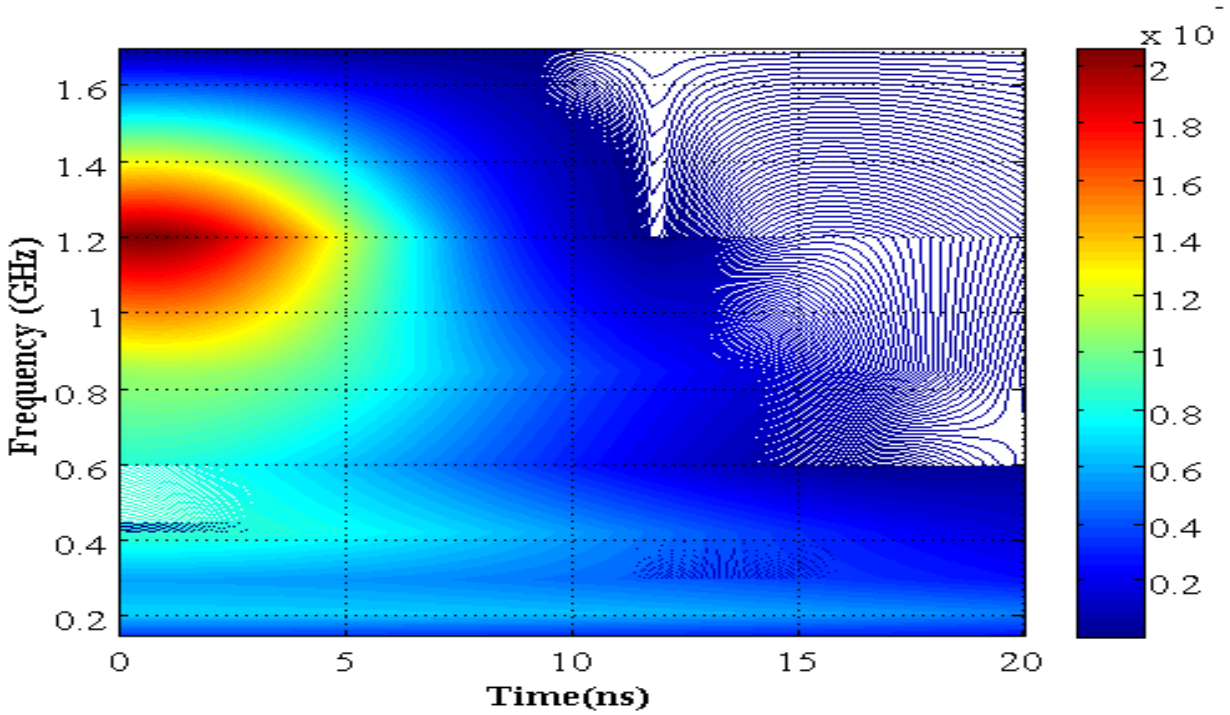

Figure 5-25 CWT of human body only.

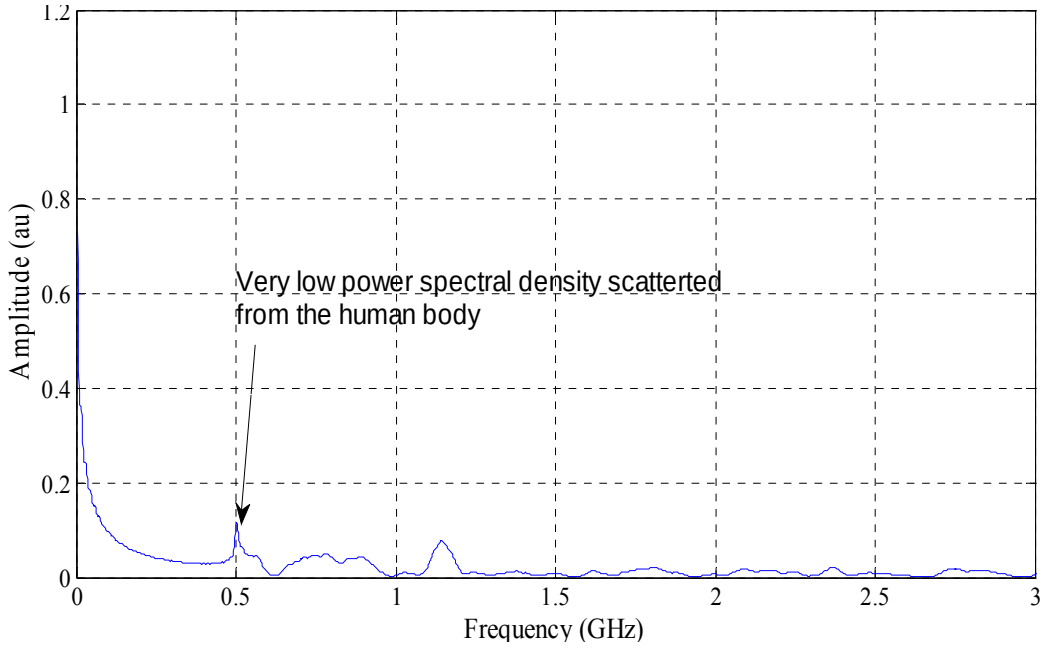

Figure 5-26 Frequency response of body only.

As shown in figure 5-24, the late time response scattering events are clearly observed in the TD. Because of the human body's dielectric properties, the re-radiated backscattered data is very weak and since the nature of the frequency is dependent on the human tissue dielectric properties, the refraction angle $\emptyset_t{}^o$ and the transmitted pulse phase velocity is frequency dependent and varied accordingly, (C. Balanis, 1989). As a result of that the pulse hits the proposed target on very small deference on frequency and time. The magnitude of the re radiated energy shown in figure 5-25 and figure 5-26 is small since the transmitted pulse is attenuated as it propagates within the lossy dielectric of the human body.

5.8.2 Onbody concealed knife

In this experimental measurement a real kitchen knife of length L=12 cm and width d = 1.2 cm, was attached to the human body and the data captured according to the experimental setup stated earlier. Figure 5-27 presents the time domain of the LTR resonance scattering event sequence of the target, while the CWT performance is presented in figure 5-28.

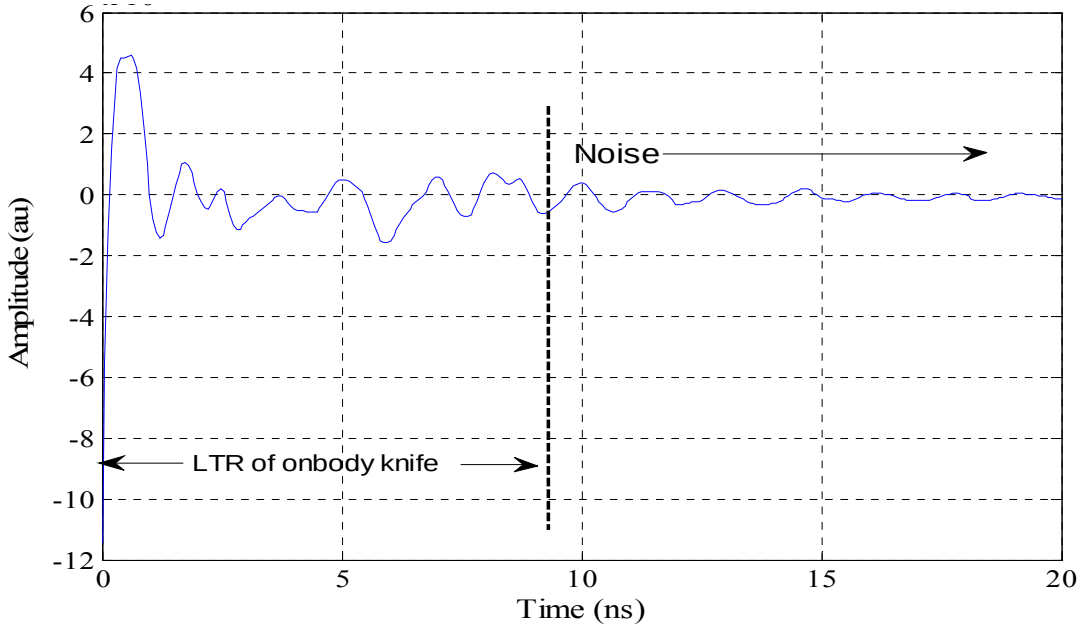

Figure 5-27 LTR of onbody knife.

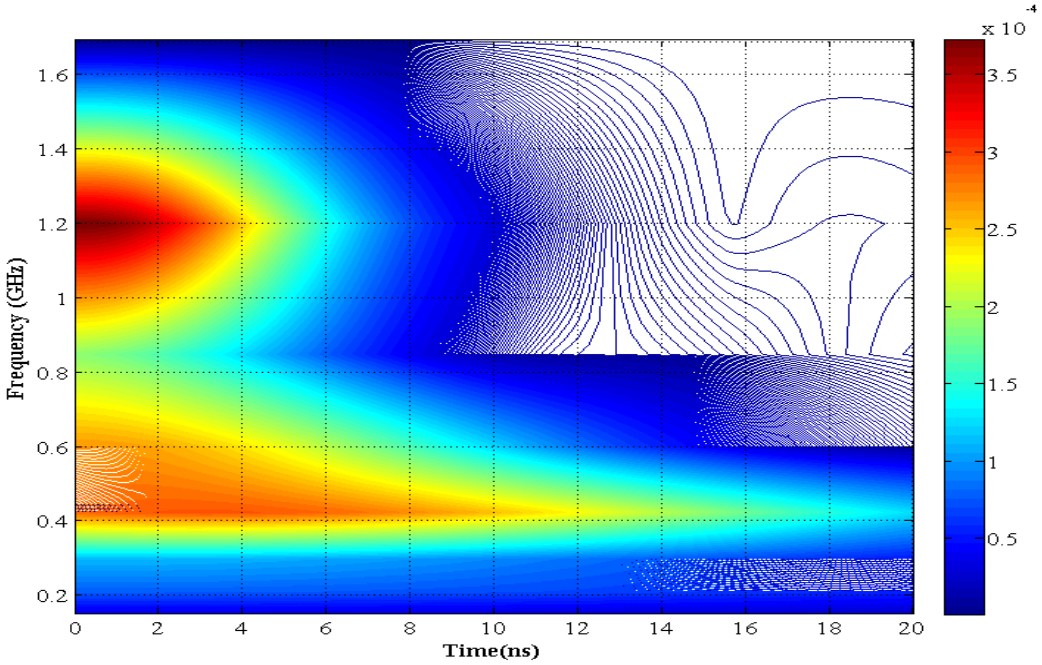

Figure 5-28 CWT performance of onbody knife.

Compared to the response of lossy human body, alone, the transmitted and received backscattered data is travelling through three mediums, free space (air), human body (lossy dielectric material properties) and the PEC target. The angle of refraction is very similar to that for the land mind detection and could be calculated to be, (Balanis, 1989)

$$\theta_r = tan^{-1}\left(\sqrt{\frac{\varepsilon_r\,\varepsilon_0}{\varepsilon_0}}\right)^{o} \tag{6.1}$$

The backscattered data is more complicated compared to experimental examples studied earlier; the scattered response of the different media interferes with each other and the LTR of the concealed object is masked as shown in the figure 5-27. The LTR scattering sequences of this complex medium illustrate that the scattering objects interacted with each other. The CWT TF analysis of the target signature is given in figure 5-27. Comparing the CWT TFD for the knife (figure 5-19) the lossy human body only, (figure 5- 25) and the onbody knife it can be clearly seen that the time frequency intensity patterns for the onbody knife retain the characteristics observed for the knife only. These energy levels corresponding to the dominant modes of the LTR concealed target.

5.8.3 Onbody concealed gun

In this section a real handgun was attached to a human body. Again the re-radiated data was measured by the VNA via the receiving antenna. The time domain scattering event sequence and frequency domain data of the scattering target data are presented in the following figures 5-29 and 5-30.

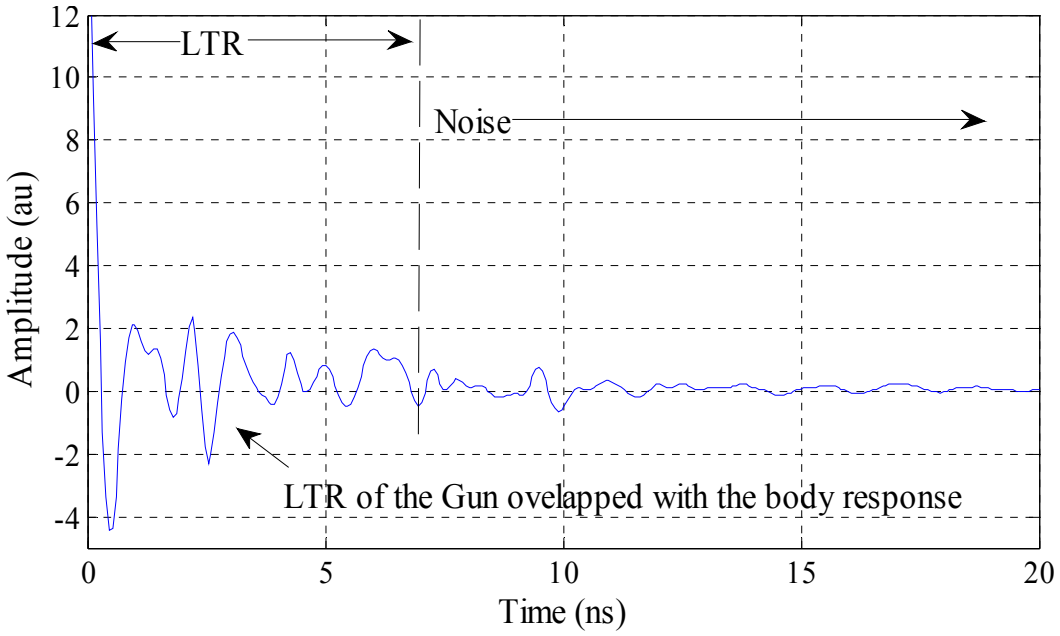

Figure 5-29 LTR of onbody gun.

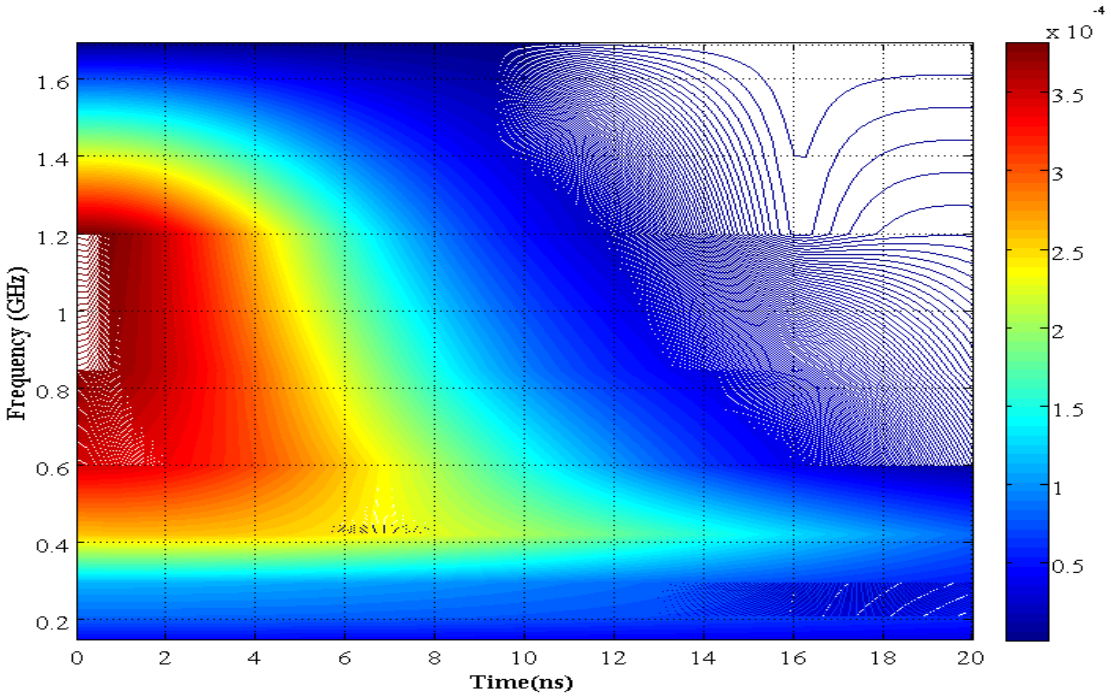

Figure 5-30 CWT performance of onbody gun.

In a manner similar to the test with the onbody knife, the non-zero conductivity of a lossy dielectric (human body) attenuates the electromagnetic wave and only the first few dominant scattering phenomena in the low frequency region are observed in the frequency domain. However figure 6-29 clearly shows that the CTW TFD for the onbody handgun contains high energy levels which are related to the presence of the gun (see figure 5-22 and figure 5-25). However, further investigation is required to confirm the nature of each resonance mode.

The CWT performance regarding practical detection of onbody concealed weapons shows that in the time frequency domain the spectrum a characteristic signal for both the knife and the handgun could be extracted. This shows that the spectral density is a very powerful means to represent target complexity and geometry. Thus it can be confirmed that the CWT response was related to the concealed test target and could be a very powerful tool in the detection of any onbody concealed objects.

5.9 Discussion

All of the carried out experiments of different objects are summarized in table 5-1 in which f the dimensions and dominate frequency of each target is given.

Table 5-1 Summary of the used objects

Target	Length (mm)	Diameter (mm)	Orientation $\emptyset^o$	Dominant frequency (GHz)
Wire 1	100	4.0	45	1.4
Wire 2	200	4.0	45	0.71
Wire 3	150	4.0	45	0.91
Wire 4	150	10.0	45	0.91
Off & onbody Knife	220	11	45	0.63
Off & onbody Gun	160	Varied	45	0.71

From the practical tests carried out in this chapter it was found that the life time and number of resonant modes of the LTR are indicative of target geometry (size, shape complexity and material). LTR responses of the simple wire targets in the time, frequency and time frequency domain are shown illustrated in figures 5-4 to 5-17. When compared to the LTR of more complex objects such as guns or knives, it can be seen the number of resonant modes of the complex objects was significantly larger than for the simple objects, see figures 5-18 to 5-23.

In the time domain all of the LTR events are observed at their respective times, as the objects radiate energy the level of the signal falls trailing off into background noise. In the frequency domain the target frequency response is represented by a number of high –

Q resonant peaks. This requires more explanation, SEM states that the LTR response of the PEC target can be represented as sum of sinusoids and damped exponential model related to the target resonances. Figures 5-7, 5-11,5-14 and 5-17 illustrate the frequency domain results of the LTRs, in which the LTRs dominant mode of the resonant frequency related to the target dimensions. It is found that when the wire diameters are increased the frequency magnitude of the re-radiated LTR target response is decreased which is due to the charge density Q of the proposed target. However when the target length is increased the LTR life time increased. On the other hand results of the complex objects presented in figure 5-18 to 5-23 show the LTRs dominant modes which reflect the target complexly and complexity. The complexity of the target increases the LTR resonance modes, in other words a complex object such as a gun produces more scattering resonant events than a simple object such as wire.

To further investigate the behaviour of LTR target response for targets of different dimensions the CWT was applied to the different LTR target responses and the TFD results have been presented, see figures 5-4, 5-6, 5-9,5-13,5-16,5-19,and 5-22, which effectively confirms that the LTR resonant modes vary as a function of target geometry.

To look for a more comprehensive explanation, wires of different lengths and diameters were considered. Sections 5.6.1 to 5.6.4 describe how the dominant (fundamental) frequency of each target has the higher energy level, this fundamental frequency corresponding to a particular dimension of the target. In addition, the life time of the energy levels is proportional with the size of the target as illustrated in Figures 6-4 and 6-

6. Also it was found that when the wire diameter changed the energy levels of the dominant frequency also varied, see figures 5-9 and 5-13, in which the energy level of the fundamental frequency is increased when the diameter increased. The results of CWT illustrate that all of the LTR scattering events or modes are clearly observed according to the energy level of every event.

Different LTR modes are clearly observed in figures 5-18 and 5-22. In Figure 5-23 it's clearly observed that high level of energy appears across all of the dominant modes of the LTR which are correlated to the target geometry. The low energy levels observed between 0.8 to 1.9 GHz in figure 5-19 correspond to the dielectric part of the knife, and the high energy peaks related to the PEC parts. According to the HWSEM model, the former resonant mode could be the result of the interaction of various scattering events correlated with the target geometry or complexity.

Figures 5-24 to 5-30 illustrate results for onbody concealed objects which have consequently different dielectric properties, time domain of the target signature is presented in figures 5-24 and 5-29. It was found that occurrences of the scattering events were delayed in the time domain when the target was attached to the human body and also it was observed that the target signature is overlapped with the human body response.

The TFDs of the onbody concealed objects are given in figures 5-25, 5-28, and 5-30. It was observed that high energy levels corresponding to the dominant frequency of the concealed target signature, compared to the results of the energy levels in figure 5-25 for

the human body only. It can be seen that when an object concealed onbody high energy levels corresponding to the target signature could be clearly seen since the human body response has low energy levels. Onbody target detection results show that use of the CWT technique is capable of detecting the existence or absence of target objects concealed onbody and is also capable to discriminate between different objects. However further investigation is required.

It would be remarked that the presence of the human body disturbs the LTR by shifting the local dielectric environment of the target and thus modifying the complex natural resonances of the targets. Further problems are come across as the human body filters and returns the scattered data, which resemble the time pulse after the pulse has crossed and excited any metal objects being carried. This has the unwanted result of complicating the LTR of the carried targets with clutter and makes real extraction of target LTR a more difficult job.

5.10 Summary

Different PEC targets have been experimented on within a free space environment and onbody by means of CWT time frequency analysis. Real different wire targets, a knife and a handgun were used as experimental examples to demonstrate how the TFDs have the capacity and the ability to detect and discriminate between these objects by their different scattering patterns and TFD. These results can be elucidated on by utilizing the HWSEM outlines, whereby the target signature, which is transitory in nature, has been elaborated upon in the sense that it is basically a set of resonance events. The presence of

a target object is marked by the high energy levels that exist within the TF spectrum. These energy levels represent the dominant frequency modes of the LTR. Experiments conducted on different sizes and lengths of a wire reflected differences in the target response and LTR life time which mostly depends mostly on the geometry of the target. Also the fundamental frequency (lower resonance frequency) is a function of the target size. It has been shown that the CWT is a tool which has the ability to detect all the scattering events and extract the lower resonance frequencies and the life time from them.

Chapter 6
Conclusion and suggested future work

6.1 Conclusion

A system for the detection and identification of onbody concealed threat objects based upon the UWB electromagnetic transient signature has been designed built and tested using real objects. The heart of the method is to illuminate the target in the far field region of an antenna by a frequency sweep in which the wavelengths of the excitation are directly related to the size of the objects being detected so that the LTR of the backscattered signal contains aspect independent resonances which are exponentially damped. As reported in the first chapter, there are two main objectives for this thesis. The first was to investigate the construction of a new antenna with relatively flat gain (non-zeros resonant) as much as possible, distortionless pulse transmission and reception, and be directive with high-radiation efficiency.

The design methodology and configuration of the TSA were presented in sections 3.2.1 and 3.3. Detection of concealed onbody weapons is limited by antenna response as any antenna ringing could mask important aspect independent scattering related to the signature of concealed object. An approach was described based on a relatively flat gain antenna across the operating bandwidth. An optimum antenna design is achieved by the adjustment of the following parameters: flare angle, cavity radius and throat width to optimize the antenna performance.

The simulated results closely resemble the measured results confirming the design procedure of the proposed antenna. Both the measured and simulated results show that a return loss of 10 dB has been achieved from about 0.25 GHz to more than 3 GHz, sufficient to cover the fundamental frequencies of most threat objects (0.25 to 3 G Hz). This criterion is necessary for successful concealed weapon detection based on the LTR scattered from the object.

The gain of the designed antenna achieves the required flat response and a VSWR around unity. The far-field radiation patterns of the purpose built TSA showed it achieves directive properties with an average front-to- back ratio which is greater than 10 dB across the whole band, making it convenient for standoff detection applications. The time domain performance of the antenna was also measured. Two identical co-polarized antennas were set facing each other across a distance of 50 cm. The results show that the antenna could send and receive very narrow pulses in a distortion free manner to meet the requirements of successful concealed weapon detection based on the late time response scattered from the illuminated objects.

In chapter 4, the performance of the antennas for illuminating the target and collecting the back-scattered response have been tested and validated. The results show that the different backscattered impulse response of different simple and complex objects were successfully captured by the antenna.

Simple and complex objects were illuminated and interrogated and their LTRs captured. The measurements were accomplished for the various targets. Distance between cross-

polarized antennas was 1 m, distance between antenna and target was around 1.5 m, target orientations was 45^o. The captured data was treated by the designed MATLAB algorithms. The background was subtracted in order to cancel out most of the interference from the surrounding area, this was done by abstract the background data when target present from the background date when target is not present. The antenna response de-convolved. The filtered frequency domain data are then transformed into time domain data via an IFFT and only the real or imaginary part of these data is used for LTR extraction; the complex nature of the signal arises as the IFFT is carried out over positive frequencies only.

The second aim of this thesis was also achieved; a new approach for concealed weapon detection based on a CWT applied to the scattering response of a target being detected has been successfully tested. In the TF domain, the occurrence of the frequency components can be easily observed which also provide further insight into transient scattering.

In chapter 5, the behaviours of TFD using different target signature of a well-known scattered such as the simple wire were examined. In particular, CWT performance showed it to be capable of revealing the major scattering events. In addition, TF analysis was applied to the simple and complex targets previously used in chapter 4. The LTR signature of each object was accurately extracted and presented in the TF domain for both the wire targets and more complex kitchen knife and small handgun. These latter threat objects were both clearly observed in TF domain and more importantly the interactions

between various wave fronts were clearly identified, which goes some way to verifying the correctness of the HWSEM model. This chapter also found that TF analysis can be used as an alternative tool to study transient electromagnetic scattering behaviour and extract the unique signature of concealed weapons. The application of TF analysis to the transient scattering from onbody concealed weapons was also considered. The signature of both an onbody knife and onbody handgun was demonstrated the feasibilities of using TFDs to study transient scattering from onbody concealed targets. The CWT's experimental performance regarding detection of onbody concealed weapons showed that in the TFD the spectral response for every target could be seen as a distribution in which the level and life-time depended on the target material and geometry. The spectral density provides very powerful information concerning target complexity and geometry. As a result of that it can be confirmed that the CWT response is directly identifies the response of the unknown concealed target and could be a very powerful tool in the detection of any onbody concealed object.

6.2 Suggested future work

The scope of this thesis was limited to a lower frequency band (0.25 – 3 GHz) and single transmitter and receiver antennas. However as explained in chapter 5, attenuation from human body significantly mask the target resonance around 3 GHz it would be probably better to work below 3 GHz and enhance the LTR signal by the following suggested points:

- An antenna array could be used to increase the gain which would help to enhance the weak LTR of the target.
- Different angles of incidence with the multiple antennas could also enhance the successful extraction of LTR related to the concealed weapons.
- For TF analysis CWT results confirm that it is a powerful tool for extracting the target signature however one of the major challenge is the discrimination between multiple threat (knife and gun) and non-threat onbody objects such as keys, mobile phones, etc., More work has to be done and for that it is suggested that a combination of CWT with Hilbert transform or Empirical Mode Decomposition (EMD) could be possible approach as these elementary tested to analysis the overlapped multi objects response.
- Another possible direction is the adaptive wavelet analysis to extract target features sets from the target signature; this may lead to novel target recognition schemes.
- On-going work will be required to classify and recognize all likely concealed targets and to build and store the information of all common firearms in a high resolution library.
- Target classification might be done by the use of adaptive technique based on the high resolution stored library.

Appendix A

Tested objects

The pictures bellow illustrate all of the objects which were used to study the LTR phenomena. The objects were oriented at $\mathbf{45^o}$ and illuminated by sweep frequency from 0.25 to 3GHz. All of the experiments were carried out in the millimetre microwave laboratory.

Figure A-1 Photo of PEC wire 1 and wire 2

Wire 1: *L= 20 cm, d = 0.2 cm*.
Wire 2: *L = 15 cm, d = 0.2 cm*

Figure A-2 Photo of PEC wire 3 and wire 4

Wire 3: *L= 20 cm, d = 1 cm*

Wire 4: *L = 15 cm, d =1 cm*

Appendix B

CST Numerical simulations

Many numerical simulations were performed to various objects with different sizes, by the using of *CST microwave studio transient solver*. Some of these objects are:

- Four different sizes wires 0.4 cm length and 1.0 cm width, with different lengths 20 cm, 10 cm.

The CST modules are located 45^{o} along z-axes and illuminated by sharp (0.7ns) pulse equivalent to sweep frequency within the desired frequency bandwidth (0.25 – 3Ghz) , the backscattered data measured by using the far field probe. Series of lab Experiments were carried out to the same simulated objects, to validate the obtained results and to seek comprehensive knowledge to the target backscattering response.

The results are in the following figures in which the CNR extraction for these modules. The early time response and the late time response are clearly distinguishable. The early time response is characterized by high frequency data while the low frequency oscillation after this is the late time response. Figure B-1 shows the target orientation.

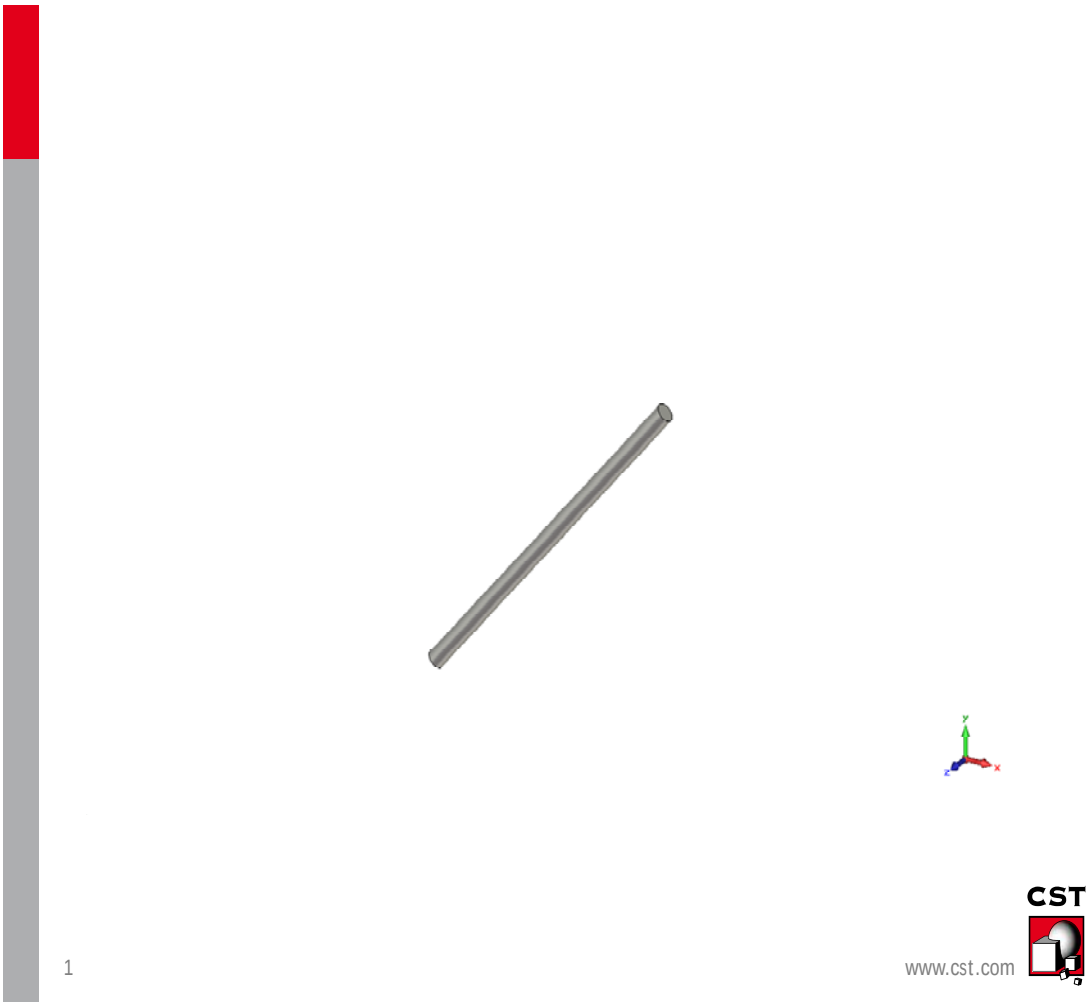

Figure B-1 Simulated PEC wire

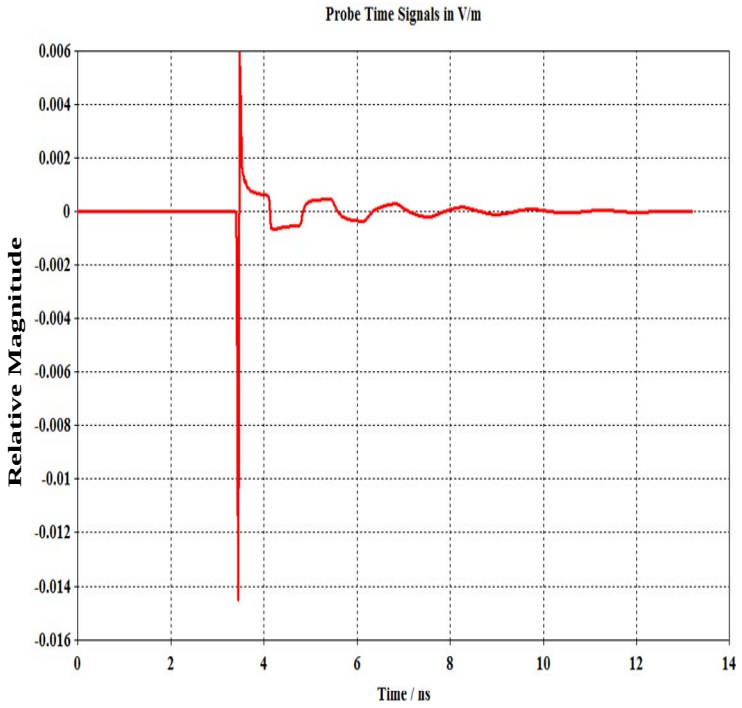

Figure B-02 CNR of the simulated PEC wire (L=20 cm and d=0.4 cm).

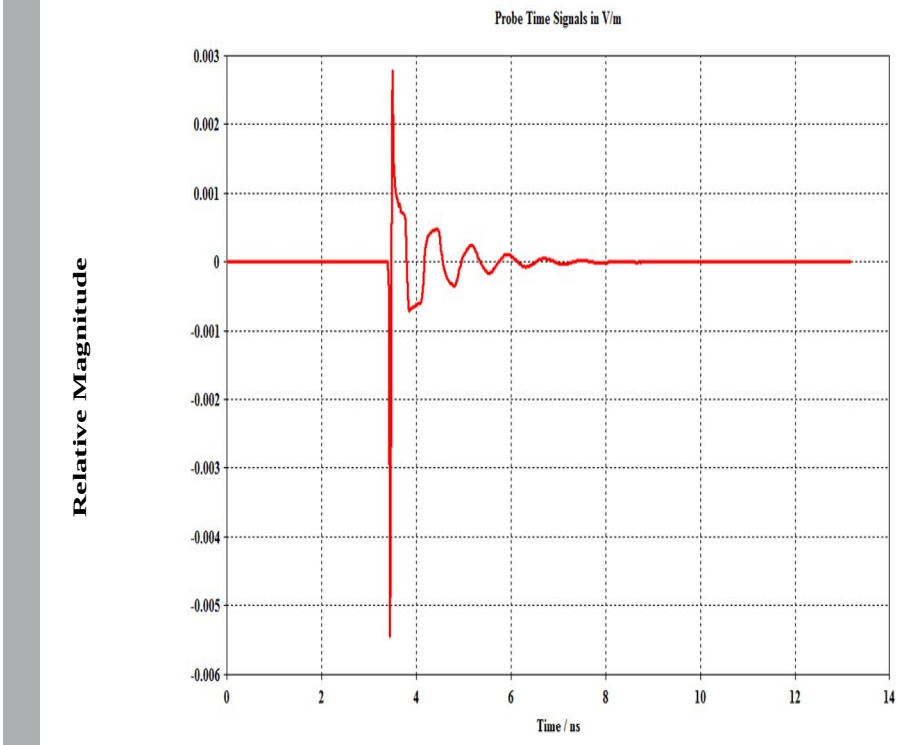

Figure B-3 CNR of the simulated PEC wire (L = 10 cm and d = 0.4 cm).

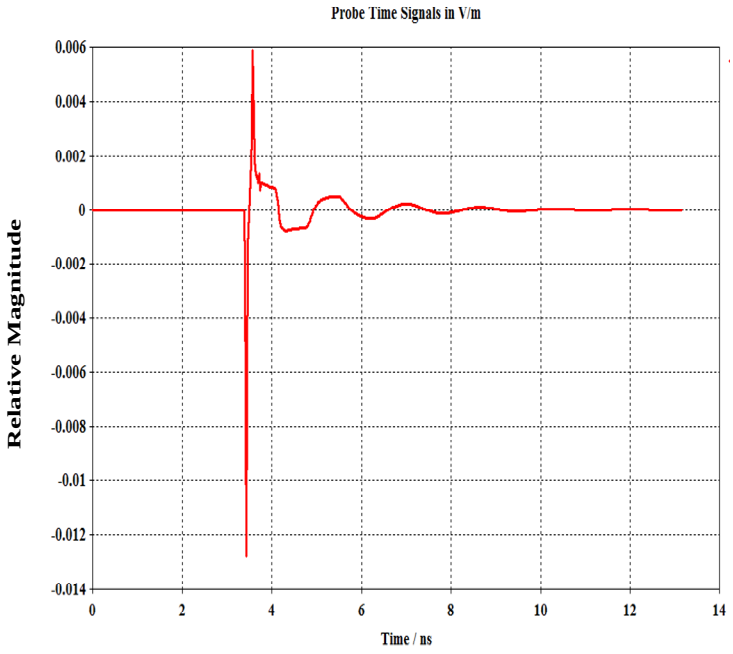

1

www.cst.com

CST

Figure B-04 CNR of the simulated PEC wire (L = 20 cm and d = 1.0 cm).

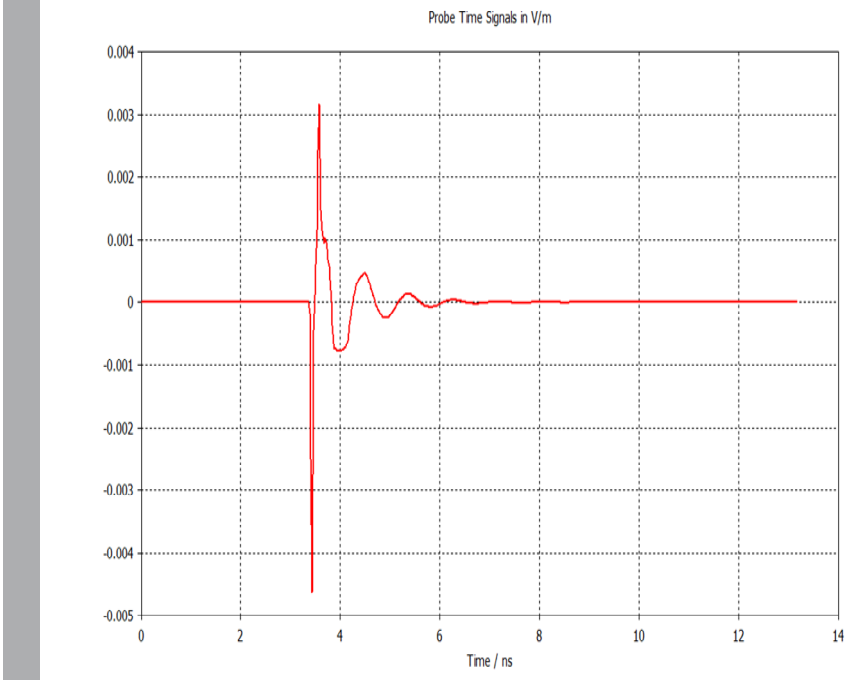

1

www.cst.com

Figure B-5 CNR of simulated PEC wire (L = 10 cm and d = 1.0 cm)

References

Abbas, M., Arazm, F., Rashed, J. & Faraji , R.(2007) ' Design and Optimization of a New 118 GHz Double Ridged Guide Horn Antenna.' *Journal of Electromagnetic Waves and Applications,* Vol.21,no.4 pp. 501-516.

Agurto, A., LI, Y., Tian, G. Y., Bowring , N. & Lockwood, S. (2007) ' A review of concealed weapon detection and research in perspective.' IEEE Int. Conf. MonE02 Networking, Sensing and Control pp. 443-448.

Andrews, D. A., Bowring, N., Rezgui, N. D., Southgate, M., Harmer, S. & Atiah, A. (2008) 'A multifaceted active swept millimetre-wave approach to the detection of concealed weapons' *SPIE int Conf erence on Security and defence, England, Cardeff.* pp. 707-711.

Anderws, D. A., Rezgui, N. D., Smith, S. E., Bowring , N., Southgate, M. & Baker, J. G. (2008) ' Detection of concealed explosives at stand-off distances using wide band swept millimetre waves.' *SPIE int Conf erence on Security and defence, England, Cardeff.*71170J.

Appel,H., J. (1981) ' Distance criteria in near-field and far-field antenna measurements'. *In: International Conference on Antennas and Propagation, 2nd, England, London*. pp.215-225.

Appleby, R.(2004) ' Passive millimetre–wave imaging and how it differs from terahertz imaging' *Philosophical Transactions of the Royal Society of London. Series A: Mathematical, Physical and Engineering Sciences,*pp. 362**,** 379.

Appleby, R. & Anderton, R. N. (2007) ' Millimeter-wave and submillimeter-wave imaging for security and surveillance.' *Proceedings of the IEEE, Vol.95**,**no.8 pp.1683-1690.*

Arivazhagan, S. & Ganesan, L.(2004) 'Automatic target detection using wavelet transform.' *EURASIP Journal on Applied Signal Processing,* pp. 2663–2674.

Auger, F. & Flandrin, P. (1995) 'Improving the readability of time-frequency and time-scale representations by the reassignment method.' *Signal Processing, IEEE Transactions on,*Vol. 43**,** pp.1068-1089.

Auger, F., Flandrin, P., Goncalves, P. & Lemoine, O. (1996) 'Time-Frequency Toolbox.For Use with Matlab.' *CNRS France&Rice University, USA*.

Balanis, C. A. (1989) *'Advanced engineering electromagnetics.', Wiley New York.*

Bastiaans, M. J. 2009.' Wigner distribution in optics",*McGraw-Hill, New York*

Baum, C. (1976) ' The singularity expansion method.' *Transient Electromagnetic Fields***,**Springer Berlin,Vol. 10 pp. 129-179.

Baum, C. E. (1971) ' On the singularity expansion method for the solution of electromagnetic interaction problems'. *Air force weapons lab Kirtland AFB NM.*

Baum, C. E., Rothwell, E. J., Chen, K. M. & Nyqist, D. P. (1991) 'The singularity expansion method and its application to target identification'. *Proceedings of the IEEE,* Vol. 79**,** pp.1481-1492.

Boashash , B. (2003) 'Time frequency signal analysis and processing: a comprehensive reference', *Elsevier Science,. Maryland USA.*

Bowen, J. (1995) ' Astigmatism in tapered slot antennas'. *International Journal of Infrared and Millimeter Waves,* Vol. 16**,** pp. 1733-1756.

Ceravolo, R. (2008) 'Time–Frequency Analysis', *Wily Online Library*

Chamberlain, N. E., Walton, E. K. & Garber, F. D. (1991) ' Radar target identification of aircraft using polarization-diverse features'. *Aerospace and Electronic Systems, IEEE Transactions on,* Vol. 27**,** pp. 58-67.

Chauveau, J., Debeaucoudrey, N. & Saillard, J.(2007) ' Selection of contributing natural poles for the characterization of perfectly conducting targets in resonance region'., *IEEE Transactions Antennas and Propagation, ,* Vol. 55**,** pp. 2610-2617.

Chen, C., and L. Peters, Jr. (1997), "Buried unexploded ordnance identification via complex naturel resonances," *IEEE Transactions , Antenna and propagation,* Vol. AP-45,No 11, pp. 1645-1654.

Chen, F. C. & Chew, W. (2003),' Time-domain ultra-wideband imaging radar experiment for verifying super-resolution in nonlinear inverse scattering'. *Journal of Electromagnetic Waves and Applications,* Vol.17**,** pp. 1243-1260.

Chen, V. C.(2008) ' Joint time-frequency analysis for radar signal and imaging.' IEEE, pp.5166-5169.

Chen, V. C. & Hao, L. (1999). 'Joint time-frequency analysis for radar signal and image processing.' *Signal Processing Magazine, IEEE,* Vol.16**,** pp. 81-93.

Chen, V. C. & Ling, H.(2002). 'Time-frequency transforms for radar imaging and signal analysis.', Artech House Publishers.

Chen, W. & Shuly, N. (2010)' Matrix pencil method for estimating parameters use in radar target identification.'. CSIRO, Vol.46.

Chevill, R. A., Mcgowan, R. W. & Grischkowsky, D. R. (2002). 'Late-time target response measured with terahertz impulse ranging.' *Antennas and Propagation, IEEE Transactions on,* Vol.45**,** pp. 1518-1524.

Choi, H. I. & Williams, W.(1989).' Improved time-frequency representation of multicomponent signals using exponential kernels.' *Acoustics, Speech and Signal Processing, IEEE Transactions on,* Vol.37**,** pp. 862-871.

Choi, I. S. & Kim, H. T. (2007).' Feature extraction of radar targets using Evolutionary Adaptive Wavelet Transform.' IEEE, pp. 129-132.

Choi, I. S. & Kim, H. T.(2008). 'Generalized early time/late time evolutionary programming based CLEAN.' *Microwave and Optical Technology Letters,* Vol.50**,** pp.208-210.

Choi, I. S., Lee, J. H., Kim, H. T. & Rothwell, E.(2003).' Natural frequency extraction using late-time evolutionary programming-based CLEAN'. *Antennas and Propagation, IEEE Transactions on,* Vol. 51**,** pp. 3285-3292.

Cohen, L. (1995). 'Time-frequency analysis', *Prentice Hall PTR.*

Cohen, L. (1989). 'Time-frequency distributions-a review.' *Proceedings of the IEEE,* Vol. 77**,** pp. 941-981.

Costianes, P. J. (2006).' An overview of concealed weapons detection for homeland security'. A*pplied Imagery and Pattern Recognition Workshop, 2005. Proceedings. 34th*, *IEEE*, pp.5-6.

Debanth, L. 2003. *Wavelets and signal processing*, Birkhauser.

Drachman, B. & Rothwell, E. (2002). 'A continuation method for identification of the natural frequencies of an object using a measured response.' *Antennas and Propagation, IEEE Transactions on,* Vol. 33**,** pp. 445-450.

Dudley, D. (1985). 'Comments on SEM and the parametric inverse problem.' *Antennas and Propagation, IEEE Transactions on,* Vol. 33**,** pp. 119-120.

Dudley, D. & Morgan, M. (1985). 'Comments on SEM and the parametric inverse problem.' *IEEE Transactions on Antennas and Propagation,* Vol. 33**,** pp. 119-120.

Elsherbini, A., Zhang, C., Lin, S., Kuhn, M., Kamel, A., Fathy, A. E. & Elhennawy, H. (2007). 'UWB antipodal vivaldi antennas with protruded dielectric rods for higher gain, symmetric patterns and minimal phase centre variations'. IEEE, pp. 1973-1976.

Ersoy, M. & Turhan-Sayan, G.(2005). 'Electromagnetic target classification of small-scale aircraft modeled by conducting wire structures using a natural resonance based feature extraction technique.' IEEE, pp. 468-471.

Felsen , L. (1985).' Comments on early time SEM.' *Antennas and Propagation, IEEE Transactions on,* Vol. 33**,** pp. 118-119.

Flandrin, P. (1984). 'Some features of time-frequency representations of multicomponent signals.' *Acoustics, Speech, and Signal Processing, IEEE International Conference on ICASSP. IEEE*,Vol. 9, pp. 266-269.

Foo, S. L. & Defence, R. (2004). 'Ultra-wideband (UWB) Remote Sensing and Radar Imaging', *Defence Research and Development Canada-Ottawa.*

Gallego, A., Medouri A. & Carrion, C. (2008).' Estimation of number of natural resonances of transient signal using E-pulse technique.' *Electronics letters,* Vol. 27**,** pp. 2253-2256.

Garg, R. (2001). '*Microstrip antenna design handbook'*, Artech House.

Gashinova, M., Cherniakov, M. & Vasalos, A. (2007). 'UWB signature analysis for detection of body-worn weapons.', *IEEE Radar,I nternational Conference, Shanghai, PP 1-4*.

Gashinova, M., Djigan, V., Daniel, L. & Chrniakov, M. (2008). 'Adaptive calibration in UWB radar'. *IEEE Radar Conferenc, Brimingham UK,* pp. 1-6.

Gaunaurd, G. C. & Strifors, H. C. (1996). 'Signal analysis by means of time-frequency (Wigner-type) distributions-applications to sonar and radar echoes'. *Proceedings of the IEEE,* Vol.84**,** pp. 1231-1248.

Gazit, E. (2005). 'Improved design of the Vivaldi antenna'. *Microwaves, Antennas and Propagation, IET Proceedings H,* Vol. 135**,** pp. 89-92.

Gibson, P. (2007). 'The vivaldi aerial' . IEEE, 101-105.

Golub, G. H. & Van Loan, C. F. (1996). 'Matrix Computations (Johns Hopkins Studies in Mathematical Sciences).

Gordon N, Sinclair, Rupert N. Anderton and Roger Appleby (2001). 'Passive millimeter-wave concealed weapon detection'.*SPIE Conference, Boston,USA*. 142.

Guillanton, E., Dauvignac, J., Pichot, C. & Cashman J. (1998). 'A new design tapered slot antenna for ultra wideband applications'. *Microwave and Optical Technology Letters,* Vol.19**,** pp. 286-289.

Gupta, K. C., Garg, R., Bahil, I. J. & Bhartia, P. (2007). 'Microstrip lines and slotlines', *Second Edition, Artech House Publisher, Norwood, MA.*

Harmer, S., Anderws, D., Bowring, N., Rezgui, N. & Southgate, M. (2009). 'Ultra wide band detection of Onbody concealed weapons using the out of plane polarized late time response', P*roceedings of the SPIE, Volume 7485, pp. 748505-748505-8* .

Harmer, S., Andrews, D., Rezgui, N. & Bowring, N. (2010).' Detection of handguns by their complex natural resonant frequencies'. *Microwaves, Antennas & Propagation, IET,* Vol. 4**,** pp. 1182-1190.

Hausner, J. & West, N. (2008). 'Radar based concealed threat detector'. IEEE, 1-8.

Heyman, E. & Felsen, L. (1983). 'Creeping waves and resonances in transient scattering by smooth convex objects'. *Antennas and Propagation, IEEE Transactions on,* Vol. 31**,** pp. 426-437.

Heyman, E. & Felsen, L. (1985). 'A wavefront interpretation of the singularity expansion method'. *Antennas and Propagation, IEEE Transactions on* Vol.33**,** pp. 706-718.

Heyman, E., Friedlander. & Felsen, L.(2002). 'Ray-mode analysis of complex resonances of an open cavity [radar targets]'. *Proceedings of the IEEE,* Vol. 77**,** pp. 780-787.

Hlawatsch, F. & Boudreaux-Bartels, G. (1992). 'Linear and quadratic time-frequency signal representations'. *Signal Processing Magazine, IEEE,* Vol. 9**,** pp. 21-67.

Hua, Y. & Sarkar, T. (1990). 'On the total least squares linear prediction method for frequency' estimation. *Acoustics, Speech and Signal Processing, IEEE Transactions on,* Vol. 38**,** pp. 2186-2189.

Hua. & Sarkar, T.(1989). 'Generalized pencil-of-function method for extracting poles of an EM system from its transient response'. *Antennas and Propagation, IEEE Transactions on,* Vol. 37**,** pp. 229-234.

Hua, Y. & Sarkar, T. (1990). 'Matrix pencil method for estimating parameters of exponentially damped/undamped sinusoids in noise'. *Acoustics, Speech and Signal Processing, IEEE Transactions on,* Vol. pp. 38**,** 814-824.

Hua, Y. & Sarkar, T. K. (1991). 'On SVD for estimating generalized eigenvalues of singular matrix pencil in noise'. *Signal Processing, IEEE Transactions on,* Vol. 39**,** pp. 892-900.

Hunt, A., Akela, H. A., & Santa B., C. (2001). 'Demonstration of a concealed weapons detection system using electromagnetic resonances, final re-port'. *National Institute of Justice US Department of Justice, NCJ,* 190134.

Ibrahim, A. S., Liu, K. J. R., Novak, D. & Waterhouse, R. B. (2007). 'A subspace signal processing technique for concealed weapons detection'. *In*, IEEE.

Ikuno, H. & Nishimoto, M. (1999). 'Wavelet analysis of scattering responses of electromagnetic waves'. *Electronics and Communications in Japan (Part II: Electronics),* Vol. 82**,** pp. 35-42.

Ilavarasan, P., Ross, J., Rothwell, E., Chen, K. M. & Nyquist, D. (2002). 'Performance of an automated radar target discrimination scheme using E pulses and S pulses'. *Antennas and Propagation, IEEE Transactions on,* Vol.41**,** pp. 582-588.

Ilavarasan, P., Rothwell, E. J., Chen, K. M. & Nyquist, D. (1995). 'Natural resonance extraction from multiple data sets using a genetic algorithm'. *Antennas and Propagation, IEEE Transactions on,* Vol.43**,** pp.900-904.

Jain, V. (1974). 'Filter analysis by use of pencil of functions: Part I'. *Circuits and Systems, IEEE Transactions on,* Vol. 21**,** pp. 574-579.

Jain, V., Sarkar, T. & Weiner, D. (2003). 'Rational modeling by pencil-of-functions method'. *Acoustics, Speech and Signal Processing, IEEE Transactions on,* Vol.31**,** pp.564-573.

Jamies, J., Hall, P. & Wood, C. (1981). 'Microstrip antenna theory and design' (Book). *Stevenage, Herts., England, Peter Peregrinus, Ltd.(IEE Electromagnetic Waves Series,* 12.

Janaswamy, R.(2002). 'An accurate moment method model for the tapered slot antenna'. *Antennas and Propagation, IEEE Transactions on,* Vol. 37**,** pp.1523-1528.

Janaswamy, R. & Schaubert, D. (2002). 'Analysis of the tapered slot antenna'. *Antennas and Propagation, IEEE Transactions on,* Vol.35**,** pp.1058-1065.

Jang, S., Choi, W., Sarkar, T. K., Salazar P. M., Kim, K. & Baum, C. E. (2004). 'Exploiting early time response using the fractional Fourier transform for analyzing transient radar returns'. *Antennas and Propagation, IEEE Transactions on,* Vol. 52**,** pp. 3109-3121.

Jeong, J. & Williams, W. (2002). 'Kernel design for reduced interference distributions'. *Signal Processing, IEEE Transactions on,* Vol.40**,** pp. 402-412.

Jin, B., Wu, Q., Wu, Y., Bian, L. & Li, L. W. (2007). 'An Approach to the Determination of the Phase Centre of Vivaldi-Based UWB Antenna'. *Ultra-Wideband Short-Pulse Electromagnetics 8***,** pp.69-73.

Kennaugh, E. & Moffatt, D. (1965). 'Transient and impulse response approximations'. *Proceedings of the IEEE,* Vol.53**,** pp.893-901.

Kim, H. & Ling, H. (1993).' Wavelet analysis of radar echo from finite-size targets'. *Antennas and Propagation, IEEE Transactions on,* Vol. 41**,** pp.200-207.

Kim, H. & Ling, H. (2008). 'Wavelet analysis of electromagnetic backscatter data'. *Electronics letters,* Vol. 28**,** pp.279-281.

Kim, K. T., Choi, I. S. & Kim, H. T. (2002). 'Efficient radar target classification using adaptive joint time-frequency processing'. *Antennas and Propagation, IEEE Transactions on,* Vol. 48**,** pp.1789-1801.

Kim, K. T., Seo, D. K. & Kim, H. T. (2002). 'Efficient radar target recognition using the MUSIC algorithm and invariant features'. *Antennas and Propagation, IEEE Transactions on,* Vol. 50**,** pp.325-337.

Ksienski, D. A. (1985). 'Pole and residue extraction from measured data in the frequency domain using multiple data sets'. *Radio Science,* Vol. 20**,** pp.13-19.

Kumaresan, R. & Tufts, D. (2003). 'Estimating the parameters of exponentially damped sinusoids and pole-zero modeling in noise'. *Acoustics, Speech and Signal Processing, IEEE Transactions on,* Vol. 30**,** pp.833-840.

Kaiser, G., *A (1994) 'Friendly Guide to Wavelets'*, Boston: Birkhauser, pp. 60-64.

Lazaro, A., Girbau, D. & Villarino, R. (2009). 'Wavelet-based breast tumor localization technique using a UWB radar'. *Progress In Electromagnetics Research,* Vol.98**,** pp.75-95.

Le-Tien, T., Talhami, H. & Nguyen, D. (1997). 'Target signature extraction based on the continuous wavelet transform in ultra-wideband radar'. *Electronics letters,* Vol. 33**,** pp. 89-91.

Lee, J. (1991). 'Slotline impedance'. *Microwave Theory and Techniques, IEEE Transactions on,* Vol.39**,** pp.666-672.

Lee, J. H. & Kim, H. T. (2008). 'Natural Frequency Extraction Using Generalized Pencil-of-Function Method and Transient Response Reconstruction'. *Progress In Electromagnetics Research,* Vol. 4**,** pp.65-84.

Lee, K. F. & Chen, W. (1997). 'Advances in microstrip and printed antennas', *Wiley.*

Lee, R. & Simons, R. N. (1996). 'Effect of curvature on tapered slot antennas'. IEEE Antennas and Propagation Soc. Symp, Vol. 1 pp.188-191.

Lewis, L., Fassett, M. & Hunt, J. (1974). 'A broadband stripline array element'. IEEE Int. Symp. Antennas Propagation Vol.12, pp. 335-337.

Leopold B. Felsen, (1984). 'Progressing and oscillatory waves for hybrid synthesis of source excited propagation and diffraction.' *Antennas and Propagation, IEEE Transactions on,* Vol. 32**,** pp. 775-796.

Li, Q., Ilavarasan, P., Ross, J. E., Rothwell, E. J., Chen, K. M. & Nyquist, D. P. (1998). 'Radar target identification using a combined early-time/late-time E-pulse technique'. *Antennas and Propagation, IEEE Transactions on,* Vol.46**,** pp.1272-1278.

Ling, H. & Kim, H. (1992). 'Wavelet analysis of backscattering data from an open-ended waveguide cavity'. *Microwave and Guided Wave Letters, IEEE,* Vol.2**,** pp.140-142.

LING, H. & KIM, H. 1992. Wavelet analysis of backscattering data from an open-ended waveguide cavity. *Microwave and Guided Wave Letters, IEEE,* 2**,** 140-142.

Ling, H., Moore, J., Bouche, D. & Saavedra, V. (2002). 'Time-frequency analysis of backscattered data from a coated strip with a gap'. *Antennas and Propagation, IEEE Transactions on,* Vol.41**,** pp.1147-1150.

Liu, Z., Macuda, T., Xue, Z., Forsyth, D. & Laganiere, R.(2010). Concealed Weapon Detection: A Data Fusion Perspective.', *Journal of Aerospace Computing, Information, and Communication* Vol. 6, pp. 196-207.

Liu Joon-Ho and K. Hyo-Tae, 'Comments on Extraction of natural frequencies od radar target from a measured response using E-pulse techniques.', *Antenna and Propagation, IEEE Transactions on,* vol. 53, pp 3853-3855.

Lui, H. S., Aldhubaib, F., Shuley, N. V. & Persson, M. (2009).' Performance analysis of resonance based radar target recognition with different excitation bandwidth using the E-Pulse technique.'*IEEE, Radar Conference EuRAD* , pp.469-472.

Lui, H. S., Shuley, N. & Longstaff, I.(2007). 'Time-frequency analysis of late time electromagnetic transients from radar targets'.*IET,Radar System Int. Conference, Edinburgh,UK* pp.1-5.

Mackay, A. & Mccowen, A. (1987). 'An improved pencil-of-functions method and comparisons with traditional methods of pole extraction'. *Antennas and Propagation, IEEE Transactions on,* Vol. 35**,** pp.435-441.

Marple S. L. (1987) 'Digital spectral analysis-with application'. *Englewood Cliffs, N.J. Prentice-Hall.*

Mao, S. G. & Chen, S. L. (2006). 'Time-domain characteristics of ultra-wideband tapered loop antennas'. *Electronics letters,* Vol.42**,** pp.1262-1263.

Mehdipour, A., Mohammadpour, A., K. & Farji D., R. (2007). 'Complete dispersion analysis of vivaldi antenna for ultra wideband applications'. *Progress In Electromagnetics Research,* Vol.77**,** pp.85-96.

Milligan, T. A. & Wiley, J. (1985). '*Modern antenna design'*, Wiley Online Library.

Mittra, R. & Pearson, L.(1978). 'A variational method for efficient determination of SEM poles.' *Antennas and Propagation, IEEE Transactions on,* Vol.26**,** pp.354-358.

Mohamed, K., Cherniakov, M., Rasid, M. & Abdullah, R. (2009). 'Automatic target detection using wavelet technique in forward scattering radar'. IEEE, Radar Conference EuRAD, Amesterdam, Nederland, pp.76-79.

Mohammadian, A. H., Rajkotia, A. & Scliman, S. S. (2004).' Characterization of UWB transmit-receive antenna system'.*IEEE, UWB System and Tech. Conference,* pp.157-161.

Mooney, J. E., Ding, Z. & Riggs, L. S. (1998). 'Robust target identification in white Gaussian noise for ultra wide-band radar systems'. *Antennas and Propagation, IEEE Transactions on,* Vol.46**,** pp.1817-1823.

Moore, J. & Ling, H. (1993). 'Time-frequency analysis of the scattering phenomenology in finite dielectric gratings'. *Microwave and Optical Technology Letters,* Vol.6**,** pp.597-600.

Morgan, M. (1984). 'Singularity expansion representations of fields and currents in transient scattering'. *Antennas and Propagation, IEEE Transactions on,* Vol.32**,** pp.466-473.

Morgan, M. (2005). 'Target ID using natural resonances'. *Potentials, IEEE,* Vol.12**,** pp.11-14.

Muqaibel, A., Safaai-Jazi, A., Woerner, B. & Riad, S. (2002). 'UWB channel impulse response characterization using deconvolution techniques'. *IEEE, circuits and systems symposium 45th,Midwest,* Vol.3, pp. 605-608.

Narsimahn, S., Haripriya, A. & Shreyamsha Kumar, B. (2008). 'Improved Wigner-Ville distribution performance based on DCT/DFT harmonic wavelet transform and modified magnitude group delay'. *Signal Processing,* Vol.88**,** pp.1-18.

Nilsson, J. W. & Riedel, S. A.' 2008'. *Electric circuits*, Pearson Prentice Hall ; London

Novak, D., Waterhouse, R. & Farnham, A. (2006). Millimeter-wave weapons detection system. *In*, 2006. IEEE, Applied Imagery and Pattern Recognition Workshop, pp.6-20.

Oh, S. & Marks, R. (1992). 'Some properties of the generalized time frequency representation with cone-shaped kernel'. *Signal Processing, IEEE Transactions on,* Vol.40**,** pp.1735-1745.

Oppenheim, A. V., Willsky, A. S. & Hamid, S. (1997). Signals and systems, *Prentic-Hall signal Processing sereies,*

Oraizi, H. & Jam, S. (2003). 'Optimum design of tapered slot antenna profile'. *Antennas and Propagation, IEEE Transactions on,* Vol.51**,** pp.1987-1995.

Ozdemir, C. & Ling, H.(2002). 'Joint time-frequency interpretation of scattering phenomenology in dielectric-coated wires'. *Antennas and Propagation, IEEE Transactions on,* Vol.45**,** pp.1259-1264.

Pascoe, K. J., (2004) '*Target Recognition Using Late-Time Returns from Ultra-Wideband, Short-Pulse Radar', Air Force Inst. Of Tech. Wright – Pattereson, AFB OH School of Engineering& Mangement.* PhD Thesis.

Percival, D. B. & Walden, A. T. (2006). 'Wavelet methods for time series analysis', *Cambridge University press,* London,UK.

Pozar, D. M. & Schaubert, D. (1995). 'Microstrip antennas: the analysis and design of microstrip antennas and arrays', *Wiley*-IEEE Press.

Qian, S. & Chen, D. (1999).' Decomposition of the Wigner-Ville distribution and time-frequency distribution series'. *Signal Processing, IEEE Transactions on,* Vol.42**,** pp.2836-2842.

Qian, S. & Chen, D. (1999).' Joint time-frequency analysis'. *Signal Processing Magazine, IEEE,* Vol. pp. 16**,** 52-67.

Rahman, J. & Sarkar, T. K. (1995).' Deconvolution and total least squares in finding the impulse response of an electromagnetic system from measured data'. *Antennas and Propagation, IEEE Transactions on,* Vol.43**,** pp.416-421.

Rezgui, N., Andrews, D., Bowring, N., Harmer, S. & Southgate, M. (2008).' Standoff detection of concealed handguns'. SPIE conference, Cardiff,UK, 69480L.

Richards, M. A. (1994).' SEM representation of the early and late time fields scattered from wire targets'. *Antennas and Propagation, IEEE Transactions on,* Vol.42**,** pp. 564-566.

Rioul, O. & Flandrin, P. (2002). 'Time-scale energy distributions: a general class extending wavelet transforms'. *Signal Processing, IEEE Transactions on,* Vol.40**,** pp.1746-1757.

Rioul, O. & Vetterli, M. (1991).' Wavelets and signal processing'. *Signal Processing Magazine, IEEE,* Vol.8**,** pp.14-38.

Robert E. Collin 'Foundations for Microwave Engineering' , *Wiley-IEEE Press; 2 edition*

Ross, M. P., Dudley, D., Mackay, A. & Mccowen, A. (1988). 'Comments on An improved pencil-of-functions method and comparisons with traditional methods of pole extraction'. *Antennas and Propagation, IEEE Transactions on,* Vol.36**,** pp.1192-1194.

Rothwell, E. & Chen, K. (2002). 'A hybrid E-pulse/least squares technique for natural resonance extraction'. *Proceedings of the IEEE,* Vol.76**,** pp. 296-298.

Rothwell, E., Chen, K. M. & Nyquist, D. (2002). 'Extraction of the natural frequencies of a radar target from a measured response using E-pulse techniques'. *Antennas and Propagation, IEEE Transactions on,* Vol.35**,** pp.715-720.

Rothwell, E. J. & Sun, W. (1990). 'Time domain deconvolution of transient radar data'. *Antennas and Propagation, IEEE Transactions on,* Vol.38**,** pp.470-475.

Sadiku, M. O., Akujuobi, C. M. & Garcia, R. C. (2005). 'An introduction to wavelets in electromagnetics'. *Microwave Magazine, IEEE,* Vol.6**,** pp.63-72.

Sarkar, T., Nebat, J., Weiner, D. & Jain, V. (1980).' Suboptimal approximation/identification of transient waveforms from electromagnetic systems by pencil-of-function method'. *Antennas and Propagation, IEEE Transactions on,* Vol.28**,** pp. 928-933.

Sarkar, T. K., Park, S., Koh, J. & Rao, S. M. (2000).' Application of the matrix pencil method for estimating the SEM (singularity expansion method) poles of source-free transient responses from multiple look directions'. *Antennas and Propagation, IEEE Transactions on,* Vol.48**,** pp.612-618.

Sarkar, T. K. & Perira, O. (1995). 'Using the matrix pencil method to estimate the parameters of a sum of complex exponentials'. *Antennas and Propagation Magazine, IEEE,* Vol.37**,** pp.48-55.

Sarkar, T. K., Yang, X. & Arvas, E. (1988). 'A limited survey of various conjugate gradient methods for solving complex matrix equations arising in electromagnetic wave interactions'. *Wave Motion,* Vol.10**,** pp.527-546.

Sato,M., Ohkubo, T. & Nitsuma, H. (1995). 'Cross-polarization borehole radar measurements with a slot antenna'. *Journal of Applied Geophysics,* Vol.33**,** pp.53-61.

Schaubert, D. (1989). 'Endfire tapered slot antenna characteristics'. *Antennas &Propagation ICAP89., Sixth Int. Conference, Coventry, UK,* Vol.1, pp.432-436

Schaubert, D. H. & Chio, T. A.(1999) 'Wideband vivaldi arrays for large aperture antennas'. *Perspetives on Radio Astronomy, Technologies for Large Antenna Arrays, Netherlands Foundation for Research in Astronomy* , pp. 49-57.

Sejdic, E., Djurovic, I. & Jiang, J. (2009). 'Time-frequency feature representation using energy concentration: An overview of recent advances'. *Digital Signal Processing,* Vol.19**,** pp.153-183.

Sejdic, E., Ozertem, U., Djurovic, I. & Erdogmus, D. (2009). 'A new approach for the reassignment of time-frequency representations'. *IEEE, Signal Processing International Conference, Taipei,* pp. 2997-3000.

Shin, J. & Schaubert, D. H. (2002).' A parameter study of stripline-fed Vivaldi notch-antenna arrays. *Antennas and Propagation, IEEE Transactions on,* Vol.47**,** pp. 879-886.

Shira, H. (1988). 'Deemphasizing low frequency defects in GTD analysis of pulsed signal scattering by a perfectly conducting flat strip'. *Antennas and Propagation, IEEE Transactions on,* Vol. 34**,** pp. 1261-1266.

Shirai, H. & Felsen, L.(1986). 'High-frequency multiple diffraction by a flat strip: Higher order asymptotics'. *Antennas and Propagation, IEEE Transactions on,* Vol.34**,** pp.1106-1112.

Shirai, H. & Felsen, L.(1986). 'Modified GTD for generating complex resonances for flat strips and disks'. *Antennas and Propagation, IEEE Transactions on,* Vol.34**,** pp.779-790.

Shirai, H. & Felsen, L.(1986). 'Wavefront and resonance analysis of scattering by a perfectly conducting flat strip'. *Antennas and Propagation, IEEE Transactions on,* Vol.34**,** pp.1196-1207.

Shuley, N. & Longstaff, D. (2004). 'Role of polarisation in automatic target recognition using resonance descriptions'. *Electronics letters,* Vol.40**,** pp. 268-270.

Shuppert, B. (1988). 'Microstrip/slotline transitions: Modeling and experimental investigation'. *Microwave Theory and Techniques, IEEE Transactions on,* Vol.36**,** pp.1272-1282.

Sutinjo, A. & Tung, E.(2004). 'The design of a dual polarized Vivaldi array'. *Microwave Journal,* Vol.47**,** pp.152-161.

Taylor, J. D. (1995). 'Introduction to ultra-wideband radar systems'*, CRC Press; 1 edition*, *NewYork,* USA.

Thayaparan, T., Stankovic, L., Amin, M., Chen, V., Cohen, L. & Boashash, B. (2010). 'Time-frequency approach to radar detection, imaging, and classification'. *Signal Processing, IET,* Vol.4**,** pp.325-328.

Thiele, E. & Taflove, A. (2002). 'FD-TD analysis of Vivaldi flared horn antennas and arrays'. *Antennas and Propagation, IEEE Transactions on,* Vol.42**,** pp.633-641.

Tseng, F. & Sarkar, T. (1987). 'Deconvolution of the impulse response of a conducting sphere by the conjugate gradient method'. *Antennas and Propagation, IEEE Transactions on,* Vol.35**,** pp. 105-110.

Tufts, D. W. & Kumaresan, R.(2005). 'Estimation of frequencies of multiple sinusoids: Making linear prediction perform like maximum likelihood'. *Proceedings of the IEEE,* Vol.70**,** pp. 975-989.

Turhan-Sayan, G. (2003). 'Natural resonance-based feature extraction with reduced aspect sensitivity for electromagnetic target classification'. *Pattern Recognition,* Vol.36**,** pp. 1449-1466.

Turhan-Sayan, G. (2005).' Real time electromagnetic target classification using a novel feature extraction technique with PCA-based fusion'. *Antennas and Propagation, IEEE Transactions on,* Vol. 53**,** pp.766-776.

Turhan-Sayan, G. & Kuzuoglu, M. (2001). 'Pole estimation for arbitrarily-shaped dielectric targets using genetic algorithm-based resonance annihilation technique'. *Electronics letters,* Vol.37**,** pp.380-381.

Torrence C. and Compo G.P. (1998). 'A practical guide to wavelet analysis'. Bull. Am. Meteorol. Soc. Vol.79 pp.61–78.

Van Blaricum, M. & Mittra, R. (1988). 'A technique for extracting the poles and residues of a system directly from its transient response'. *Antennas and Propagation, IEEE Transactions on,* Vol.23**,** pp. 777-781.

Vanblaricum, M. & Mittra, R. (1978). 'Problems and solutions associated with Prony's method for processing transient data'. *Antennas and Propagation, IEEE Transactions on,* Vol.26**,** pp. 174-182.

Vasalos, A., Vasalos, I., Ryu, H. G. & Fotinea, S. E. (2010).' LTR analysis and signal processing for concealed explosive detection'. *IEEE Microwave Conference, Germany*, pp.166-169.

Wadell, B. C. (1991). 'Transmission line design handbook', *Artech House* Boston, USA.

Wang, Y., Longstaff, I. & Leat, C.(2000). 'Measurement of complex natural resonances of targets in free space and lossy media'. *Journal of Electromagnetic Waves and Applications,* Vol.14**,** pp.1245-1246.

Wei, Q., Xin, J., Shu-Qian, L. & Yan-Hong, W. (2010). 'SAR interference signal feature vector extraction and simulation based on wavelet packet analysis'.IEEE,Signal Processing Systems 2nd International Conference., Dalian, , Vol.3, pp. 284-287.

Xia, W., He, Z. & Liao, Y. (2008). 'Subspace-based method for multiple-target localization using MIMO radars'.*IEEE, Signal Processing and Information Technology*, pp.715-720.

Xianming, Q., Zhi Ning, C. & Michael Yan Wah, C. (2008). 'Parametric study of ultra-wideband dual elliptically tapered antipodal slot antenna'. *International Journal of Antennas and Propagation,* Vol.2008, Article ID 267197.

Yang, Y., Wang, Y. & Fathy, A. E. (2008). 'Design of compact Vivaldi antenna arrays for UWB see through wall applications'. *Progress In Electromagnetics Research,* Vol.82**,** pp.401-418.

Yarovoy, A. G., Van G., P. & Ligthart, L. P. (2000). 'Ground penetrating impulse radar for landmine detection'. *GPR 2000, Processe of the Eighth International Conference on Ground Pentrating Radar, SPIE,* Vol.4, pp. 856-860.

Ye, H. & Jin, Y. Q. (2010). 'Dual GPOF/DCIM for Fast Computation of Sommerfeld Integrals and EM Scattering From an Object Partially Embedded in Dielectric Half-Space'. *Antennas and Propagation, IEEE Transactions on,* Vol.58**,** pp.1801-1807.

Yngvesson, K. S., Schaubert, D. H., Korzeniowski, T. L., Kollberg, E. L. & Thungren, T. (1985). 'Endfire tapered slot antennas on dielectric substrates'. *IEEE Transactions on Antennas and Propagation,* Vol.33**,** pp.1392-1400.

Younan, N. (2002). 'Radar target identification via a combined E-pulse/SVD-Prony method'., *IEEE, Radar Conference 2000, USA*, pp.799-803.

J. Young, (1976). 'Radar imaging from ramp response signatures'. *Antennas and Propagation, IEEE Transactions on,* Vol.24**,** pp.276-282.

Young, Randy K.,(1992) ' Wavelet Theory and Its Applications*',* *Springer, 1st edition USA,* PP. 13-20.

Zhao, Y., Atlas, L. E. & Marks, R. J.(1990). 'The use of cone-shaped kernels for generalized time-frequency representations of nonstationary signals'. *Acoustics, Speech and Signal Processing, IEEE Transactions on,* Vol.38**,** pp.1084-1091.